

AD _____

Award Number: W81XWH-09-1-0673

TITLE: IL-6 Receptor Isoforms and Ovarian Cancer

PRINCIPAL INVESTIGATOR: Susan E. Waltz, Ph.D.

CONTRACTING ORGANIZATION: University of Cincinnati
Cincinnati, OH 45221

REPORT DATE: ~~Feb 2009~~ ~~AFH~~

TYPE OF REPORT: ~~Other~~

PREPARED FOR: U.S. Army Medical Research and Materiel Command
Fort Detrick, Maryland 21702-5012

DISTRIBUTION STATEMENT: Approved for Public Release;
Distribution Unlimited

The views, opinions and/or findings contained in this report are those of the author(s) and should not be construed as an official Department of the Army position, policy or decision unless so designated by other documentation.

Table of Contents

	<u>Page</u>
Introduction.....	4
Body.....	4
Key Research Accomplishments.....	9
Reportable Outcomes.....	9
Conclusion.....	9
References.....	10
Appendices.....	11

Introduction

The overall goal of the proposed study has been to test the hypothesis that membrane and soluble IL6R play distinct roles in driving tumor progression. Two major Tasks were funded as outlined in the Statement of Work, which encompasses examining IL6R expression in ovarian patient tumor samples and performing experiments to define the function of IL6R in the tumor proper and host microenvironment.

Body

The overall goals have been accomplished and the data published related to Task 1 (1). Task 1 entailed the "Identification of IL6R isoforms in patient samples." In the reported studies, elevated levels of IL6, total IL6R, differential spliced forms of IL6R, ADAM10 and ADAM17 were found in ovarian tumors. In addition, these studies further demonstrated that both tumor and host cells contribute to soluble IL6R expression in the tumor microenvironment.

Task 2 entailed "*In vivo* experiments to determine functions of IL6R isoforms and tumor:stroma relationships. For this task, mouse breeding colonies and genotyping procedures were set up. A recent paper was also published related to the characterization and general phenotype of these mice (2). Xenograft studies using ovarian cancer cell lines in SCID mice demonstrated that host IL6R may be an important means by which IL6R levels are increased in the tumor microenvironment along with the importance of IL6R in the tumor proper (1). Further studies have been published which also show that overexpression of IL6R and to a more modest extent IL6, in ovarian cancer cells promotes their colonization on the omentum *ex vivo* and increased their adherence to plastic as well as plates coated with laminin and collagens I and II (3). To test the significance of host derived tumor growth, ovarian tumor cells were next injected intraperitoneally (IP) into mice deficient in either IL6 or IL6R. In examining tumor adherence to the omentum following IP injection, mice with a complete loss of IL6 or IL6R exhibited less ovarian cancer cell adherence to the omentum. To obtain information as to the host cell type in which IL6R expression is needed for tumor adherence, ovarian cancer cells were injected into mice with conditional losses of IL6R in either hepatocytes or in myeloid cells (monocytes/granulocytes). Interestingly, tumor adherence was reduced in both hosts with IL6R loss, although IL6R loss in host myeloid cells lead to a greater inhibition of tumor adherence to the omentum compared to loss in IL6R from hepatocytes. At this point, the project was halted as the initial PI left the institution. A few months later, a new PI was designated (Susan Waltz) and the mouse breeding colonies were re-initiated. Unfortunately, having to regenerate the animal colonies entailed approximately 8-12 months to obtain the complex IL6R^{-/-} mice and the IL6R conditional mutants as the original colonies were sacrificed prior to the designation of a new PI. Over the course of the past year, the focus of the new PI has been to generate the appropriate mouse colonies and cell lines to continue experiments designated in Task 2. The primary goal of these final studies has been to examine the significance and potential mechanisms associated with host IL6R on ovarian cancer growth and metastasis. The following is a synopsis of the final data that has been obtained since the new PI was designated through completion of the funded studies:

IL6 and IL6R stimulate migration in ovarian cancer cell lines.

Among gynecologic cancers, ovarian cancer has the highest death rate. Treatment may involve debulking surgery followed by chemotherapy but metastasis often reoccurs. Localized metastasis within the peritoneum is the most common method of spread and occurs via malignant ascites or direct extension. IL6 is highly expressed in malignant ascites and serum. Data recently published by the previous PI, Dr. Angela Drew, demonstrated that IL6 and IL6R

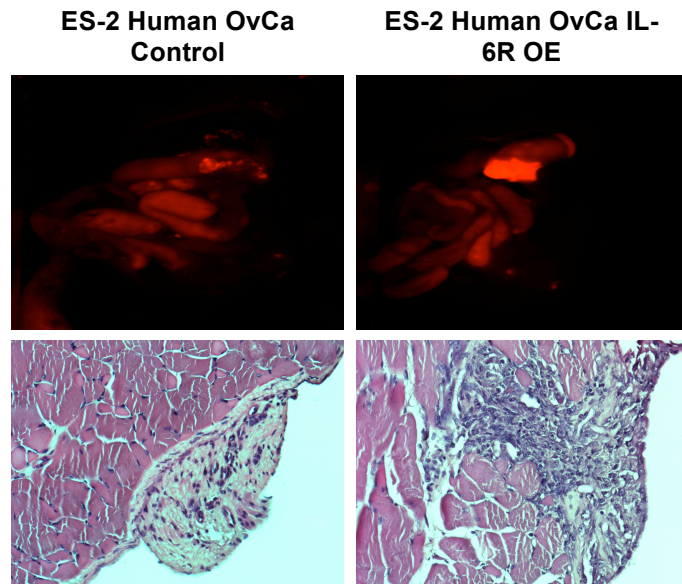


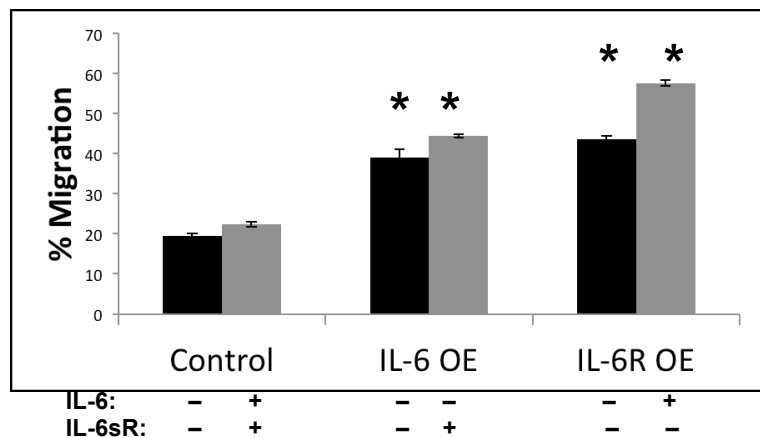
Figure 1. IL6R overexpression increases metastasis to the omentum. ES-2-RFP ovarian cancer cells and ES-2-RFP IL6R cells, which were engineered to overexpress IL6R were IP injected into SCID mice and tumor cell spread was monitored by fluorescence (Top) and by histological analysis (Bottom).

overexpression in ovarian cancer cell lines promoted metastasis to the omentum following intraperitoneal injection (3). In following up on these data, we demonstrated that the ovarian cancer cell line ES-2 overexpressing IL6R not only increased metastasis to the omentum following intraperitoneal (IP) injection into mice but that cells overexpressing IL6R exhibited increased migration/invasion within the peritoneal cavity (**Figure 1**).

To follow up on increased migratory ability of tumor cells overexpressing IL6R, we next sought to determine whether IL6 signaling regulates tumor cell migration. To accomplish this, ES-2 human ovarian cancer cells, as well as ES-2 cells overexpressing IL6 or IL6R were plated on tissue culture plates and scratch wounds were made. Over the course of the experiment, photographs of the cultures were taken temporally and the percent migration was measured based on wound closure. As depicted in

Figure 2, both IL6 and IL6R overexpression lead to significantly more cell migration compared to control cells. Slight increases, although not significant, were observed following the addition of exogenous IL6 or soluble IL6R. This data suggests that tumor cell derived IL6/IL6R signaling may be an important factor regulating the local migration/invasive ability of ovarian cancer cells and that further supplementation of IL6 or IL6R may only marginally be required beyond that present in the tumor cell proper to increase this effect.

Figure 2. IL6 and IL6R overexpression lead to increased cell migration in ES-2 ovarian cancer cells. Control ES-2 cells or cells overexpressing IL6 or IL6R were examined for the percent migration (wound closure) after 30 hours following a scratch wound. In addition, cells were exogenously treated with IL-6 or soluble IL-6R. *, P<0.05 Compared to the corresponding control group.



Published studies examining IL6^{-/-} and IL6R^{-/-} mice demonstrated a complexity of IL6 signaling for wound healing in mice with IL6^{-/-} mice exhibiting delayed healing of incisional skin wounds compared to wild type mice (2). Interestingly, IL6R^{-/-} did not display a delay in wound healing *in vivo*. In examining mechanisms that may explain the differences in wound healing phenotypes, signaling pathways downstream of IL6 signaling were examined. STAT3 phosphorylation was

similarly reduced in mice with IL6 and IL6R deficiencies compared to control 30 minutes after wounding. However phosphorylation of MAPK (Erk1/2) was undetectable in IL6^{-/-} mice yet increased in IL6R^{-/-} mice suggesting an importance of Erk activation in wound healing. To examine the importance of these signaling cascades in wound healing *in vivo*, mice (wild type, IL6^{-/-} and IL6R^{-/-} mice) were topically treated with U0126, an inhibitor of MEK1/2 during the incisional wound period and wounding evaluated. In total, these *in vivo* wound healing studies indicated that enhanced ERK activation is important in assisting wound contraction/healing (2).

To test if MAPK signaling may be an important factor in ovarian tumor cell migration, ES-2 cells with or without IL6 or IL6R overexpression were treated with 40 μ M U0126 *in vitro* and migration/wound closure experiments monitored as in **Figure 2**. As depicted in **Figure 3**, U0126 treatment significantly inhibited the migration of ES-2 cells alone. Impressively, Erk inhibition also ablated the enhanced migration observed in ES-2 cells overexpressing IL6 or IL6R.

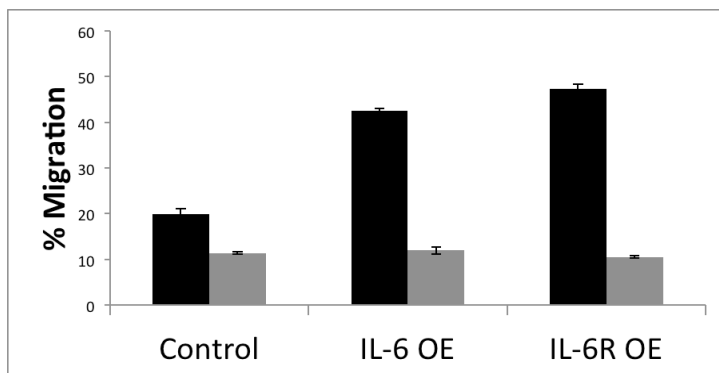


Figure 3. MEK1/2 inhibition ablates wound healing following IL6 and IL6R overexpression in ES-2 ovarian cancer cells. Control ES-2 cells or cells overexpressing IL6 or IL6R were examined for the percent migration (wound closure) after 30 hours following a scratch wound. Black bars represent wound healing following vehicle treatment while grey bars represent wound healing following addition of 40 μ M U0126. All grey bars are significantly reduced compared to their corresponding black bar control group.

To examine signaling pathways in ovarian cancer cells that are associated with activation of the IL6 signaling pathway and enhanced cell migration, cells were plated as in **Figure 2**, wounded (scratched) and given vehicle, AG490 (Stat Inhibitor) or U0126. After 30 hours, cell lysates were examined by Western analysis. As shown in **Figure 4**, inhibition by U0126 completely ablated Erk phosphorylation and correlated with decreased wound healing as depicted in **Figure 3**. STAT3 inhibition did not have a dramatic effect on Erk levels and was also unable to negate the effects of IL6 or IL6R mediated augmentation of cell migration (data not shown). These studies suggest that IL6 and IL6R overexpression in the ovarian cancer cell proper can lead to an increase in tumor cell migration/invasion, which may be dependent on maintaining Erk phosphorylation. Interestingly, these studies differ with the role of IL6 and IL6R *in vivo* of which IL6 is required for efficient wound healing while IL6R is dispensable. However, the results are consistent in that Erk activation appears to be an important pathway for wound healing.

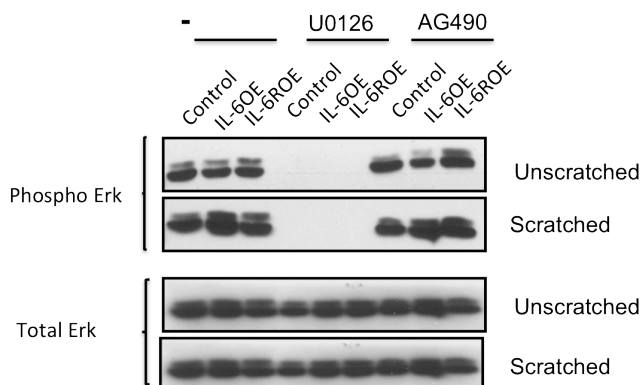


Figure 4. Wound healing is associated with Erk activation. ES-2 cells with IL6 or IL6R overexpression were scratch wounded or not followed by treatment with vehicle (-), U0126 or AG490. After 30 hours, cell lysates were examined for Erk phosphorylation.

Omental colonization is promoted by host IL6R expression and may be inhibited by the addition of soluble IL6R. To further evaluate the importance of host IL6R in the colonization of ovarian tumor cells to the omentum, we examined *ex vivo* omental colonization by ID8 cells to isolated murine omenta from wild type, IL6R^{-/-} and IL6R flox/AlbCre mice (mice with a conditional deletion of IL6R in hepatocytes). ID8 cells were obtained from the University of Kansas and were chosen due to the fact that they are syngeneic with the omenta isolated from C57Bl/6 mice so as to eliminate any phenotype related to the cells being recognized as foreign by the host immune system. The ID8 cells were labeled with tomato red fluorescent protein and were mixed with omenta noted. As is observed in Figure 5, ID8 cells were unable to efficiently colonize the omenta from both IL6R^{-/-} and IL6R flox/AlbCre mice. Data from the IL6R flox/AlbCre mice suggests that sufficient soluble IL6R may be produced in the liver to aid in ovarian cell colonization/metastasis, as in the absence of this source, colonization is similar to that observed in IL6R^{-/-} mice. This data also suggests that the levels of IL6R may be important in this process.

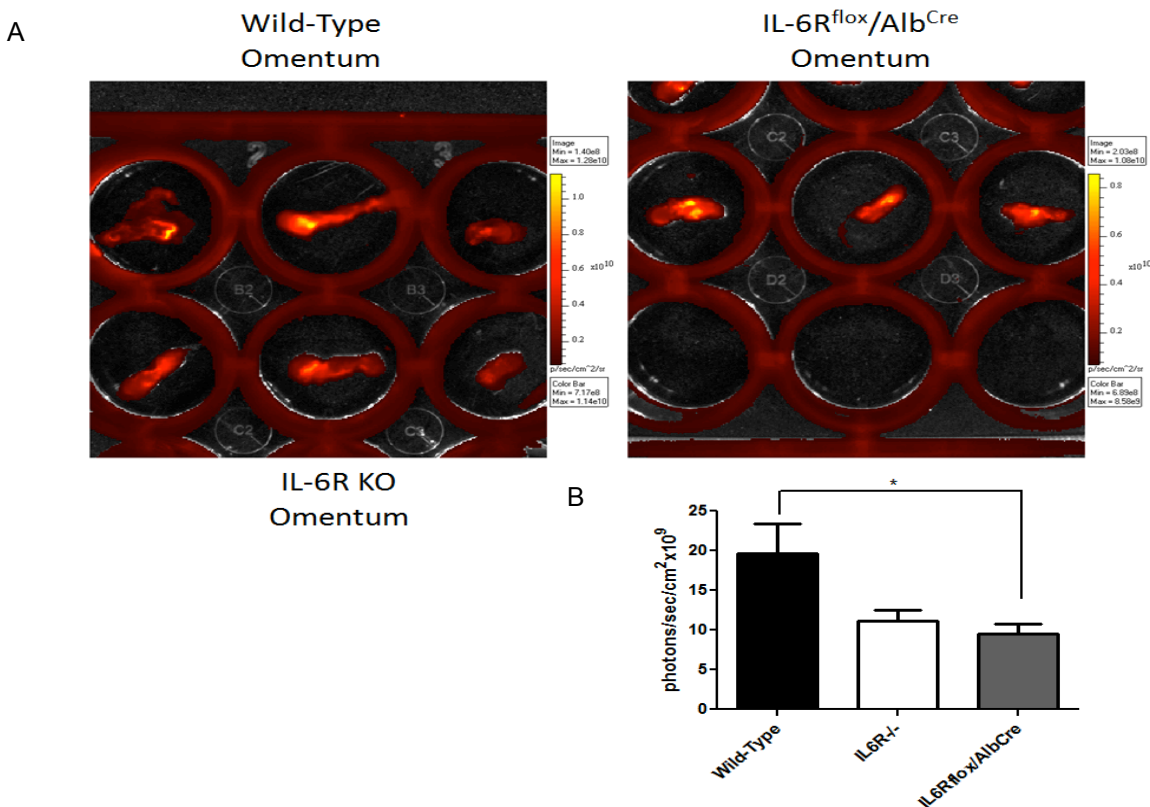


Figure 5. Assessment of *ex vivo* colonization of ID8-Tomato Red Cells to Omenta. (A) ID8 mouse ovarian cancer cells, derived from C57Bl/6 mice, were transduced with tomato red lentivirus and examined by fluorescence microscopy for red protein expression. Naïve omenta were excised from 7-11 week old wild-type, IL6R^{-/-} and IL6R^{flox/Albumin^{Cre}} mice using an ice-cold PBS technique previously published. Briefly, the spleen, pancreas and omentum were dissected *en bloc* and placed in ice cold PBS. After a few minutes, the omentum, which rises to the top, was removed and placed in a 24-well dish with 2×10^6 ID8-Tomato Red cells and co-cultured with agitation at 37°C, 5% CO₂ for 6 hours. After this time, fluorescence was examined using a Xenogen IVIS microscopy system. Note the different scales on the right. (B) Total flux measurements in photons/sec/cm² x 10⁹ were analyzed and graphed using the Xenogen IVIS microscopy system ($N=3$ per genotype, * $P<0.05$ by Student's t-Test).

Given the data in **Figure 5** which suggests that soluble IL6R from the host may dramatically promote the colonization of ovarian cancer cells to the omentum, we next sought to test this hypothesis. We isolated omenta from wild type (WT), IL6R^{-/-} and IL6R flox/AlbCre mice. The omenta were mixed with ID8 cells as in **Figure 5** along with either vehicle or soluble IL6R/IL6. As shown in **Figure 6**, the number of ID8 colonies on the omentum of IL6R and IL6R flox/AlbCre mice is reduced compared to controls. However, ID8 attachment was rescued in the IL6R mutant mice following supplementation with soluble IL6R and IL6. These studies suggest that blocking IL6 signaling may be an effective therapeutic approach to prevent ovarian cancer cell spread.

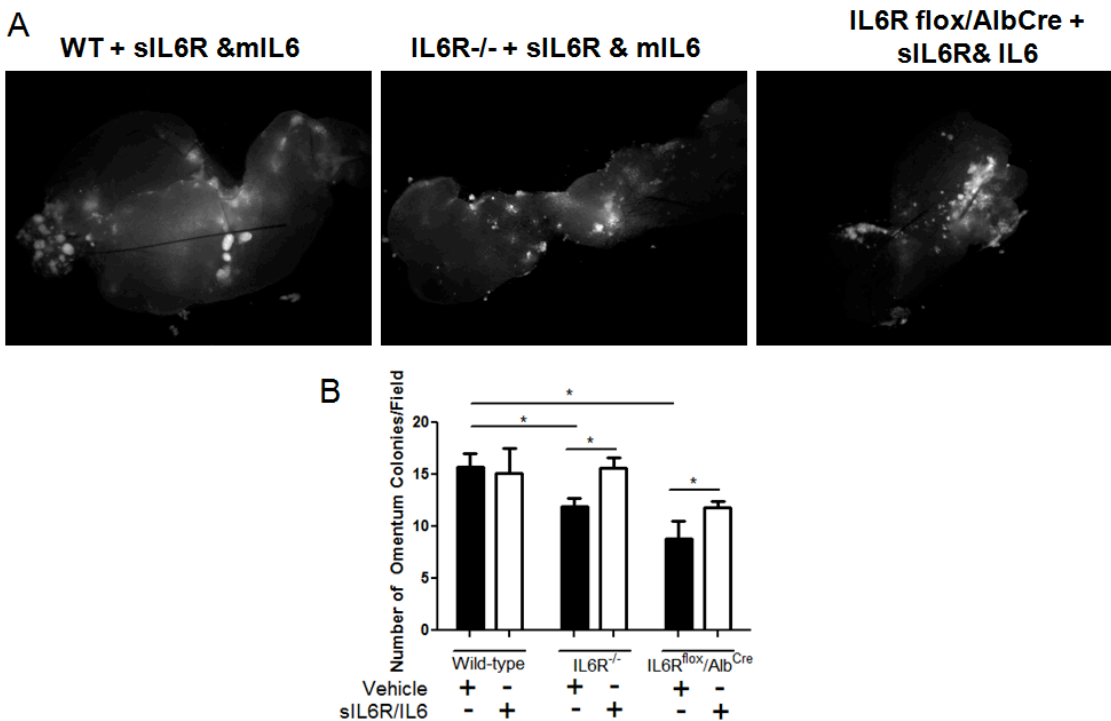


Figure 6. Omental colonization is enhanced in the absence of IL6R by the addition of soluble IL6R and ligand. (A) Naive omenta were dissected from 11-16 week old wild-type, IL6R^{-/-} and IL6R^{flox}/Albumin^{Cre} as in Figure 1. 2x10⁶ ID8-Tomato Red cells supplemented with 100 ng/ml soluble mouse IL6R (sIL6R) and 10 ng/ml mouse IL-6 (IL6) were incubated with these omenta for 16 hours with agitation at 37°C, 5% CO₂ after which time colonies were examined by fluorescence microscopy and counted at 20X (B).

Key Research Accomplishments

- Staffing accomplished to support continuation of project.
- Obtained and generated IL6R floxed mice (IL6R^{fl/fl}), IL-6R deficient mice (IL6R^{-/-}), and IL6R flox/AlbCre mice. Initiated breeding colonies to generating control and experimental animals.
- Initiated procedures to successfully genotype mice from breeding colonies.
- Identification of IL6R in the ovarian tumor microenvironment.
- Obtained ID8 cells and generated Tomato Red expressing ID8 cells to follow by fluorescent imaging.
- Demonstration that differentially spliced isoforms of IL6R are prominent in ovarian cancer.
- Host expression of IL6R contributes to the total amount of IL6R present in the tumor microenvironment.
- Finding that IL6R expression enhances the earliest metastasis of ovarian cancer.
- Myeloid cell expression and hepatic expression of IL6R are critical to influence early tumor cell adhesion to the omentum.
- Demonstrated that IL6 and IL6R stimulate migration of ovarian cancer cells and invasion into the omentum.
- Overexpression of IL6 and IL6R in ovarian cancer cells leads to increased cell migration *in vitro*.
- Migration of IL6 and IL6R overexpressing ovarian cancer cells is associated with Erk phosphorylation and blockade of Erk activation inhibits IL6 signaling induced migration.
- *In vivo*, host IL6R deficiency or lack of IL6R production in hepatocytes leads to a reduction in colonization of ovarian cancer cells, ID8 cells, to the omentum *ex vivo*.
- Soluble IL6R and IL6 are able to enhance omental colonization of ovarian cancer cells to omentum isolated from IL6R and IL6R flox/AlbCre host mice.

Reportable Outcomes

Cell lines:

Obtained through an approved material and transfer agreement (MTA) a tumorigenic mouse ovarian cancer cell line referred to as ID8 cells. These cells were generated at the University of Kansas from C57B6 mice. The prime advantage of the use of these cell lines is to be able to examine ovarian dissemination and growth in syngeneic immune-competent mice. We have successfully grown these cells in culture and have generated stable cell clones which express Tomato Red so that these cells can be followed through fluorescent imaging techniques *in vivo*.

Gene Targeted Animals:

Generated breeding colonies for IL6R^{-/-}, and IL6R flox/AlbCre mice to generate conditional deletions of IL6R in hepatocytes.

Research opportunities provided for individuals based on studies in this award:

Molly McFarland-Mancini, Postdoctoral Fellow, 2006-2009

Premkumar Giridhar, Postdoctoral Fellow, 2009-2010

William D. Stuart, Principal Research Scientist, 2011-2012

Andrew Paluch, Graduate Student, 2012

Manuscripts published and under preparation:

- Rath, K.S., Funk, H.M., Bowling, M.C., Richards, W.E., and Drew, A.F. 2010. Expression of soluble interleukin-6 receptor in malignant ovarian tissue. *Am J Obstet Gynecol* 203:230 e231-238.
- McFarland-Mancini, M.M., Funk, H.M., Paluch, A.M., Zhou, M., Giridhar, P.V., Mercer, C.A., Kozma, S.C., and Drew, A.F. 2010. Differences in wound healing in mice with deficiency of IL-6 versus IL-6 receptor. *J Immunol* 184:7219-7228.
- Giridhar, P.V., Funk, H.M., Gallo, C.A., Porollo, A., Mercer, C.A., Plas, D.R., and Drew, A.F. 2011. Interleukin-6 receptor enhances early colonization of the murine omentum by upregulation of a mannose family receptor, LY75, in ovarian tumor cells. *Clinical & experimental metastasis* 28:887-897.
- Paluch A, Stuart WD, and Waltz SE. Manuscript in preparation. IL6 signaling promotes ovarian tumor cell migration and omental attachment which is regulated by Erk activation and soluble IL6 signaling.

Conclusion

The combined studies supported by this grant have provided important experimental evidence related to IL6 signaling in the ovarian tumor cell proper and in the host microenvironment. The results show that IL6R is present in the tumor microenvironment along with differentially spliced isoforms. This expression in the tumor microenvironment is upregulated compared to normal tissues. Moreover, we show that overexpression of either tumor derived or host IL6R is important in ovarian cancer cell metastasis. We further show that signaling thru IL6 in the tumor cells leads to enhanced tumor cell migration that can be blocked by inhibiting Erk signaling. In addition, we provide evidence that soluble IL6 signaling may be an important target to regulate ovarian metastasis as reduction of IL6R leads to reduced omental colonization of ovarian cancer cells which can be reverted by addition of soluble IL6 signaling.

References

1. Rath, K.S., Funk, H.M., Bowling, M.C., Richards, W.E., and Drew, A.F. 2010. Expression of soluble interleukin-6 receptor in malignant ovarian tissue. *Am J Obstet Gynecol* 203:230 e231-238.
2. McFarland-Mancini, M.M., Funk, H.M., Paluch, A.M., Zhou, M., Giridhar, P.V., Mercer, C.A., Kozma, S.C., and Drew, A.F. 2010. Differences in wound healing in mice with deficiency of IL-6 versus IL-6 receptor. *J Immunol* 184:7219-7228.
3. Giridhar, P.V., Funk, H.M., Gallo, C.A., Porollo, A., Mercer, C.A., Plas, D.R., and Drew, A.F. 2011. Interleukin-6 receptor enhances early colonization of the murine omentum by upregulation of a mannose family receptor, LY75, in ovarian tumor cells. *Clinical & experimental metastasis* 28:887-897.

Appendices

The following three publications are being attached to support the details of the funded tasks accomplished.

- Rath, K.S., Funk, H.M., Bowling, M.C., Richards, W.E., and Drew, A.F. 2010. Expression of soluble interleukin-6 receptor in malignant ovarian tissue. *Am J Obstet Gynecol* 203:230 e231-238.
- McFarland-Mancini, M.M., Funk, H.M., Paluch, A.M., Zhou, M., Giridhar, P.V., Mercer, C.A., Kozma, S.C., and Drew, A.F. 2010. Differences in wound healing in mice with deficiency of IL-6 versus IL-6 receptor. *J Immunol* 184:7219-7228.
- Giridhar, P.V., Funk, H.M., Gallo, C.A., Porollo, A., Mercer, C.A., Plas, D.R., and Drew, A.F. 2011. Interleukin-6 receptor enhances early colonization of the murine omentum by upregulation of a mannose family receptor, LY75, in ovarian tumor cells. *Clinical & experimental metastasis* 28:887-897.

ONCOLOGY

Expression of soluble interleukin-6 receptor in malignant ovarian tissue

Kellie S. Rath, MD; Holly M. Funk, BSc; Marcia C. Bowling, MD; William E. Richards, MD; Angela F. Drew, PhD

OBJECTIVE: The objective of the study was to investigate interleukin-6 receptor (IL6R) isoforms and sheddases in the ovarian tumor microenvironment.

STUDY DESIGN: Expression of IL6R and sheddases was measured in tissue samples of papillary serous ovarian carcinomas and benign ovaries by real-time polymerase chain reaction and immunohistochemistry. Murine xenograft samples were tested by enzyme-linked immunosorbent assay to discriminate and evaluate tumor and host contributions of IL6R.

RESULTS: IL6R expression was increased in malignant ovarian tumors and localized to epithelial cells. Expression of a soluble splice variant of

IL6R was increased in malignant tumors, as were the sheddases for the full-length isoform. An in vivo xenograft model showed that host IL6R expression is also increased and regulated by tumor-associated inflammation.

CONCLUSION: IL6R is overexpressed in epithelial ovarian malignancies because of increases in a soluble IL6R variant, in the sheddases for full-length IL6R and host IL6R expression. Soluble IL6R may be an efficacious target for reducing IL6-mediated ovarian tumor progression.

Key words: a disintegrin and metalloprotease domain 10, a disintegrin and metalloprotease domain 17, cytokine receptor, inflammation, interleukin-6, ovarian tumor

Cite this article as: Rath KS, Funk HM, Bowling MC, et al. Expression of soluble interleukin-6 receptor in malignant ovarian tissue. *Am J Obstet Gynecol* 2010;203:230.e1-8.

Ovarian cancer is the most deadly of the gynecological malignancies.¹ Most gynecologic oncologists initially treat the disease with debulking surgery, followed by adjuvant chemotherapy with platinum and taxane agents. After an initial response to chemotherapy, the

cancer will recur in the majority of patients but with chemoresistant properties. The efficacy of second-line and salvage therapies for patients who fail initial surgical and medical therapy is limited at best. A greater understanding of the mechanisms by which ovarian cancers metastasize and develop chemoresistance is essential for reducing the high mortality associated with these malignancies.

Interleukin-6 (IL-6) is an important proinflammatory cytokine that is frequently up-regulated in acute and chronic inflammatory conditions, including many cancers (reviewed elsewhere²). IL-6 signaling occurs through a hexameric complex of IL-6, a specific α receptor (IL6R; glycoprotein [gp]80), and a shared β -signaling receptor (gp130).³ Dimerization of gp130 leads to activation of Janus tyrosine kinases and subsequent translocation of signal transducer and activator of transcription (Stat) transcription factors.⁴ Stat3 is the major Stat induced by IL-6 signaling, and its nuclear translocation induces a transcriptional program resulting in inflammation, cell survival, or differentiation, depending on the cellular context.^{5,6} In addition to membrane-bound IL6R, several soluble isoforms also exist.⁷

Expression of both membrane-bound and soluble forms of IL6R are largely restricted to hepatocytes and immune cells, and therefore, signaling through membrane-bound IL6R is restricted to these cells. However, the soluble isoforms of IL6R are excreted from these cells types and unexpectedly function as agonists for IL6R signaling and hence allow IL6R-mediated signaling in cells that do not express IL6R. This occurs through initial binding of IL-6 to soluble extracellular IL6R and subsequent binding of this complex to the membrane-bound signaling receptor, gp130.

This binding results in dimerization of gp130, which, in turn, leads to stat3 activation that occurs in a similar fashion to that induced by membrane-bound IL6R. Because gp130 is ubiquitously expressed, the potential to respond to IL-6 is conferred on all cells in the presence of soluble IL6R. This process, known as transsignaling,⁸ has been found to be important in multiple disease states including rheumatoid arthritis, asthma, inflammatory bowel disease, and colon cancer.⁹⁻¹¹ It has been shown that many of the inflammatory functions of IL-6 signaling can be prevented by inhibiting the soluble isoform of IL6R with a solu-

From the Department of Cancer and Cell Biology (Drs Rath and Drew and Ms Funk) and the Division of Gynecologic Oncology, Department of Obstetrics and Gynecology (Drs Rath and Richards), University of Cincinnati School of Medicine, and the Department of Obstetrics and Gynecology (Dr Bowling), Christ Hospital, Cincinnati, OH.

Received Dec. 22, 2009; revised Jan. 29, 2009; accepted March 18, 2010.

Reprints: Angela F. Drew, PhD, Department of Cancer and Cell Biology, Vontz Center for Molecular Studies, University of Cincinnati, 3125 Eden Ave., Cincinnati, OH 45267-0521. angela.drew@uc.edu.

This study was supported in part by the American Cancer Society Grant RSG-06-141-01-CSM (to A.F.D.) and the Department of the Army, Department of Defense Ovarian Cancer Research Program grant (OC080273) (to A.F.D.).

0002-9378/\$36.00

© 2010 Mosby, Inc. All rights reserved.

doi: 10.1016/j.ajog.2010.03.034

TABLE 1
Patient characteristics

Patient no.	Age	Pathology	Stage
1-16	39-71	Normal ovarian tissue	
17	69	Mixed papillary serous and undifferentiated tumor	IV
18	56	Papillary serous	II
19	62	Papillary serous	IIIC
20	47	Papillary serous	IIIC
21	75	Papillary serous	IIIC
22	50	Papillary serous	IV
23	39	Papillary serous, high grade	IIIC
24	36	Papillary serous cystadenocarcinoma	IB
25	68	Papillary serous	III
26	77	Papillary serous	IV
27	55	Papillary serous	III

Rath. IL-6 receptor in ovarian tumors. Am J Obstet Gynecol 2010.

ble form of gp130.¹² Therefore, the soluble isoform plays important roles in inflammatory contexts by allowing a heightened response to IL-6 in all cell types at the site of inflammatory challenge.

Soluble IL6R can be generated by 2 distinct processes: differential splicing and proteolytic cleavage.¹³⁻¹⁵ The differentially spliced isoform lacks a transmembrane domain and is secreted as a soluble, functional receptor.¹⁶ The proteolytic enzymes responsible for cleavage of full-length IL6R are a disintegrin and metalloprotease domain (ADAM)-17, also known as tumor necrosis factor alpha-converting enzyme and to a lesser extent, ADAM10.¹⁷⁻¹⁹ These sheddases

cleave full-length IL6R in a membrane proximal site to release a soluble, functional receptor. A study of IL-6 signaling in an angiotensin-induced cardiac model suggested that the 2 forms of soluble IL6R may have different functions leading to either hypertrophy or hypertension.²⁰

It is well established that IL-6 is up-regulated in both the serum and ascites of ovarian cancer patients and is associated with disease progression.²¹⁻²³ IL-6 has also been implicated in chemotherapeutic resistance in ovarian cancer cell lines and in patients with ovarian cancer.^{22,24,25} However, the status of IL6R expression in ovarian cancer has not been adequately addressed to date. One

study reports increased expression of soluble IL6R in the sera of patients in the early stages of various tumor types, but specific data for ovarian cancer were not available.²⁶ Despite the importance of the soluble isoforms of IL6R in inflammation, there has not been a characterization of these isoforms in ovarian cancer.

Given that we have previously shown that inflammation drives the spread of ovarian tumors in murine models,²⁷ a thorough evaluation of inflammatory IL6R isoforms in the tumor microenvironment is needed. Here we describe the increased expression of IL-6, total IL6R, differentially spliced IL6R, ADAM10, and ADAM17 in ovarian tumors. Furthermore, we show that both tumor and host cells contribute to soluble IL6R expression in the tumor environment.

MATERIALS AND METHODS

Patient tissue collection and cell lines

Tissue samples from malignant and non-malignant ovaries were collected from patients undergoing routine gynecologic procedures at the University Hospital and the Christ Hospital in Cincinnati, OH (Table 1). Normal ovarian tissue was collected from patients 1-16. Malignant tissue collected from patients 17-27 were from primary ovarian epithelial carcinomas. Tissues were immediately snap frozen in liquid nitrogen at the time of surgery and stored at -80°C until analysis. Human ES-2 and SKOV3, clear cell and serous papillary ovarian carcinoma cell lines, respectively, were obtained from American Type Culture Collection (Manassas, VA). Cells were maintained in Dulbecco's Modified Eagles media with 10%

TABLE 2
Primers used in RT-PCR analysis

Gene	5'	3'
IL-6	CTCACCTCTTCAGAACGAATTGACAAACAAA	GGTACTCTAGGTATACCTCAAACCTCCAAAA
IL6R	GCTGTGCTCTTGGTGAGGAAGTTT	CTGAGCTCAAACCGTAGTCTGTAGAAA
IL6R variant 1 (full-length)	GCCTCCCAGTGCAAGATTCTTCTT	CCGCAGCTTCCACGCTTCTTCTT
IL6R variant 2 (differentially spliced)	GCGACAAGCCTCCCAGGTT	CCGCAGCTTCCACGCTTCTTCTT
ADAM10	AATGGATTGTGGCTCATTGGTGGG	TGGAAGTGGTTTAGGAGGAGGCCAA
ADAM17	CTTATGTTGGCTCTCCCAGAGCAAA	CATCCGGATCATGTTCTGCTCCAAAA

Rath. IL-6 receptor in ovarian tumors. Am J Obstet Gynecol 2010.

fetal calf serum and tested negative for mycoplasma contamination.

Animal studies

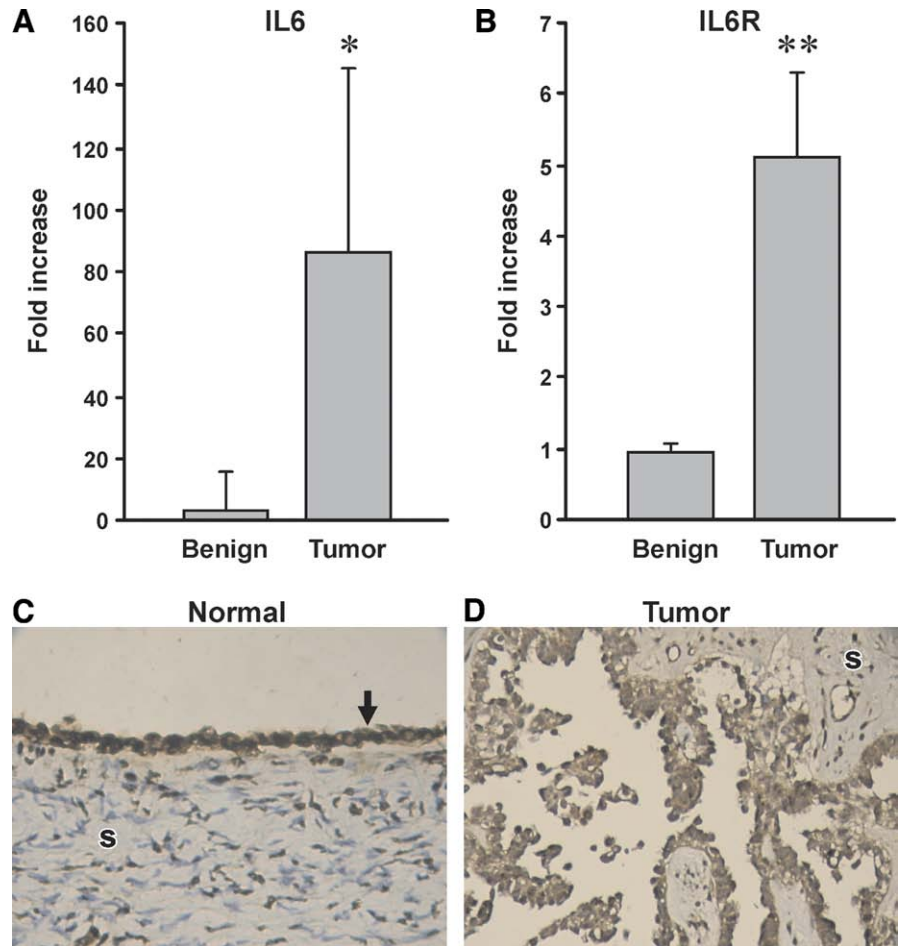
Human tumor cell lines (ES-2 and SKOV3) were harvested, resuspended in Matrigel (basement membrane protein gel, BD Biosciences, Franklin Lakes, NJ), and implanted in the ovaries of severe combined immunodeficiency (SCID) mice (Charles River Laboratories, Wilmington, MA), as previously described.²⁷ Groups of mice (n = 6) were administered acetyl salicylic acid (ASA; 100 mg/kg; Sigma, St Louis, MO), phosphate-buffered saline, or thioglycolate (0.5 mL of a 3% solution; Fluka, Buchs, Switzerland) by twice-weekly intraperitoneal injection. Additional mice without tumors were administered ASA, saline, or thioglycolate. Peritoneal lavage with phosphate-buffered saline was performed on anesthetized mice. Lavage fluid was centrifuged and stored at -80°C until analysis. Guidelines for the care and use of laboratory animals approved by the University of Cincinnati Institutional Animal Care and Use Committee were followed.

RNA isolation and reverse transcription–polymerase chain reaction (RT-PCR)

Ribonucleic acid (RNA) was extracted from patient tissue samples with the RNeasy lipid kit (Qiagen, Valencia, CA) and quantified with a spectrophotometer (Nanodrop, Wilmington, DE). Reverse transcription was performed with the ThermoScript II kit (Invitrogen, Carlsbad, CA). Real-time polymerase chain reaction (PCR) was performed with primers specific for IL-6, both isoforms of IL6R (total IL6R), full-length IL6R (variant 1), differentially spliced IL6R (variant 2), ADAM10, and ADAM17 (Table 2) with a Realplex Mastercycler (Eppendorf, Netheler, Germany). Primer specificity was confirmed by checking product sizes on an agarose gel and performing a melt-curve analysis on each run. Gene expression was normalized against the human L32 housekeeping gene, as previously described.²⁸

FIGURE 1

Increased expression of IL-6 and IL6R in malignant ovarian tumors



RNA was extracted from ovarian samples from patients with benign gynecologic conditions or ovarian malignancies and assessed for **A**, IL-6 or **B**, total IL6R by quantitative RT-PCR. Asterisk indicates $P < .05$; double asterisk indicates $P < .001$. Immunohistochemical analysis of ovaries from patients with **C**, no malignancy or **D**, malignant tumors demonstrated intense IL6R positivity in the surface epithelium (arrow) and tumor cells but not the stroma (indicated as s). Original magnification for **C** and **D**: $\times 200$.

IL-6, interleukin-6; IL6R, interleukin-6 receptor; RT-PCR, reverse transcription–polymerase chain reaction.

Rath. IL-6 receptor in ovarian tumors. *Am J Obstet Gynecol* 2010.

Immunohistochemistry

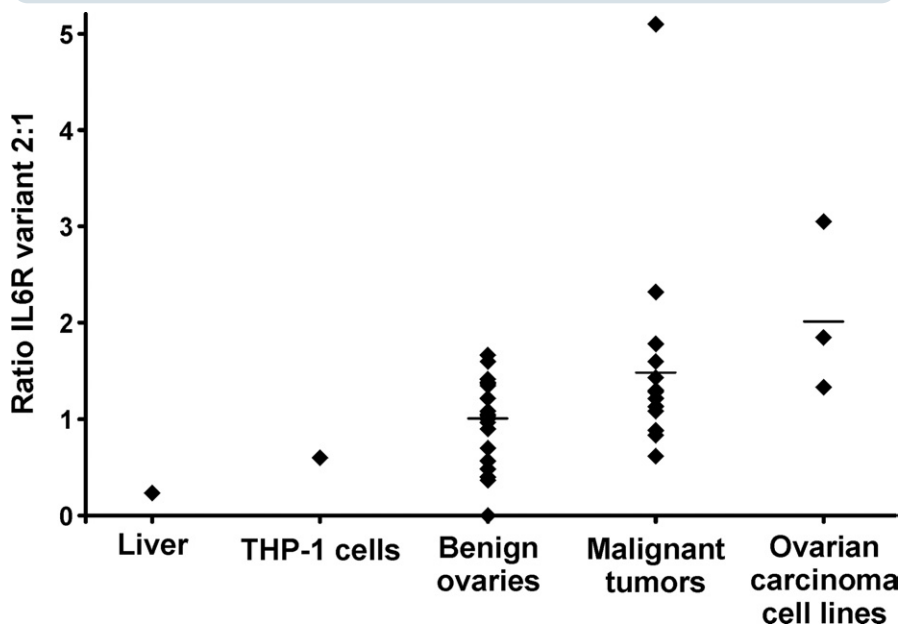
Immunohistochemistry was performed on paraffin-embedded samples of both benign and malignant ovarian tissue to detect IL6R. Briefly, samples were deparaffinized, and antigen retrieval was performed in citrate buffer (10 mM with 0.05% Tween 20, pH 6.0) for 10 minutes at 95°C . Slides were incubated overnight with rabbit antihuman IL6R (sc-661; detects both isoforms) at a dilution of 1:400 at 4°C , followed by biotinylated goat antirabbit immunoglobulin G (1:200).

ABC Elite kit (Vector, Burlingame, CA) and 3,3 diaminobenzidine substrate (Sigma) were used in the detection, followed by hematoxylin counterstain.

IL6R ELISA

Peritoneal lavage fluid from mice was analyzed by enzyme-linked immunosorbent assay (ELISA) (R&D Systems, Minneapolis, MN), according to the manufacturer's instructions, to assess expression of human and murine soluble IL6R. Cross-reactivity between human

FIGURE 2
Differentially spliced variant of IL6R



Expression of the differentially spliced variant of IL6R is preferentially increased in malignant ovarian tumors and ovarian carcinoma cell lines compared with benign ovaries, human liver, or the THP-1 monocytic cell line. Data indicate the ratio of differentially spliced IL6R mRNA compared with full-length IL6R mRNA, normalized to normal ovaries. Each data point represents one patient. $P < .05$ for benign ovaries vs malignant tumors or cell lines.

IL6R, interleukin-6 receptor; mRNA, messenger RNA.

Rath. IL-6 receptor in ovarian tumors. *Am J Obstet Gynecol* 2010.

and mouse IL6R is negligible with the use of these species-specific IL6R ELISA kits. The enzymatic reactions were detected at 570 nm and subtracted from background at 450 nm with a spectrophotometric plate reader.

Statistical methods

Data are represented as mean \pm SEM were analyzed by the Mann-Whitney *U* test.

RESULTS

Twenty-seven patient samples were collected: 16 with benign ovarian pathology and 11 with ovarian carcinoma (Table 1). Patient age ranges were not significantly different for benign ovary samples (39–71 years; average, 49.1 years) and malignant tumor samples (36–77 years; median, 59.5 years). All tumors were papillary serous and predominantly stage IIIC according to International Feder-

ation of Gynecology and Obstetrics classification.

To quantify the production of IL-6 and IL6R in benign ovaries and malignant ovarian tumors, we assessed RNA expression by real-time PCR. We found dramatic up-regulation of IL-6 in malignant ovaries compared with benign ovaries (Figure 1, A), consistent with previous reports.^{21–23} Expression of IL6R was also found to be up-regulated in ovarian malignancies (Figure 1, B).

We next sought to identify, by immunohistochemistry, the cell types responsible for IL6R expression in normal and malignant ovarian tissue. IL6R was predominantly expressed in the epithelium of normal ovaries and only minimally in the stroma (Figure 1, C). In serous papillary tumors, IL6R expression was strong in tumor cells and negligible in the tumor stroma (Figure 1, D). Ovarian IL6R expression was therefore a

function of both normal and malignant epithelium.

Given the markedly higher proportion of cells expressing IL6R in malignant ovaries, it would be reasonable to expect that the difference in messenger RNA (mRNA) expression levels between normal and malignant tissue would be even greater. This apparent underrepresentation by quantitative PCR could be due to differences in transcriptional or translational efficiencies or to soluble IL6R protein localizing to malignant ovaries despite being produced elsewhere.

Soluble IL6R is known to be important in many inflammatory contexts.⁹ To determine whether malignant ovarian tumors were predominantly expressing the full-length (variant 1) or the differentially spliced isoform that lacks the transmembrane domain (variant 2), we used real-time PCR with primers specific for each isoform. Interestingly, we found that the ratio of variant 2 relative to variant 1 was higher in malignant tumor samples than in a human monocytic cell line, normal liver, or benign ovarian samples (Figure 2).

IL6R expression is largely restricted to hepatocytes and immune cells (and some tumor cells); however, expression of soluble IL6R at sites of inflammation, tumors, or both allows IL-6 signaling in other cell types. To determine whether soluble host IL6R expression contributes to the increase in IL6R in the context of an ovarian cancer in vivo, we used a murine xenograft model. Human ovarian carcinoma cell lines were implanted orthotopically into the ovaries of immune-compromised SCID mice.

We implanted cell lines positive (SKOV3) and negative (ES2) for IL6R expression. The rate of tumor formation by SKOV3 cells implanted in the ovary was approximately 50%. Human IL6R was detected in mice in which SKOV3 cell tumors developed but not in ovaries in which tumors did not develop or in ES-2 cell-derived tumors (100% take rate), indicating the specificity of the ELISA (Figure 3, A). Mice that developed ovarian carcinoma had elevated levels of host (mouse) peritoneal soluble IL6R when compared with mice that did not develop carcinoma (Figure 3, B). Tumor

development was identified by gross analysis at necropsy and confirmed by histological analysis (data not shown).

To determine the role of inflammation in host IL6R expression in ovarian tumors, mice were treated with ASA to suppress inflammation, thioglycollate to increase inflammation, or phosphate-buffered saline (vehicle control) during tumor progression. Soluble levels of mouse IL6R were highest in mice treated with thioglycollate and lowest in mice treated with ASA (Figure 4, A).

This pattern of expression closely paralleled that of tumor burden in the mice, as assessed by ascite development and percentage of the diaphragm covered with tumor (Figure 4, B and *inset*). Mice that received inflammation-modulating drugs but that were not implanted with tumor cells expressed only baseline levels of IL6R (Figure 4, A). These data indicate that the increased expression of host soluble IL6R expression was a direct result of the presence of tumor in the peritoneum but was also influenced by the degree of inflammation.

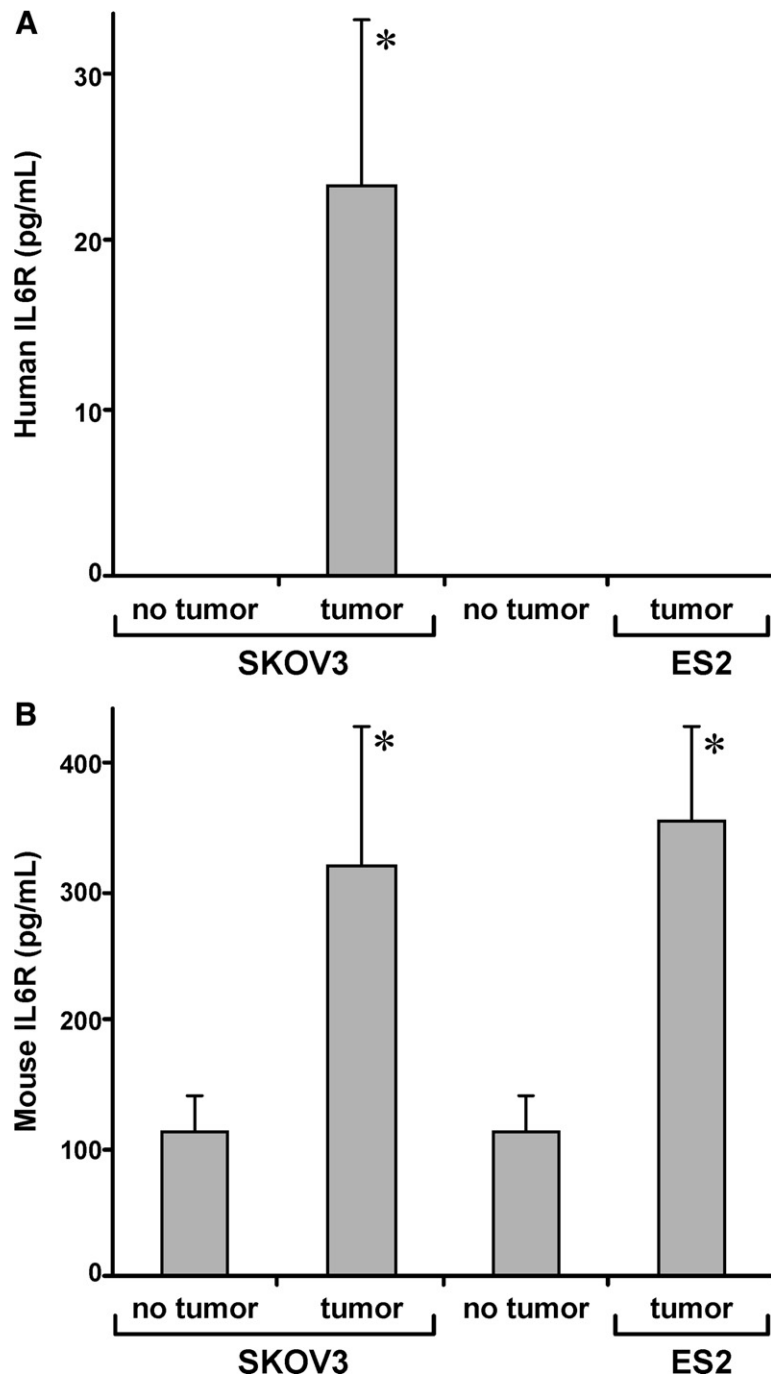
Finally, we evaluated the expression of the 2 known physiological sheddases for full-length IL6R, ADAM17, and ADAM10. We found that the expression of ADAM17 and ADAM10 was increased in malignant ovaries, as compared with benign tissue (Figure 5). The dramatic local increase in expression of these proteases in malignant ovarian tumors provides another mechanism by which soluble IL6R can be generated in the tumor microenvironment.

COMMENT

IL6R plays numerous roles in inflammatory responses and tumor progression.^{2,29} In this study, we found that IL6R is expressed in normal and malignant epithelium. We have demonstrated several mechanisms by which increased levels of soluble IL6R occur in the tumor microenvironment, including increased expression of a differentially spliced soluble isoform, up-regulation of sheddases for the membrane-bound form, and increased host expression of soluble IL6R. The increase of IL6R facilitates enhanced responsiveness to IL-6 in ovarian malignancy.

FIGURE 3

Soluble IL6R protein in mice with human ovarian tumor xenografts

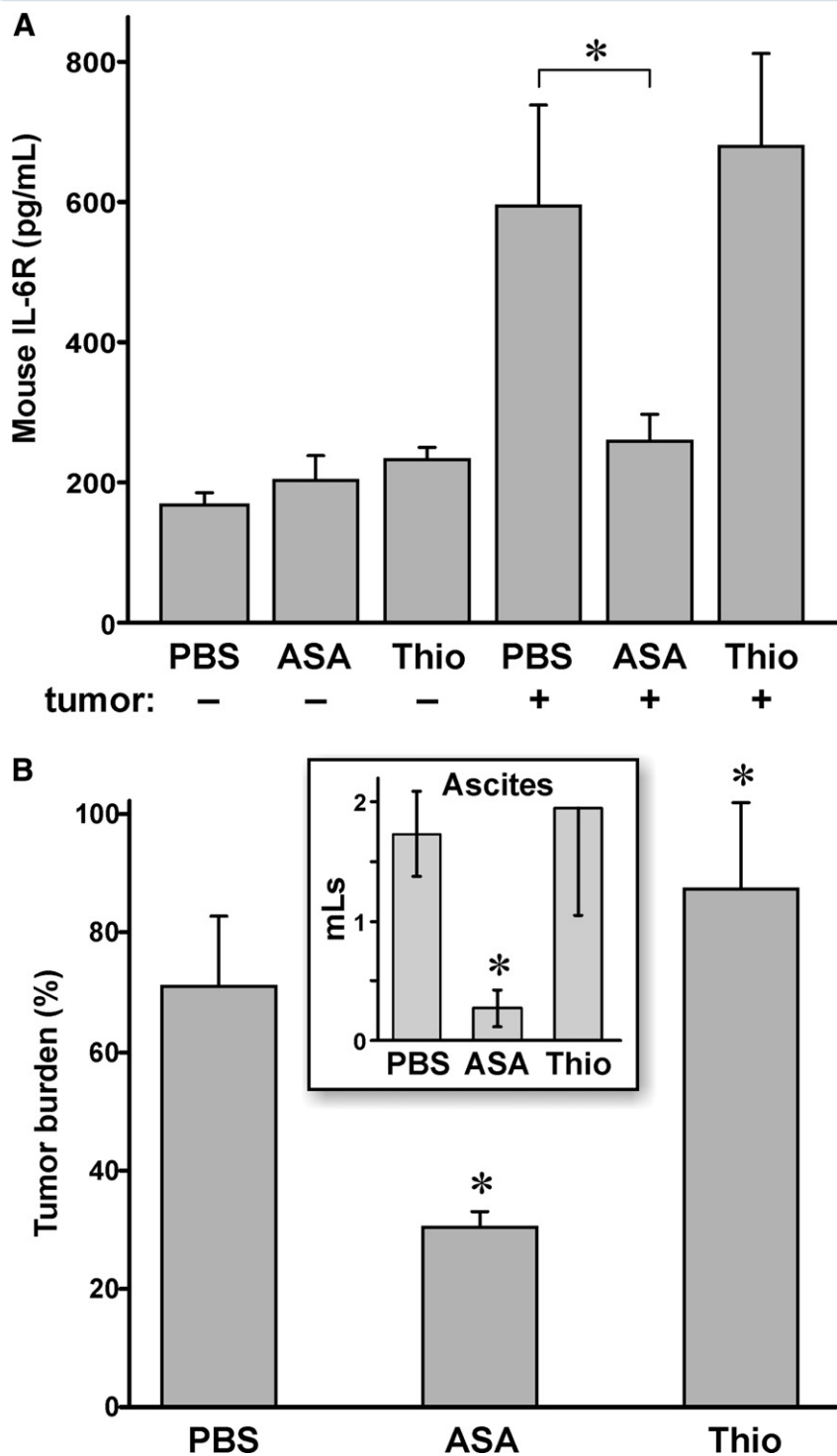


Increased expression of mouse and human soluble IL-6R protein in mice with human ovarian tumor xenografts. **A**, Expression of human sIL6R was increased in the peritoneal lavage fluid of mice that developed human SKOV3 carcinomas, as compared with mice in which tumors did not develop ($P < .025$). No human IL6R was detected in untreated mice or mice implanted with human ES-2 tumor cells, indicative of the lack of IL6R expression by this tumor cell line. **B**, Baseline levels of mouse IL6R were detected in the peritoneal lavage fluid of untreated mice and mice in which SKOV3 tumors failed to develop. Markedly increased levels of mouse IL6R occurred in mice with either human carcinoma cell line. Asterisk indicates $P < .05$.

IL6R, interleukin-6 receptor; sIL6R, soluble IL-6R.

Rath. IL-6 receptor in ovarian tumors. *Am J Obstet Gynecol* 2010.

FIGURE 4
IL6R expression is influenced by mediators
of inflammation during tumor progression



A, Suppressing inflammation with ASA during tumor progression significantly reduced host (mouse) IL6R expression ($P < .05$). Augmenting inflammation with thioglycollate showed a trend toward increased mouse IL6R expression. **B**, The pattern of IL6R expression during inflammation modulation closely resembled that of ascites production (*inset*) and tumor burden. Asterisk indicates $P < .05$.

ASA, acetyl salicylic acid; IL6R, interleukin-6 receptor.

Rath. IL-6 receptor in ovarian tumors. *Am J Obstet Gynecol* 2010.

nancies, contributing to increased phosphorylation of Stat3 and up-regulation of cell-survival pathways.^{24,30,31}

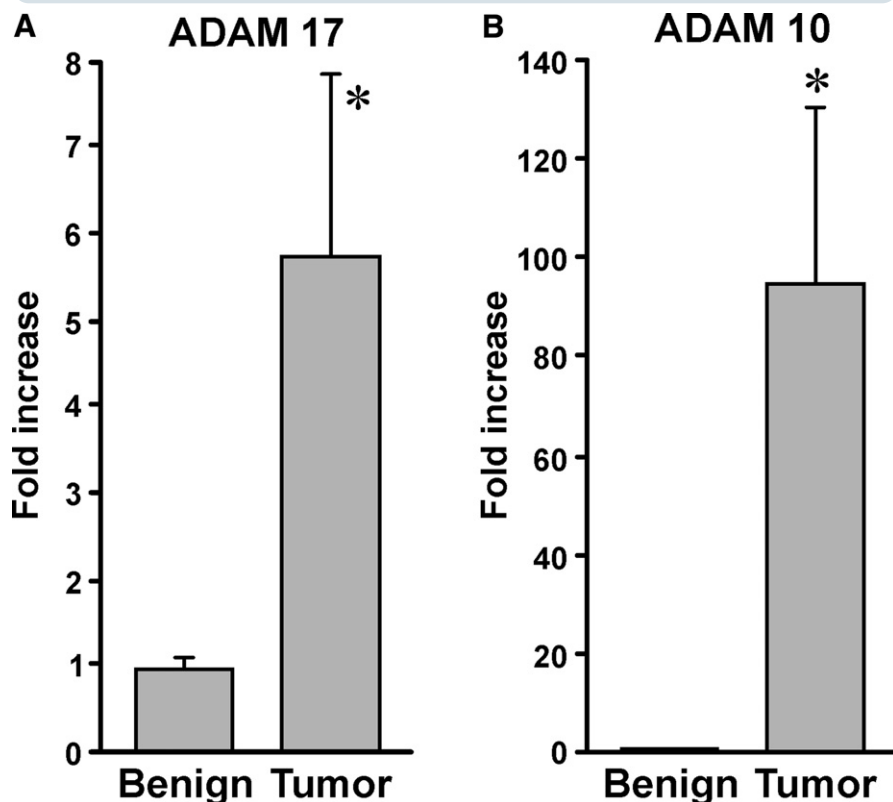
With no inherent kinase activity, IL6R functions to recognize its specific ligand and to induce dimerization of gp130, the signaling component of the complex. IL6R carries out this role in either soluble or membrane-bound forms; thus, the soluble receptor is effectively an agonist for IL-6 signaling. In fact, blocking only the soluble form of IL6R with exogenous soluble gp130 prevents many, if not all, of the known functions of IL-6 in inflammatory contexts.^{11,12}

In the current study, we demonstrate that tumor cells preferentially express a differentially spliced isoform of IL-6R that lacks the transmembrane domain. Expression of this soluble differentially spliced isoform has previously been reported in a subset of monocytes and in several carcinoma cell lines.³² In addition, our findings suggest that soluble IL6R may also be generated in malignant ovaries by cleavage of the membrane-bound form by increased levels of ADAM10 and ADAM17 proteases. Production of soluble IL6R in ovarian tumor cells may serve to increase IL-6 responsiveness in surrounding tumor cells, stromal cells, or peritoneal mesothelial cells.

Little has been learned about the contribution of the stroma to the expression of IL6R within the context of a tumor, owing to the difficulty in identifying the source of soluble IL6R. Here we have utilized a xenograft model and species-specific ELISAs to allow the distinction between tumor (human) and host (murine) IL6R.

Our data show that, in addition to tumor cell production of IL6R, host cells make a significant contribution to the increased expression of soluble IL6R in the peritoneal environment and that IL6R levels reflect the degree of peritoneal inflammation. It was not possible to determine whether host-derived IL6R is the differentially spliced isoform because this variant is lacking in mice. It is tempting to speculate that immune cells are a predominant source of host IL6R because they are abundant in the ascites

FIGURE 5
Increased expression of ADAM17 and ADAM10
in malignant ovarian tumor tissue



Expression of **A**, mRNA for ADAM17 and **B**, ADAM10 were increased in the ovaries of patients with ovarian cancer compared with benign ovaries. *Asterisk indicates* $P < .001$.

ADAM10, a disintegrin and metalloprotease domain 10; *ADAM17*, a disintegrin and metalloprotease domain 17; *mRNA*, messenger RNA. Rath. *IL-6 receptor in ovarian tumors. Am J Obstet Gynecol* 2010.

fluid³³⁻³⁵ and are known to be a source of shed IL6R in inflammatory contexts.³⁶

Given the importance of IL-6 signaling in inflammation, tumor growth, differentiation, and chemoresistance, the identification of IL6R isoforms in malignant ovarian tumors may provide novel therapeutic opportunities. Here we show that expression of soluble isoforms of IL6R is increased by multiple mechanisms, including preferential production of a differentially spliced variant, increased production of sheddases for membrane-bound IL6R, and up-regulation of host inflammation-induced soluble IL6R in the tumor microenvironment. Together these data suggest that trans-signaling through IL6R is a feature of ovarian tumors and that targeting IL6R may provide a novel treatment to

decrease the morbidity and mortality of this disease. ■

ACKNOWLEDGMENT

We gratefully acknowledge the assistance of Karen Winstead of the University of Cincinnati Tumor Bank, Dr Maryellen Daston for document editing, and Glenn Doerman for graphical assistance.

REFERENCES

1. American Cancer Society. Cancer facts and figures; 2008. Available at: www.cancer.org/downloads/STT/2008CAFFfinalsecured.pdf. Accessed May 5, 2010.
2. Hong DS, Angelo LS, Kurzrock R. Interleukin-6 and its receptor in cancer: implications for translational therapeutics. *Cancer* 2007;110:1911-28.
3. Taga T, Hibi M, Hirata Y, et al. Interleukin-6 triggers the association of its receptor with a possible signal transducer, gp130. *Cell* 1989;58:573-81.

4. Stahl N, Farruggella TJ, Boulton TG, Zhong Z, Darnell JE Jr, Yancopoulos GD. Choice of STATs and other substrates specified by modular tyrosine-based motifs in cytokine receptors. *Science* 1995;267:1349-53.

5. Yamanaka Y, Nakajima K, Fukada T, Hibi M, Hirano T. Differentiation and growth arrest signals are generated through the cytoplasmic region of gp130 that is essential for Stat3 activation. *EMBO J* 1996;15:1557-65.

6. Wegenka UM, Buschmann J, Luttkien C, Heinrich PC, Horn F. Acute-phase response factor, a nuclear factor binding to acute-phase response elements, is rapidly activated by interleukin-6 at the posttranslational level. *Mol Cell Biol* 1993;13:276-88.

7. Jones SA, Rose-John S. The role of soluble receptors in cytokine biology: the agonistic properties of the sIL-6R/IL-6 complex. *Biochim Biophys Acta* 2002;1592:251-63.

8. Mackiewicz A, Schooltink H, Heinrich PC, Rose-John S. Complex of soluble human IL-6-receptor/IL-6 up-regulates expression of acute-phase proteins. *J Immunol* 1992;149:2021-7.

9. Jones SA, Richards PJ, Scheller J, Rose-John S. Review: IL-6 transsignaling: the in vivo consequences. *J Interferon Cytokine Res* 2005;25:241-53.

10. Becker C, Fantini MC, Schramm C, et al. TGF-beta suppresses tumor progression in colon cancer by inhibition of IL-6 trans-signaling. *Immunity* 2004;21:491-501.

11. Nowell MA, Richards PJ, Horiuchi S, et al. Soluble IL-6 receptor governs IL-6 activity in experimental arthritis: blockade of arthritis severity by soluble glycoprotein 130. *J Immunol* 2003;171:3202-9.

12. Rabe B, Chalaris A, May U, et al. Transgenic blockade of Interleukin-6-trans-signaling abrogates inflammation. *Blood* 2008;111:1021-8.

13. Horiuchi S, Koyanagi Y, Zhou Y, et al. Soluble interleukin-6 receptors released from T cell or granulocyte/macrophage cell lines and human peripheral blood mononuclear cells are generated through an alternative splicing mechanism. *Eur J Immunol* 1994;24:1945-8.

14. Mullberg J, Schooltink H, Stoyan T, Heinrich PC, Rose-John S. Protein kinase C activity is rate limiting for shedding of the interleukin-6 receptor. *Biochem Biophys Res Commun* 1992;189:794-800.

15. Thabard W, Barille S, Collette M, et al. Myeloma cells release soluble interleukin-6R-alpha in relation to disease progression by two distinct mechanisms: alternative splicing and proteolytic cleavage. *Clin Cancer Res* 1999;5:2693-7.

16. Lust JA, Jelinek DF, Donovan KA, et al. Sequence, expression and function of an mRNA encoding a soluble form of the human interleukin-6 receptor (sIL-6R). *Curr Top Microbiol Immunol* 1995;194:199-206.

17. Jones SA, Novick D, Horiuchi S, Yamamoto N, Szalai AJ, Fuller GM. C-reactive protein: a physiological activator of interleukin 6 receptor shedding. *J Exp Med* 1999;189:599-604.

18. Marin V, Montero-Julian F, Gres S, Bongrand P, Farnarier C, Kaplanski G. Chemotactic

agents induce IL-6R-alpha shedding from polymorphonuclear cells: involvement of a metalloproteinase of the TNF-alpha-converting enzyme (TACE) type. *Eur J Immunol* 2002;32:2965-70.

19. Matthews V, Schuster B, Schutze S, et al. Cellular cholesterol depletion triggers shedding of the human interleukin-6 receptor by ADAM10 and ADAM17 (TACE). *J Biol Chem* 2003;278:38829-39.

20. Coles B, Fielding CA, Rose-John S, Scheller J, Jones SA, O'Donnell VB. Classic interleukin-6 receptor signaling and interleukin-6 trans-signaling differentially control angiotensin II-dependent hypertension, cardiac signal transducer and activator of transcription-3 activation, and vascular hypertrophy in vivo. *Am J Pathol* 2007;171:315-25.

21. Moradi MM, Carson LF, Weinberg B, Haney AF, Twiggs LB, Ramakrishnan S. Serum and ascitic fluid levels of interleukin-1, interleukin-6, and tumor necrosis factor-alpha in patients with ovarian epithelial cancer. *Cancer* 1993;72:2433-40.

22. Plante M, Rubin SC, Wong GY, Federici MG, Finstad CL, Gastl GA. Interleukin-6 level in serum and ascites as a prognostic factor in patients with epithelial ovarian cancer. *Cancer* 1994;73:1882-8.

23. Scambia G, Testa U, Benedetti Panici P, et al. Prognostic significance of interleukin 6 se-

rum levels in patients with ovarian cancer. *Br J Cancer* 1995;71:354-6.

24. Duan Z, Foster R, Bell DA, et al. Signal transducers and activators of transcription 3 pathway activation in drug-resistant ovarian cancer. *Clin Cancer Res* 2006;12:5055-63.

25. Penson RT, Kronish K, Duan Z, et al. Cytokines IL-1beta, IL-2, IL-6, IL-8, MCP-1, GM-CSF and TNF-alpha in patients with epithelial ovarian cancer and their relationship to treatment with paclitaxel. *Int J Gynecol Cancer* 2000;10:33-41.

26. Kovacs E. Investigation of interleukin-6 (IL-6), soluble IL-6 receptor (sIL-6R) and soluble gp130 (sgp130) in sera of cancer patients. *Biomed Pharmacother* 2001;55:391-6.

27. Robinson-Smith TM, Isaacsohn I, Mercer CA, et al. Macrophages mediate inflammation-enhanced metastasis of ovarian tumors in mice. *Cancer Res* 2007;67:5708-16.

28. Drew AF, Blick TJ, Lafleur MA, et al. Correlation of tumor- and stromal-derived MT1-MMP expression with progression of human ovarian tumors in SCID mice. *Gynecol Oncol* 2004;95:437-48.

29. Nilsson MB, Langley RR, Fidler IJ. Interleukin-6, secreted by human ovarian carcinoma cells, is a potent proangiogenic cytokine. *Cancer Res* 2005;65:10794-800.

30. Silver DL, Naora H, Liu J, Cheng W, Montell DJ. Activated signal transducer and activator of transcription (STAT) 3: localization in focal ad-

hesions and function in ovarian cancer cell motility. *Cancer Res* 2004;64:3550-8.

31. Syed V, Ullinski G, Mok SC, Ho SM. Reproductive hormone-induced, STAT3-mediated interleukin 6 action in normal and malignant human ovarian surface epithelial cells. *J Natl Cancer Inst* 2002;94:617-29.

32. Jones SA, Horiuchi S, Novick D, Yamamoto N, Fuller GM. Shedding of the soluble IL-6 receptor is triggered by Ca²⁺ mobilization, while basal release is predominantly the product of differential mRNA splicing in THP-1 cells. *Eur J Immunol* 1998;28:3514-22.

33. Mantovani A, Polentarutti N, Peri G, et al. Cytotoxicity on tumor cells of peripheral blood monocytes and tumor-associated macrophages in patients with ascites ovarian tumors. *J Natl Cancer Inst* 1980;64:1307-15.

34. Haskill S, Becker S, Fowler W, Walton L. Mononuclear-cell infiltration in ovarian cancer. I. Inflammatory-cell infiltrates from tumour and ascites material. *Br J Cancer* 1982;45:728-36.

35. Melichar B, Savary CA, Patenia R, Templin S, Melicharova K, Freedman RS. Phenotype and antitumor activity of ascitic fluid monocytes in patients with ovarian carcinoma. *Int J Gynecol Cancer* 2003;13:435-43.

36. Chalaris A, Rabe B, Paliga K, et al. Apoptosis is a natural stimulus of IL6R shedding and contributes to the proinflammatory trans-signaling function of neutrophils. *Blood* 2007;110:1748-55.

Differences in Wound Healing in Mice with Deficiency of IL-6 versus IL-6 Receptor

Molly M. McFarland-Mancini,^{*,1} Holly M. Funk,^{*,1} Andrew M. Paluch,^{*} Mingfu Zhou,^{*} Premkumar Vummidi Giridhar,^{*} Carol A. Mercer,[†] Sara C. Kozma,^{*} and Angela F. Drew^{*}

IL-6 modulates immune responses and is essential for timely wound healing. As the functions mediated by IL-6 require binding to its specific receptor, IL-6R α , it was expected that mice lacking IL-6R α would have the same phenotype as IL-6-deficient mice. However, although IL-6R α -deficient mice share many of the inflammatory deficits seen in IL-6-deficient mice, they do not display the delay in wound healing. Surprisingly, mice with a combined deficit of IL-6 and IL-6R α , or IL-6-deficient mice treated with an IL-6R α -blocking Ab, showed improved wound healing relative to mice with IL-6 deficiency, indicating that the absence of the receptor contributed to the restoration of timely wound healing, rather than promiscuity of IL-6 with an alternate receptor. Wounds in mice lacking IL-6 showed delays in macrophage infiltration, fibrin clearance, and wound contraction that were not seen in mice lacking IL-6R α alone and were greatly reduced in mice with a combined deficit of IL-6 and IL-6R α . MAPK activation-loop phosphorylation was elevated in wounds of IL-6R α -deficient mice, and treatment of wounds in these mice with the MEK inhibitor U0126 resulted in a delay in wound healing suggesting that aberrant ERK activation may contribute to improved healing. These findings underscore a deeper complexity for IL-6R α function in inflammation than has been recognized previously. *The Journal of Immunology*, 2010, 184: 7219–7228.

Interleukin 6 is a pleiotropic cytokine with roles in generating acute phase responses, inflammation, and lymphocyte differentiation. Numerous cell types produce IL-6, especially at sites of inflammation. IL-6 functions are mediated by binding to its specific receptor, IL-6R α (gp80 and CD126). IL-6R α is the only known receptor for IL-6, and its expression is predominantly restricted to hepatocytes and immune cells. Recently, ciliary neurotrophic factor (CNTF) and IL-27, two other members of the IL-6 family, have been demonstrated to bind IL-6R α in vitro but with lower affinity than IL-6, and thus, the in vivo relevance of these findings remains unclear (1, 2). IL-6 engagement of IL-6R α induces homodimerization of the ubiquitously expressed, common IL-6 family signaling receptor gp130 (IL-6 signaling transducer). Mammalian IL-6, however, cannot directly engage gp130 in the absence of IL-6R α (3).

IL-6R α contains an extracellular Ig-like domain, a cytokine receptor homology module, a transmembrane domain, and a non-signaling intracellular domain. The cytokine receptor homology module is made up of two fibronectin type III domains and is

responsible for recognition and binding of IL-6 and gp130 (reviewed in Ref. 4). Typical for a cytokine receptor, IL-6R α does not possess kinase activity. Ligand-bound IL-6R α induces dimerization of gp130 (5). The Janus family kinases, JAK1, JAK2, and TYK2, are constitutively associated with the cytoplasmic tail of gp130 and phosphorylate gp130 dimers (6, 7). The transcription factors Stat3 and, to a lesser extent, Stat1 dock at any of four C-terminal tyrosines on gp130 (8, 9). JAKs phosphorylate the Stat proteins inducing Stat dimerization, translocation to the nucleus, and transcription of genes with IL-6-responsive elements (10). IL-6-induced Stat3 activation is negatively regulated by suppressor of cytokine signaling 3 and Src homology region 2 domain-containing phosphatase 2 binding to a membrane-proximal gp130 phospho-tyrosine residue (Y759), resulting in Ras activation and ERK signaling (11–13). Both Stat3 and Erk activation result in cell proliferation, survival, differentiation, and inflammation, and both are frequently upregulated in tumors.

IL-6 signaling can also occur through a soluble form of the receptor that can bind IL-6 and subsequently induce gp130 dimerization (3). This process is known as trans-signaling and allows cells that do not express IL-6R α to respond to IL-6 (14). Soluble forms of IL-6R α occur as the result of either of two distinct processes: alternative splicing or proteolytic cleavage (15–17). The importance of each isoform in physiologic processes is not clearly understood. It is known from mice overexpressing human soluble IL-6R α that the soluble isoform plays a role in sensitizing cells to IL-6 signaling and prolonging IL-6 half-life (18). Inhibition of the soluble form of IL-6R α in vivo is sufficient to block many of the known functions of IL-6 signaling, such as modulation of the inflammatory response (19, 20). Neutrophil infiltration and apoptosis are early events in the inflammatory response that trigger IL-6R α shedding and subsequent monocyte infiltration (19–22). Despite high expression of membrane-bound IL-6R α , human osteoblasts are unable to respond to IL-6 unless the receptor is cleaved to produce the soluble form (23). It has not

^{*}Department of Cancer and Cell Biology, Vontz Center for Molecular Studies, University of Cincinnati, Cincinnati, OH 45267; and [†]PDS Biotechnology, Lawrenceburg, IN 47025

¹M.M.M.-M. and H.M.F. contributed equally to this work.

Received for publication June 18, 2009. Accepted for publication April 15, 2010.

This work was supported by a grant from the American Cancer Society (RSG-06-141-01; to A.F.D.) and the Department of the Army, Department of Defense Ovarian Cancer Research Program (OC080273; to A.F.D.).

Address correspondence and reprint requests to Dr. Angela F. Drew, Department of Cancer and Cell Biology, Vontz Center for Molecular Studies, University of Cincinnati, 3125 Eden Avenue, Cincinnati, OH 45267-0521. E-mail address: adrew41@gmail.com

Abbreviations used in this paper: Arg1, arginase 1; CNTF, ciliary neurotrophic factor; DIG, digoxigenin; ES, embryonic stem; fbg, fibrinogen; s, soluble; SAA, serum amyloid A; WT, wild-type.

Copyright © 2010 by The American Association of Immunologists, Inc. 0022-1767/10/\$16.00

been well established whether any nonredundant function exists for the membrane-bound form of IL-6R α .

IL-6-deficient (*Il6*^{-/-}) mice were generated ~15 y ago (24, 25). Their multiple phenotypic abnormalities are not surprising, because of the pleiotropic functions ascribed to IL-6. Although *Il6*^{-/-} mice have no apparent developmental abnormalities, they have an impaired capacity to mount immune responses to several pathogens and to generate acute-phase responses (24). In addition, they have reduced capacity for liver regeneration and develop age-related obesity (26, 27). *Il6*^{-/-} mice display resistance to experimental autoimmune conditions, such as encephalitis, and protection against bone loss after ovariectomy (25, 28). Studies using experimental tumor models in *Il6*^{-/-} mice have reported both tumor-protective and tumor-promoting effects for IL-6, depending on the tumor model used (29–31). A better understanding of the functions of IL-6 and its receptor in different contexts may provide opportunities for more effective manipulation of IL-6 signaling in the treatment of inflammation and cancer.

Il6^{-/-} mice display significant defects in wound healing. Wound healing is a tightly regulated process in which platelets and fibrin immediately fill the wound bed with an insoluble clot, and significant neutrophil immigration occurs shortly thereafter (reviewed in Ref. 32). Re-epithelialization proceeds by adjacent keratinocyte proliferation and migration over the wound area. Neutrophils in wounds are important for microbe neutralization, but their absence from sterile wounds does not delay healing (33, 34). Monocyte/macrophages are subsequently recruited and play roles in the clearance of debris and the provision of growth and angiogenic factors. Macrophages in wounds typically express markers indicating alternate activation pathways with functions in tissue remodeling and angiogenesis, rather than classically activated macrophages that function to kill pathogens. Wounds in mice with inhibited macrophage function display excess fibrin and cellular debris and heal more slowly than those in untreated mice (35). Wound healing is delayed in *Il6*^{-/-} mice as a result of impaired re-epithelialization, angiogenesis, and macrophage infiltration (36, 37).

In this paper, we report on mice with complete and conditional deficiencies of IL-6R α , which were generated to better understand the relationship between soluble and membrane-bound receptor and to identify any phenotypic discrepancies that may exist, as compared with *Il6*^{-/-} mice. Although IL-6 and IL-6R α are believed to be exclusive and essential components of IL-6 signaling in vivo, we report both similarities and differences between the phenotypes of *Il6*^{-/-} and *Il6ra*^{-/-} mice. These studies indicate an unanticipated compensatory improvement in wound healing in *Il6ra*^{-/-} mice but not in *Il6*^{-/-} mice, which suggests a greater complexity in IL-6R α function than was previously appreciated.

Materials and Methods

Generation of *Il6ra*-knockout mice

Il6ra-deficient mice were generated by the insertion of a targeting vector into the *IL-6ra* genomic locus. The targeting vector included the selection cassette loxP-frt-pMC1neoA-frt in which the neo gene is flanked by frt sites. Murine *IL-6ra* exons 4, 5, and 6 were inserted between the loxP sequences. The construct was introduced into embryonic stem (ES) cells on a C57BL/6 background for homologous recombination. To prevent changes in the level of gene expression in mice carrying the floxed allele, the resulting loxP sites of the recombined allele were located in nonconserved intronic sequences known to share no sequence conservation between mouse and human and to be devoid of transcription factor binding sites. Recombined ES cell clones were identified by PCR, and a successful single insertion was confirmed by Southern blot analysis. Blastocysts containing ES cells with the floxed allele were implanted, and germline mice were bred with EIIa-cre mice on a C57BL/6 background, resulting in the deletion of *IL-6ra* exons 4, 5, and 6 (the cytokine receptor binding module) and the Neo cassette. Further breeding with C57BL/6 mice was

carried out to remove the Cre construct, and mice were then bred to homozygosity for the deleted *IL-6ra* allele. Genotypes were confirmed by PCR analysis and Southern blotting. Studies included in this paper have been reviewed and approved by the University of Cincinnati Institutional Animal Care and Use Committee.

Southern blot analysis

Genomic DNA was prepared by phenol/chloroform extraction and digested overnight with restriction enzymes. Samples were loaded onto a 0.8% agarose gel in tris-acetate EDTA buffer and electrophoresed. The gel was stained with ethidium bromide for 10 min in tris-acetate EDTA buffer, imaged by UV, and then transferred overnight in 20 \times SSC onto a positively charged nylon membrane (Roche, Basel, Switzerland). Digoxigenin (DIG)-labeled probes were prepared using the PCR DIG Probe Synthesis Kit (Roche), according to the manufacturer's instructions. The membrane was hybridized with 50 ng/ml DIG-labeled probe, followed by chemiluminescent detection with anti-DIG alkaline phosphatase Ab and CSPD substrate.

Generation and maintenance of mice with conditional expression of *IL-6Ra*

Mice with a floxed allele of *IL-6ra* (*Il6ra*^{fl/+}) were first crossed with FLPe^{+/+} mice (38) to delete the FRT-flanked Neo cassette in the targeting vector. Progeny with successful excision of Neo, as determined by PCR, were crossed with mice expressing Cre recombinase under the control of the albumin promoter (AlbCre⁺) (39) or the lysozyme M promoter (LysM-Cre⁺) (40). Progeny lacking the FLPe allele were selected for further breeding. *Il6ra*^{fl/fl}/AlbCre^{+/+} mice were maintained as homozygotes for both alleles. *Il6ra*^{fl/fl}/LysMCre^{+/+} mice used in experiments were bred from colonies of *Il6ra*^{fl/fl} and *Il6ra*^{fl/fl}/LysMCre^{+/+} mice. All mouse strains were on a C57BL/6 background.

Genotyping

DNA from ear clippings was isolated by using the SYBR Green Extract-N-Amp Tissue PCR kit (Sigma-Aldrich, St. Louis, MO). Primers for the wild-type (WT) *IL-6ra* allele (5'-CTGGGACCCGAGTTACTACTT-3' and 5'-CAGCAACACCGTGAACCTCTT-3'), the floxed *IL-6ra* allele (5'-GCCTGGGTGGAGAGGCTTTTT-3' and 5'-CCCAGTGAGCTCCACCATCAA-3'), and the excised *IL-6ra* allele (5'-CTGGGACAGGGAAGGCTTTT-3' and 5'-CCCAGTGAGCTCCACCATCAA-3') were used in real-time PCR analysis. AlbCre, LysMCre, and FLPe mice were genotyped as per protocols from their originating laboratories (JAX Mice Database, The Jackson Laboratory, Bar Harbor, ME).

Harvesting of normal and inflammatory-challenged tissues

Spleen, liver, and lung tissues were collected from euthanized mice for analysis. Plasma was prepared from EDTA-treated blood collected from the retro-orbital plexus. Hepatocytes were prepared from anesthetized mice by *in situ* liver perfusion and Percoll gradient separation, as described previously (41). Thioglycolate-elicited macrophages and granulocytes were collected by peritoneal lavage 24 or 48 h after *i.p.* injection of 3% thioglycolate broth. Cells were incubated on plastic for 1 h to enrich for adherent macrophages. Acute-phase responses were assessed in plasma and livers collected from mice given a *s.c.* injection of 100 μ l turpentine at various intervals prior to sacrifice.

Air-pouch experiments were performed as described previously (20). Briefly, mice were injected *s.c.* in the center of the back with 6 and 4 ml sterile air at days -6 and -3, respectively, to create an air pouch. Inflammation was elicited at day 0 by injecting 1 ml 1% carrageenan (Sigma-Aldrich) in PBS into the air pouch. Lavage was performed at days 3 and 7 after carrageenan administration. Lavage fluid was spun onto slides with a cytospin (Thermo Shandon, Pittsburgh, PA) and stained with Kwik-Diff (Thermo Shandon). Differential cell counts were performed by a hematologist (C.A.M.) on three to four microscope fields per sample.

Full-thickness excisional wounds were prepared on shaved dorsal skin by 4-mm-punch biopsy (small wounds; Acuderm, Fort Lauderdale, FL) or with a fine-scissor cutting around a 1-cm² template (large wounds). Mice were housed individually, and wounds were left undressed. Wounds were photographed and examined daily, and the percentage of wound closure was assessed as the size of the remaining wound area relative to the original template. Wounds were collected after 1, 2, 5, 8, and 11 d for analysis. For MEK inhibition, wounds were treated daily with topical U0126 (10 μ g dissolved in 25 μ l DMSO; Selleck Chemicals, Houston, TX) or vehicle alone. In other experiments, mice were given daily peritoneal injections of Abs specific for mouse IL-6R α (500 μ g/mouse; BioExpress, West Lebanon, NH), mouse gp130 (7.5 μ g/mouse; eBioscience, San Diego, CA), mouse IL-27/p28 (37 μ g/mouse; Shenandoah Biotech, Warwick, PA), or rat IgG (Sigma-Aldrich) diluted to a similar concentration in PBS.

Real-time PCR analysis

RNA from WT and *Il6ra*^{-/-} mice was isolated using the Nucleospin II Kit (Macherey-Nagel, Bethlehem, PA). One microgram of mRNA was reverse transcribed with the ThermoScript II Kit (Invitrogen, Carlsbad, CA). Twenty nanograms of cDNA was used for subsequent PCR analysis. Quantitative PCR was performed using the Realplex Mastercycler (Eppendorf) and the following primers: L32 (*Rpl32*) 5'-CTTAGAGGACACGTTGTGAGCAATC-3' and 5'-GCTGTGCTGCTCTTCTACAATGGCTTTT-3'; haptoglobin, 5'-TATGGATGCCAAAGGCAGCTTCC-3' and 5'-TCGCTGTGTTTCAGGAAGAGGTTT-3'; serum amyloid A (SAA), 5'-AGAGGACATGAGGACACCATTTGCT-3' and 5'-AGGACGCTCAGTATTGTCAGGCA-3'; and fibrinogen, 5'-GATGAACAAATGTACGCAGGCCA-3' and 5'-GCCCAAATAATGCCGTCGTCGAAA-3'. Each analysis was repeated at least twice to ensure reproducibility. To ensure specificity, real-time melt curves were analyzed, and band sizes were checked on agarose gels. Values were normalized against murine L32, housekeeping gene.

Western blotting and ELISA

Protein lysates were prepared from liver and spleen tissue and quantified by protein assay (Bio-Rad DC; Bio-Rad, Hercules, CA) for Western blotting. Reduced samples were electrophoresed on 8% polyacrylamide gels and transferred to polyvinylidene difluoride membranes (Millipore, Bedford, MA). Membranes were blocked in 5% milk for 1 h. Primary Ab dilutions were applied at 4°C overnight at the following dilutions: rabbit anti-mouse IL-6Rα IgG (1/400; Santa Cruz Biotechnology, Santa Cruz, CA), rabbit anti-β-actin (1/1000; Cell Signaling Technology, Beverly, MA), phospho-Stat3 (1/800, Ser⁷²⁷; Cell Signaling Technology), Stat3 (1/1000, C-20; Santa Cruz Biotechnology), phospho-p44/42 MAPK, ERK1/2, and p44/42 MAPK (1/1000, numbers 4370 and 4695; Cell Signaling Technology). Primary Abs were detected with donkey anti-rabbit IgG-HRP (1/10,000; Novus Biologicals, Littleton, CO) and luminol (ECL Plus; PerkinElmer, Wellesley, MA). ELISAs were used to detect murine soluble IL-6Rα (R&D Systems, Minneapolis, MN) and SAA (Invitrogen) in EDTA-treated plasma.

Histology and immunohistochemistry

Wound tissues were collected into Glyofix fixative (Thermo Shandon) at necropsy and processed into paraffin. A separate group of wounds was fixed in zinc fixative (BD Biosciences, San Jose, CA) for CD31 immunostaining. 4 μm sections were prepared and routinely stained with H&E. Re-epithelialization was assessed by measuring the percentage of the wound area covered with keratinocytes. Immunohistochemistry was performed on dewaxed tissues after Ag retrieval by heating in citrate buffer or EDTA (F4/80). Sections were blocked with 10% serum, 5% BSA in TBS. Primary Abs were used at the following dilutions: F4/80 (1/400; eBioscience), CD31 (BD Biosciences), fibrinogen [1/1000 (42)], and arginase I (1/100; BD Biosciences). Arginase staining was performed with the Mouse-on-Mouse Blocking kit (Vector Laboratories, Burlingame, CA). Endogenous peroxidase was blocked prior to adding biotinylated secondary Abs (1/200; Vector Laboratories). ABC Elite kit (Vector Laboratories) and diaminobenzidine (Sigma-Aldrich), VectorRed (Vector Laboratories), or Fast Red (Sigma-Aldrich) substrates were used. Morphometry was performed by investigators unaware of the genotypes of the mice. Vascular density was assessed by counting luminal structures in three high-power fields per wound. Macrophages were quantified by measuring the percentage of two randomly selected high-power fields within the wound area that were positive for the substrate (VectorRed) above a predetermined threshold (ImageJ software). Fibrin staining was assessed by a pathologist unaware of the mouse genotypes.

Statistics

Statistics were performed by the Mann-Whitney *U* test for pairwise comparisons or the Kruskal-Wallis test for multiple comparisons. Data are expressed as average ± SEM.

Results

Generation of *Il6ra*^{-/-} mice

Mice with a floxed allele of *IL-6ra* (*Il6ra*^{fl/+}) were generated by homologous recombination with a vector containing LoxP sites around exons 4–6 and a neomycin cassette (Fig. 1A). *Il6ra*^{fl/+} mice were crossed with EIIa-Cre mice, and the offspring were interbred to obtain mice with a complete deficiency of IL-6Rα (EIIa-Cre^{+/-}/IL-6Rα^{-/-}) (Fig. 1A). Southern blotting indicated an absence of the WT 11-kb genomic DNA fragment and the presence of the

predicted 9-kb excised allele in mice homozygous for the floxed allele (Fig. 1B). Subsequent breeding to remove the Cre-recombinase gene was performed. The absence of mRNA for *IL-6ra* was determined by real-time PCR on liver and lung tissue (Fig. 1C). IL-6Rα protein was absent from liver and spleen lysates prepared from *Il6ra*^{-/-} mice and present in WT (*Il6ra*^{+/+}) and heterozygous (*Il6ra*^{+/-}) mice (Fig. 1D). Similarly, soluble IL-6Rα was abundant in *Il6ra*^{+/+} and *Il6ra*^{+/-} mice and undetectable in *Il6ra*^{-/-} mice (Fig. 1E). Although the presence of a truncated IL-6Rα protein in *Il6ra*^{-/-} mice cannot be formally excluded, such a product is unlikely because of 1) the presence of an incomplete domain, 2) unpaired cysteine residues because of the deletion of the cytokine homology domain, and 3) the inability of a polyclonal Ab raised against the entire extracellular domain of IL-6Rα to recognize any product in null mice while detecting abundant product in WT mice. *Il6ra*^{-/-} mice were normal in appearance and were born in the expected Mendelian ratio.

Il6ra^{-/-} mice have a defective response to IL-6

IL-6 is critical for the acute-phase response to s.c. injected turpentine (43, 44). To assess the response of *Il6ra*^{-/-} mice, groups of mice were s.c. injected with turpentine. Hepatic production of the acute-phase reactants fibrinogen, haptoglobin, and SAA was markedly diminished or absent in *Il6ra*^{-/-} mice, as assessed by real-time PCR (Fig. 2A) and by ELISA for SAA (Fig. 2B). Similar results were obtained in *Il6*^{-/-} mice (Fig. 2A, 2B), as reported previously (43). Thus, IL-6 signaling function is abrogated in *Il6ra*^{-/-} mice in the context of generating an acute-phase response.

IL-6 has been shown to be important in the progression of inflammatory responses from a neutrophil-dominant phase to a macrophage-dominant phase (21). To determine whether this is also the case in *Il6ra*^{-/-} mice, we created s.c. air pouches in mice and injected carrageenan as described previously (20). Although the proportion of neutrophils and macrophages in the pouch fluid was not different between the groups 3 d after carrageenan administration, neutrophil resolution was impaired after 7 d (Fig. 2C), and macrophage infiltration was delayed (Fig. 2D) in both *Il6*^{-/-} and *Il6ra*^{-/-} mice. Given that IL-6Rα is believed to be the exclusive binding partner required to facilitate the interaction with the common IL-6 family receptor gp130, it was not surprising to find that deficiencies of either IL-6 or IL-6Rα induced the same phenotypic abnormalities compared with WT mice.

Hepatocyte production of IL-6Rα is critical for the acute-phase response but myeloid cells secrete most of the circulating IL-6Rα

IL-6Rα expression has been reported to be predominantly restricted to hepatocytes and immune cells. To elucidate the importance of each compartment in IL-6Rα-dependent processes, we generated mice with conditional deficiency of IL-6Rα in either hepatocytes or lysozyme M-expressing cells (macrophages and granulocytes) by crossing *Il6ra*^{fl/fl} mice with mice expressing Cre recombinase under the control of the albumin (AlbCre) or lysozyme M (LysMCre) promoters, respectively. Significant reduction in IL-6Rα expression was observed in hepatocytes of AlbCre^{+/-}/*Il6ra*^{fl/fl} mice (Fig. 3A) and in thioglycolate-elicited macrophages of LysMCre^{+/-}/*Il6ra*^{fl/fl} mice (Fig. 3B). Interestingly, expression of soluble IL-6Rα in plasma was more dependent on immune cell secretion than on hepatic production, because LysMCre^{+/-}/*Il6ra*^{fl/fl} mice had lower levels of IL-6Rα levels (39.95% of WT) than AlbCre^{+/-}/*Il6ra*^{fl/fl} mice (67.95%) (Fig. 3C). No differences were seen between WT and *Il6ra*^{fl/fl} mice lacking Cre (data not shown). It is also noteworthy that macrophages, granulocytes, and hepatocytes together apparently account for almost all of the circulating IL-6Rα in unchallenged mice, because the sum of the proportional

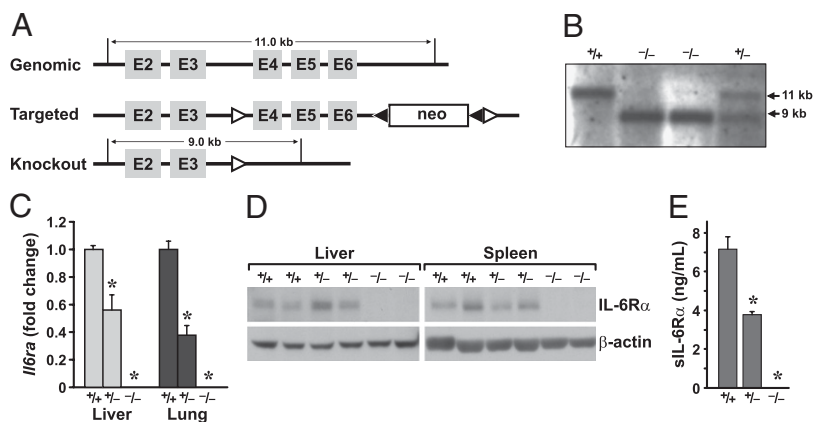


FIGURE 1. Generation of *IL-6ra*-deficient mice. *A*, Schematic depicting exons 2–6 of the genomic *IL-6ra* gene, the targeted construct containing LoxP sites (Δ) around exons 4–6 and a neo cassette, and the recombinant allele after Cre recombinase-mediated excision. *B*, Southern blot analysis of tail DNA from WT, homozygous, and heterozygous *IL-6ra*-targeted alleles, indicating expected band sizes of 11 kb (WT) and 9 kb (knockout). *C*, Real-time PCR with primers specific for exon 5 of murine *IL-6ra* indicating an absence of *IL-6ra* RNA in homozygous knockout mice. Data are expressed as fold change relative to WT mice. *D*, Western blot analysis of liver and spleen tissue collected from mice (two of each genotype) with WT, heterozygous, and homozygous alleles for IL-6R α . *E*, Absence of sIL-6R α in plasma of homozygous *Il6ra*^{-/-} mice ($n = 12$) but not in *Il6ra*^{+/+} ($n = 11$) or *Il6ra*^{+/-} mice ($n = 12$), as measured by ELISA. * $p < 0.05$. sIL-6R, soluble IL-6R.

deficits in circulating IL-6R α in AlbCre^{+/-}/*Il6ra*^{fl/fl} (30.6% deficit) and LysMCre^{+/-}/*Il6ra*^{fl/fl} (62.7% deficit) mice equaled 93.4% of the levels in WT mice. To determine the contributions of hepatocytes and immune cells to soluble IL-6R α during inflammatory challenge, plasma and livers were collected from mice subjected to turpentine injection or cutaneous wounding. Despite increased expression of mRNA for *IL-6ra* in livers of WT mice subjected to acute-phase protein induction (Ref. 45 and our own unpublished data), no increase in the expression of soluble IL-6R α was seen in mice challenged with turpentine or cutaneous wounding (Fig. 3C, 3D).

We next compared acute-phase reactants in mice with conditional expression of IL-6R α . As expected, generation of an acute-phase response was completely muted in AlbCre^{+/-}/*Il6ra*^{fl/fl} mice compared with WT or *Il6ra*^{fl/fl} mice (Fig. 3E, 3F). This is consistent with hepatocytes being the predominant cell type responsible for acute-phase responses. No significant difference was seen

between LysMCre^{+/-}/*Il6ra*^{fl/fl} mice and WT (Fig. 3E, 3F) or LysMCre^{-/-}/*Il6ra*^{fl/fl} mice (data not shown). Despite in vitro reports that soluble IL-6R α can enhance acute-phase protein expression in HepG2 cells (46), no hepatic acute-phase response was detected in AlbCre^{+/-}/*Il6ra*^{fl/fl} mice despite their having two-thirds of the WT expression of soluble IL-6R α (Fig. 3C, 3D). Apparently, membrane-bound IL-6R α is essential for the hepatic acute-phase response to IL-6.

The deficit in wound healing is not as severe in *Il6ra*^{-/-} mice as in *Il6*^{-/-} mice

It has previously been reported that wound healing is markedly delayed in *Il6*^{-/-} mice (36, 37). We generated full-thickness small and large excision wounds to determine whether IL-6R α ^{-/-} mice shared a similar phenotype. To our surprise, we found that *Il6ra*^{-/-} mice did not share the same dramatic delay in wound healing seen

FIGURE 2. *Il6ra*^{-/-} and *Il6*^{-/-} mice share a functional deficit in IL-6 signaling. A dramatic reduction in acute-phase protein production in response to turpentine challenge was seen in *Il6ra*^{-/-} and *Il6*^{-/-} mice by real-time RT-PCR of liver RNA (*A*) and SAA ELISA of plasma (*B*). *C* and *D*, Differential counts were performed on Kwik-diff–stained cells withdrawn from a sterile inflammatory air pouch lesion induced by carrageenan. Resolution of neutrophils (*C*) and increased influx of monocyte/macrophages (*D*) occurs in WT mice by day 7 but are delayed in *Il6*^{-/-} and *Il6ra*^{-/-} mice. Data are expressed as a percentage of total cells.

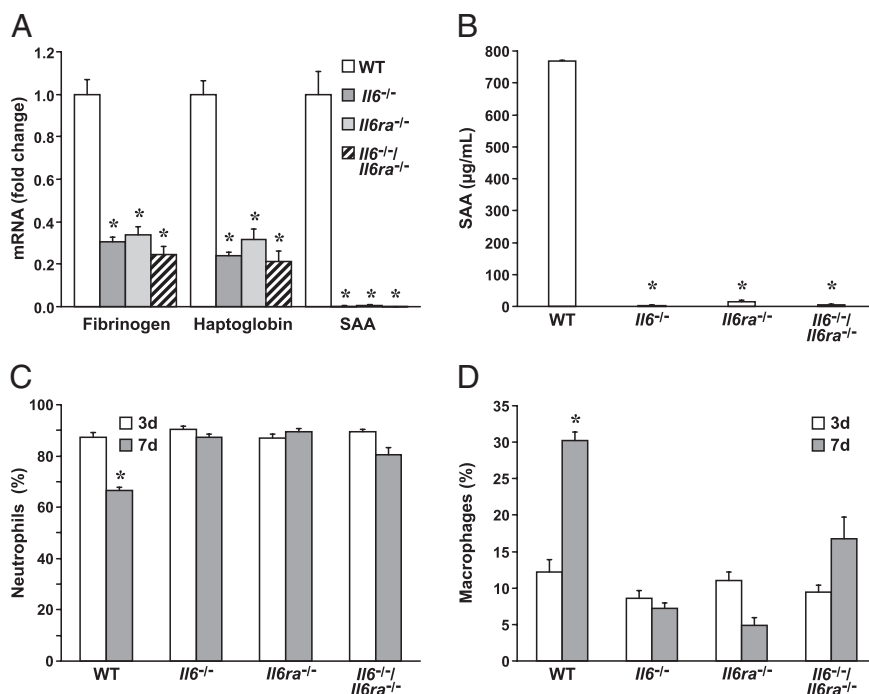
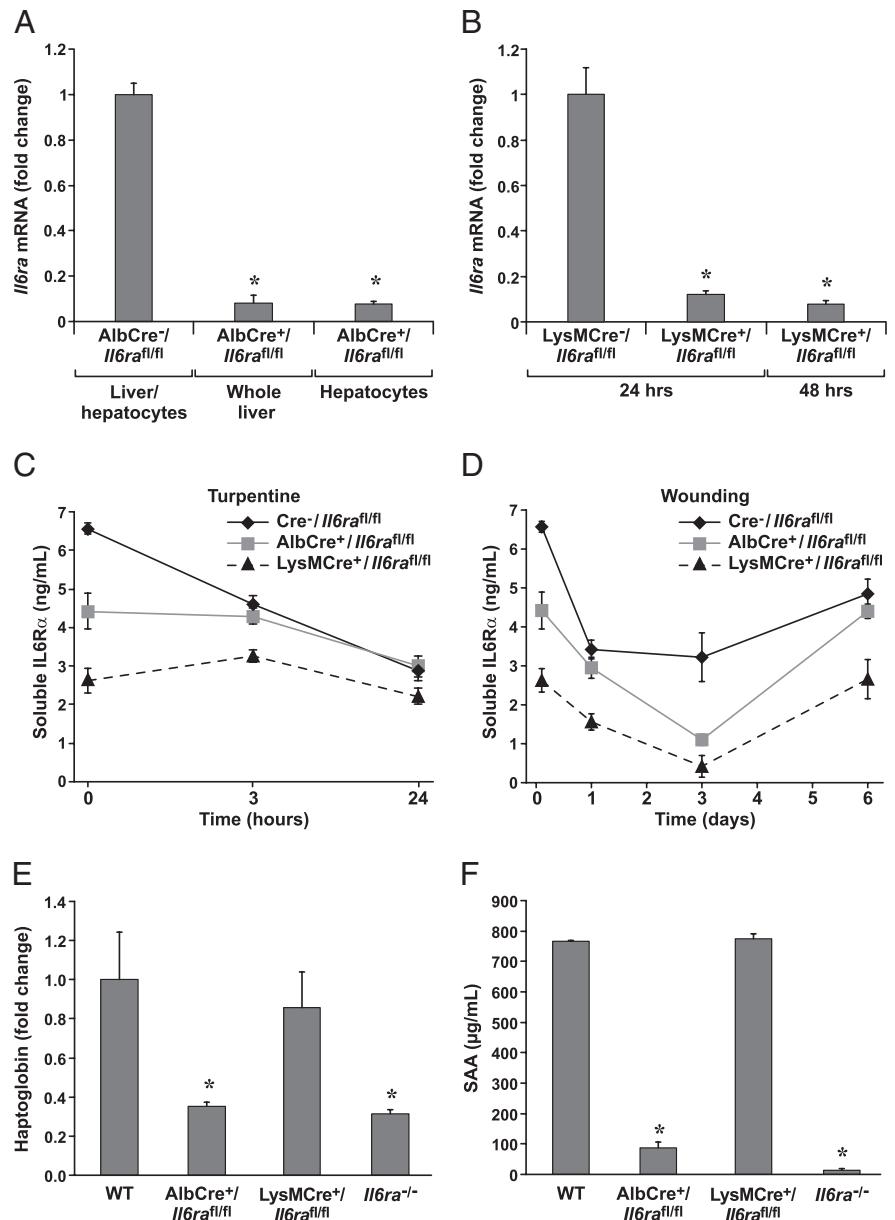


FIGURE 3. Macrophages, neutrophils, and hepatocytes make a significant contribution to circulating levels of soluble IL-6R α and to acute-phase responses. Knockdown of IL-6R α was confirmed by RT-PCR in *Il6ra*^{fl/fl} mice bred with mice expressing Cre recombinase under the control of the albumin promoter (A) or the lysozyme M promoter (B), as compared with *Il6ra*^{fl/fl} mice lacking Cre expression. Isolated hepatocytes and whole-liver homogenates were used to test for *IL-6ra* mRNA expression in AlbCre^{+/+}*Il6ra*^{-/-} mice. Thioglycolate-elicited peritoneal cells were collected from LysMCre^{+/+}*Il6ra*^{-/-} mice after 24 and 48 h and enriched for macrophages by adherence to plastic. C and D, Expression of soluble IL-6R α was reduced in plasma of mice with Cre-mediated deletion of *IL-6ra* (time 0) and further diminished, proportionately, after challenge with turpentine (C) or by cutaneous wounding (D). E and F, Acute phase reactions following turpentine challenge were diminished in mice lacking *IL-6ra* in hepatocytes but not in granulocytes, as assessed by mRNA for hepatic haptoglobin (E) and plasma SAA protein (F). **p* < 0.05; ***p* < 0.0001.



in *Il6*^{-/-} mice. Instead, *Il6ra*^{-/-} mice with large excision wounds healed almost as well as WT mice upon gross examination (Fig. 4A). *Il6*^{-/-} mice exhibited reduced wound closure rates and frequently had open wounds for several days longer than WT or *Il6ra*^{-/-} mice (Fig. 5A). Differences in small biopsy punch wounds (4 mm in diameter) were subtle, as wounds healed rapidly (data not shown). However, large wounds of *Il6*^{-/-} mice frequently became expanded beyond the boundaries of the original wound (Fig. 4A), presumably by scratching or dragging of the wound with the mouse's limbs. This assumption was made because the extended edge of the wound was always on the caudal edge, which is more accessible to the legs of mice, and because this action was occasionally observed. Ulcers generated from this activity were seen in only one WT mouse (1 of 12 mice; 8%) with resolution within 24 h. *Il6*^{-/-} mice all developed ulcers (12 of 12 mice, 100%), which had not healed at 8 d but were healing in some mice by the 11th day. Only 2 of 11 *Il6ra*^{-/-} mice (18%) developed ulcers adjacent to the wound area, and both were resolved within 24 h. Whether the formation of these ulcers was prompted by prolonged irritation from an open wound,

psychological/stress-induced defects in *Il6*^{-/-} mice (47), or phenotypic defects in wound contraction was not determined.

Histological evaluation of the wound was performed to quantify differences in the multiple processes involved in successful wound healing. Re-epithelialization was markedly delayed in both *Il6*^{-/-} and *Il6ra*^{-/-} mice compared with WT mice in both large (Figs. 4B, 5C) and small wounds (Fig. 5D). Separate experiments performed in mice with conditional expression of IL-6R α indicated that hepatic expression of IL-6R α was more important for re-epithelialization than that of myeloid cells (Fig. 5E). Delayed re-epithelialization in *Il6ra*^{-/-} mice was an unexpected finding because macroscopic wound closure rates were similar to WT mice. Instead, wound contraction rates were similar in WT and *Il6ra*^{-/-} mice but delayed in *Il6*^{-/-} mice, accounting for the macroscopic observation of a smaller defect in *Il6ra*^{-/-} mice than in *Il6*^{-/-} mice (Fig. 5A, 5B). Deficits in the formation of granulation tissue were seen in both *Il6*^{-/-} and *Il6ra*^{-/-} mice but were more pronounced in *Il6*^{-/-} mice. Deficits included delays in macrophage infiltration (Fig. 4C, 4D), fibrin clearance (Fig. 4E), and vascularization (Fig. 4F). These deficits have previously been

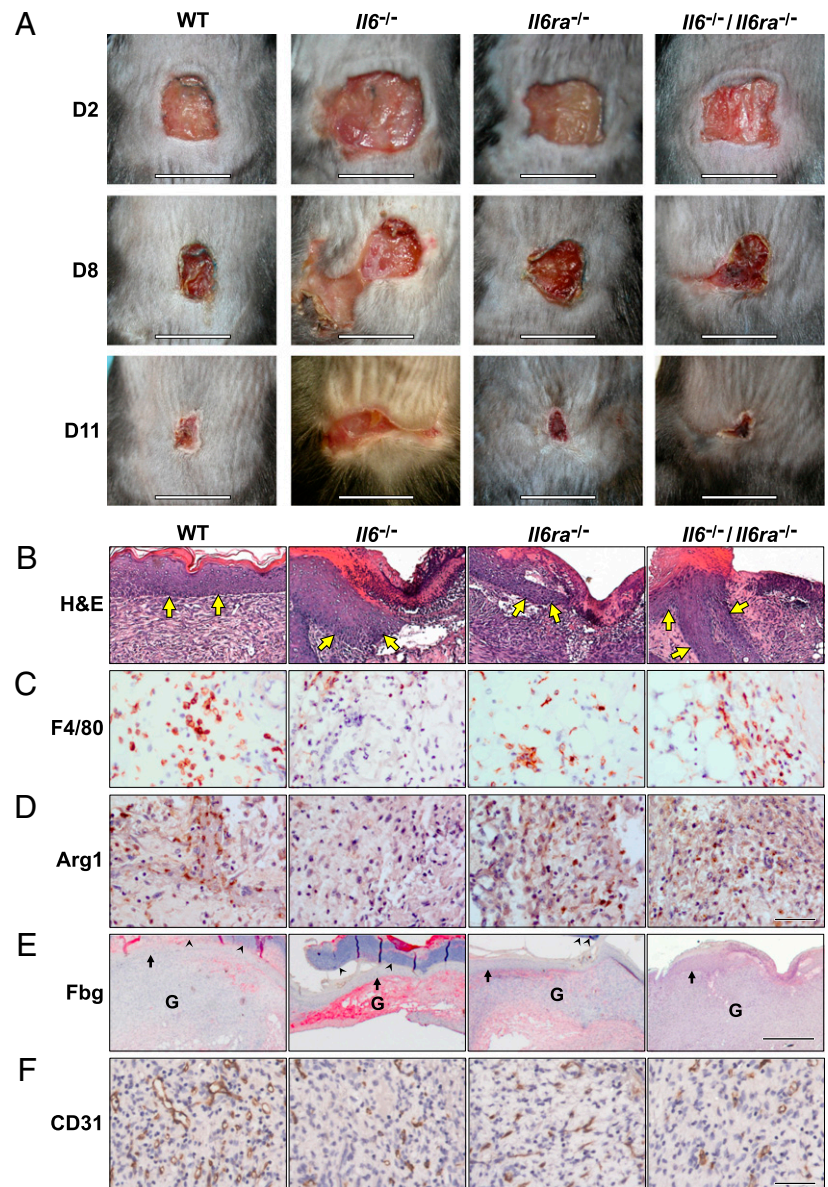


FIGURE 4. Cutaneous wound healing occurs more efficiently in *Il6ra*^{-/-} and *Il6*^{-/-}/*Il6ra*^{-/-} mice than in *Il6*^{-/-} mice. **A**, Photomicrographs of large excisional wounds made in dorsal skin after 2, 8, and 11 d. Scale bar, 1 cm. **B**, H&E sections indicating complete re-epithelialization (arrows) in WT mice and impaired re-epithelialization in other groups of mice (arrows) 11 d after large excisional wounding (original magnification $\times 100$). **C–F**, Immunohistochemical analysis of large wounds for macrophages [F4/80 Ab, day 6 (**C**); arginase 1 (Arg1), day 5 (**D**); and fibrinogen (fbg, day 8, pink/red reaction product) (**E**)]. “G” indicates granulation tissue, arrows indicate the newly formed epithelial layer, and arrowheads point to the superficial eschar. **F**, Blood vessels were indicated by immunohistochemistry for CD31 (PECAM, day 5). Scale bar, 100 μ M (**D**, **F**); 500 μ M (**E**). Original magnification $\times 400$ (**C**, **D**, **F**) and $\times 25$ (**E**). Arg1, arginase 1; fbg, fibrinogen.

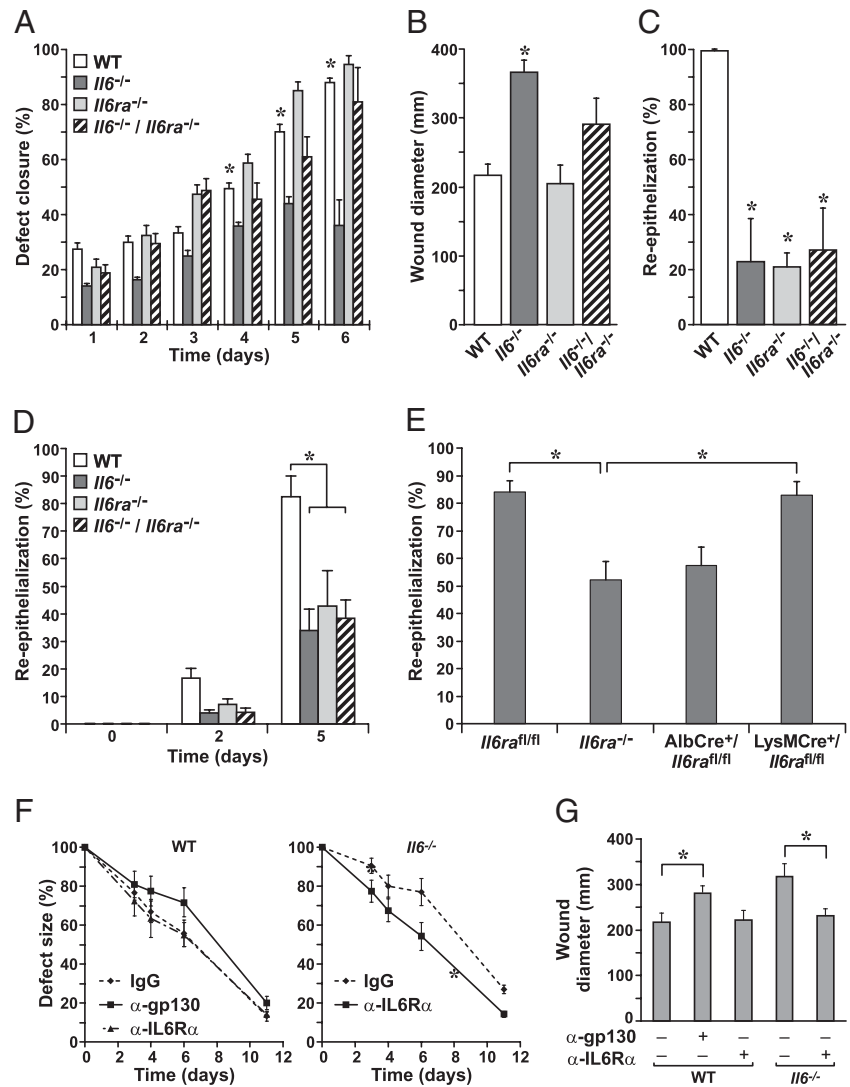
reported in *Il6*^{-/-} mice (37, 48). Both fibrin clearance and granulation tissue formation can be attributed to macrophage activity in healing wounds. Granulation tissue formation in *Il6ra*^{-/-} and *Il6*^{-/-}/*Il6ra*^{-/-} mice was variable and ranged from being similar to WT to the severe deficits seen in *Il6*^{-/-} mice. However, large wounds of *Il6*^{-/-} mice consistently displayed the most severely impaired wound healing with regard to all parameters studied except re-epithelialization (Figs. 4, 5A, 5B).

As differences were seen in wound healing between *Il6*^{-/-} and *Il6ra*^{-/-} mice, we wanted to determine whether IL-6 uses another receptor in the absence of IL-6R α or whether the absence of the receptor itself may account for the improved wound-healing phenotype in *Il6ra*^{-/-} mice. Some promiscuity exists in the IL-6 family of cytokines as high concentrations of CNTF or the IL-27 subunit p28 have been shown to induce a low level of signaling through IL-6R α (1, 2, 49), and differing phenotypes have been reported between receptor and ligand knockouts for CNTF. However, mammalian IL-6 is not known to have any activity independent of IL-6R α . We hypothesized that if IL-6 could signal through another receptor, then wound healing would be expected to be delayed in mice with a combined deficit of IL-6 and IL-6R α . Instead, closure of large excisional wounds in *Il6*^{-/-}/*Il6ra*^{-/-} mice

occurred on a time frame most similar to *Il6ra*^{-/-} mice, as did the formation of granulation tissue (Fig. 4). Apparently, absence of the receptor is more important for rescuing wound healing in *Il6ra*^{-/-} mice than is promiscuous IL-6 activity.

To confirm that the depletion of IL-6R α improves wound contraction in *Il6*^{-/-} mice, we treated mice with Abs specific for IL-6R α and gp130. As expected, depletion of gp130 delayed wound contraction in WT mice (Fig. 5F, 5G), consistent with its previously defined role in wound healing (50) but had no effect on *Il6*^{-/-} mice (data not shown). However, although depletion of circulating IL-6R α did not affect wound contraction in WT mice, it dramatically improved wound contraction in *Il6*^{-/-} mice (Fig. 5F, 5G), similar to data obtained in mice with a combined genetic deficit of IL-6 and IL-6R α . These data are consistent with the notion that IL-6R α both facilitates wound healing in an IL-6-dependent fashion but also impairs wound healing in a manner that does not involve IL-6. To determine whether IL-27 p28 binding to IL-6R α accounts for this negative effect of IL-6R α in wound contraction, we treated mice with an Ab specific for murine p28. The dose used was sufficient to prevent exogenous p28 from inducing primary murine macrophages from expressing IL-10 and suppressing IL-17 in vitro (data not shown). No difference in

FIGURE 5. Cutaneous wounds in *Il6ra*^{-/-} mice contract similarly to WT mice but display delayed re-epithelialization. Wound-closure rates in mice were quantified superficially (A) by placing a 1-cm² grid over large excisional wounds and microscopically (B) by measuring the width of the granulation tissue in histological preparations taken from the center of large wounds. C and D, Re-epithelialization was assessed in H&E preparations as the percentage of the wound surface over the newly formed granulation tissue that is covered by keratinocytes in large wounds at day 11 (C) and in small punch biopsy wounds after 0, 2, and 5 d (D). E, Re-epithelialization is delayed to a greater extent in *AlbCre*^{+/+}/*Il6ra*^{-/-} mice than in *LysMCre*^{+/+}/*Il6ra*^{-/-} mice. Small punch wound after 5 d. F, Large wounds were generated in WT (left panel) and *Il6*^{-/-} mice (right panel) prior to daily i.p. administration of control Ab (IgG) or Abs specific for mouse gp130 or mouse IL-6R α , and wound contraction was assessed macroscopically. G, Wound diameter was assessed microscopically 11 d after wounding and daily treatment with Abs, as shown.



wound contraction was seen with this treatment in either WT or *Il6*^{-/-} mice (data not shown).

To identify a mechanism that could explain the timely wound healing observed in the absence of IL-6, we investigated signaling pathways known to be induced by IL-6R α signaling. Stat3 phosphorylation was reduced to a similar extent in *Il6*^{-/-}, *Il6ra*^{-/-}, and *Il6*^{-/-} / *Il6ra*^{-/-} mice (Fig. 6A) compared with WT mice at 30 min after wounding and is therefore unlikely to explain differences between genotypes. At later time points, Stat3 phosphorylation in knockout mice was not different from that in WT mice (data not shown). However, phosphorylation of the MAPK ERK1/2 was undetectable in *Il6*^{-/-} mice yet increased in *Il6ra*^{-/-} relative to WT mice 1 d after wounding (Fig. 6A). ERK phosphorylation in *Il6*^{-/-} / *Il6ra*^{-/-} was similar to that of WT mice but notably higher than that of *Il6*^{-/-} mice. Given the importance of ERK activation in promoting wound healing, we wondered whether ERK activation could account for the difference seen between mice lacking IL-6 or IL-6R α . To test this hypothesis, we treated mice with a MEK1/2 inhibitor (U0126) to prevent ERK activation. Topical application of U0126 reduced ERK phosphorylation in wounds of both WT and *Il6ra*^{-/-} mice compared with vehicle-treated controls (Fig. 6B). The difference in wound contraction rates was significantly delayed in *Il6ra*^{-/-} mice treated with U0126 compared with vehicle control-treated mice but did not reach

significance in WT mice (Fig. 6C). These data suggest that, despite diminished Stat3 activation in *Il6*^{-/-} and *Il6ra*^{-/-} mice, enhanced ERK activation in *Il6ra*^{-/-} mice may rescue wound contraction.

Discussion

In this paper, we provide the first report of mice with a complete deficiency of IL-6R α and of mice with conditional deletion of IL-6R α . *Il6ra*^{-/-} mice share many of the phenotypic abnormalities reported in *Il6*^{-/-} mice. However, *Il6ra*^{-/-} mice do not display the dramatic delay in wound healing seen in *Il6*^{-/-} mice. Wound healing in mice with a combined deficit of IL-6 and IL-6R α resembles wound healing in WT and *Il6ra*^{-/-} mice more than that in *Il6*^{-/-} mice, suggestive of a previously unknown role for IL-6R α that does not involve IL-6.

Similar to *Il6*^{-/-} mice, *Il6ra*^{-/-} mice show deficiencies in the modulation of inflammatory responses. Using a model of sterile inflammation, we show that *Il6ra*^{-/-} mice demonstrate a similar defect in neutrophil resolution and in progression to a macrophage-dominated response as *Il6*^{-/-} mice. Similarly, mice of both genotypes share a complete inability to generate an acute-phase response after inflammatory challenge with turpentine. Mice with a conditional deletion of IL-6R α in hepatocytes but not in macrophages or granulocytes shared the inability of *Il6ra*^{-/-} mice to generate a response to turpentine. These results confirm the importance of the hepatocyte in this response and indicate that

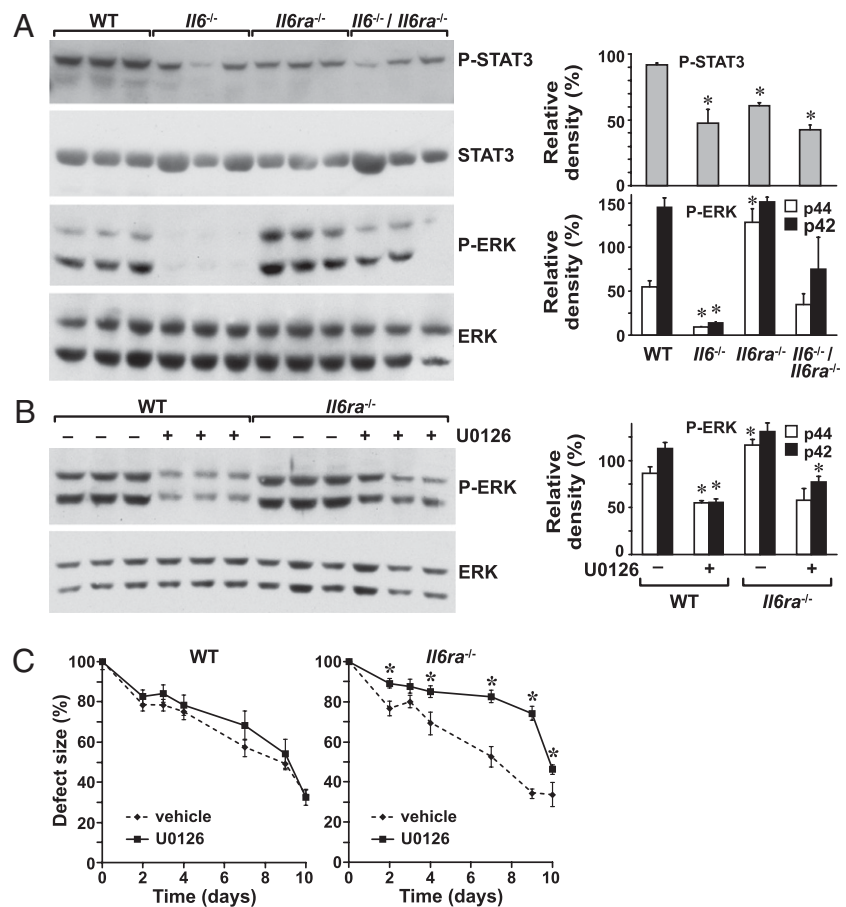


FIGURE 6. ERK activation is increased in *Il6ra*^{-/-} mice compared with WT mice. *A*, Total and phosphorylated (p) Stat3 and ERK were assessed in small punch biopsy wounds collected after 30 min (Stat3) or 1 d (ERK) by Western blotting. Densitometry results for the blots are provided to the right. **p* < 0.05. *B*, Total and p-ERKs were assessed in small wounds generated in WT and *Il6ra*^{-/-} mice treated topically with vehicle (DMSO) or with the MEK inhibitor U0126. Wounds were harvested after 1 d, and western blotting was performed on lysates. *C*, Wound contraction was assessed macroscopically in large wounds of WT (left panel) and *Il6ra*^{-/-} mice treated daily with vehicle (DMSO) or U0126. **p* < 0.05.

soluble IL-6R α expression by inflammatory cells is neither required nor sufficient. Given that mice with IL-6R α deficiency in hepatocytes still have almost two-thirds of the levels of circulating soluble IL-6R α as WT mice yet have the same defect in generating an acute-phase response as *Il6ra*^{-/-} mice, we conclude that membrane-bound IL-6R α on hepatocytes is essential for the acute-phase response.

Through studies in mice with conditional expression of IL-6R α , we demonstrated that macrophages and granulocytes produce the majority of soluble circulating IL-6R α (62.7%) in unchallenged and challenged mice and that hepatocytes produce most of the remainder (30.6%). The greater contribution by immune cells is consistent with immune cell-derived IL-6R α being secreted and transported to distant inflammatory sites. Soluble IL-6R α delivered to an inflammatory area allows IL-6 signaling through all cells present and, hence, a rapid response to injury or infection. Hepatic expression of IL-6R α , however, appears to be more relevant to cell-type-specific rapid acute-phase responses specifically mediated by hepatocytes. However, it should be noted that differences in soluble IL-6R α expression may exist in mice and humans, because mice are restricted to proteolytic cleavage and do not produce the differentially spliced form. It is of interest that the combined hepatic and granulocytic contribution of IL-6R α apparently accounts for almost all (93.4%) of the soluble IL-6R α expression in mice. It is possible that compensation from other compartments may occur in mice lacking IL-6R α in particular cell types or that incomplete knockdown of IL-6R α in macrophages and granulocytes with the lysozyme M promoter [95–99% efficiency in mature cells; 75–79% efficiency in bone marrow-derived cells (40)] accounts for residual IL-6R α expression. However, the finding that macrophages, granulocytes, and hepatocytes are the major producers

of soluble IL-6R α is consistent with tissue expression studies (51). Our study did not address lymphocyte production of soluble IL-6R α , but it is likely that these cells produce the remaining circulating IL-6R α in unchallenged mice and that their production increases during immune responses (52).

On the basis of the similarities that we found between the phenotypes of *Il6*^{-/-} and *Il6ra*^{-/-} mice, it was somewhat surprising to find differences between these genotypes in wound-healing responses. Inflammation is an influential part of wound healing, and early granulation tissue contains many of the inflammatory cell types, cytokines, and angiogenic vessels typical of inflammation. Deficits in macrophage infiltration and subsequent fibrin clearance in *Il6*^{-/-} mice were not typical in wounds of *Il6ra*^{-/-} mice. The improved wound-healing phenotype in IL-6R α ^{-/-} mice indicates a divergence in functionality between IL-6 and IL-6R α and possibly a compensatory mechanism in the absence of IL-6R α . As mice with a combined deficiency of IL-6 and IL-6R α demonstrated a wound-healing phenotype closely aligned with that of *Il6ra*^{-/-} mice, it is likely that the absence of IL-6R α played a greater role in rescuing the phenotype in *Il6ra*^{-/-} mice than did IL-6 promiscuity. However, mice with both deficits did not heal as efficiently as *Il6ra*^{-/-} mice. Therefore, we cannot eliminate the possibility that IL-6 may also signal through a different receptor in these mice.

Many interrelated processes involved in wound healing were improved in *Il6ra*^{-/-} mice compared with *Il6*^{-/-} mice, including macrophage infiltration, fibrin clearance, and angiogenesis. That re-epithelialization was delayed in both *Il6*^{-/-} and *Il6ra*^{-/-} mice was surprising given the differences in wound closure rates. It seems that restored wound contraction and granulation tissue formation in *Il6ra*^{-/-} mice accounts for the appearance that wounds are healing

efficiently, despite the delay in keratinocyte migration over the wound bed. Interestingly, experiments in mice with conditional expression of IL-6R α indicated that hepatocyte IL-6R α was more important in cutaneous wound re-epithelialization than that of macrophages and granulocytes. This finding is unexpected given that most circulating IL-6R α comes from macrophages and granulocytes and because these cell types are numerous in healing wounds. Apparently, one or more of the numerous acute-phase reactants or growth factors produced by the liver in response to IL-6 contribute to re-epithelialization.

In both knockout mice and Ab-depletion studies, we showed that depletion of IL-6R α rescues wound healing in *Il6*^{-/-} mice. No difference in Stat3 phosphorylation was seen between any of the wounds in the knockout mice, which in each case was less than the phosphorylated Stat3 observed in WT mice. Similarly, the lack of re-epithelialization in both *Il6*^{-/-} and *Il6ra*^{-/-} mice, a Stat3-dependent process, argues against this mechanism alone accounting for the rescued wound healing observed in *Il6ra*^{-/-} mice. Our data imply that IL-6R α contributes positively to wound healing in an IL-6- and Stat3-dependent manner but potentially hinders wound contraction in an IL-6-independent fashion. This mechanism is unlikely to involve other IL-6 family ligands because they predominantly induce Jak/Stat signaling. However, because select ligands in the IL-6 family, specifically IL-27 p28 and CNTF, have been shown to mediate low-affinity binding to IL-6R α in vitro (1, 2), we investigated the effect of blocking IL-27 p28 in vivo. We reasoned that if the interaction of this ligand with IL-6R α accounted for the inhibitory effects of wound contraction by IL-6R α , then blocking p28 with a specific Ab should rescue wound contraction in *Il6*^{-/-} mice. Instead, no differences in wound contraction were seen in either WT or *Il6*^{-/-} mice treated with Abs to p28. CNTF blocking experiments were not performed because CNTF production is restricted to glial and CNS cells, and CNTF does not possess a signal peptide for secretion. Instead, we investigated ERK activation as both a downstream mediator of IL-6R α signaling (13, 53, 54) and as an important effector of wound contraction (55). ERK phosphorylation was increased in wounds of *Il6ra*^{-/-} mice but not *Il6*^{-/-} mice, and blocking ERK activation with a MEK inhibitor delayed wound healing in *Il6ra*^{-/-} mice. These data suggest that increased ERK activation increases wound contraction in *Il6ra*^{-/-} mice but not in *Il6*^{-/-} mice. We observed that topical application of the MEK inhibitor U0126 inhibited wound contraction to a greater extent in *Il6ra*^{-/-} mice than in WT mice. Although it is tempting to speculate that wound healing in the absence of IL-6R α may be more dependent on ERK activation than in WT mice, such a conclusion would be premature, because more studies are needed to determine the contributions of the MAPK or other signaling pathways and mechanisms to the healing process in *Il6ra*^{-/-} mice. In addition, it should be noted that the importance of such a mechanism remains to be determined, because it may prove to be specific to mice or may occur only in the context of the nonphysiological absence of IL-6R α .

Questions still remain regarding the mechanism by which depletion of IL-6R α could lead to increased ERK activation, independently of IL-6 signaling. It could be that IL-6R α plays a role in gp130 internalization and membrane expression, or a cytoplasmic phosphorylation site of IL-6R α (56) may be involved in ERK suppression in the wound microenvironment. Sparse data suggest that gp130 and/or IL-6R α interact with several adaptor proteins upstream of ERK activation, such as Grb1, Src homology region 2 domain-containing phosphatase 2, Vav, and Src family kinases (8, 53, 57–60). The depletion of IL-6R α protein may deregulate the balance between these positive and negative effectors of the MAPK pathway, leading to increased

ERK activation. In support of this idea, treatment of HepG2 cells with soluble IL-6R α in the absence of IL-6 led to a complete inhibition of early growth response protein 1, a gene downstream of ERK activation (61). Similarly, cross-talk between gp130 and/or IL-6R α and the EGF family receptors has been reported in several tumor cell lines (62–66) and in primary mammary epithelial cells (67). It is also possible that increased ERK activation in the absence of IL-6R α is due to indirect effects on the expression or activity of other cytokines or on receptors other than gp130. It is not clear what the effect of IL-6R α deficiency would have on these interactions. However, given the similarity between healing wounds and the tumor microenvironment and given that Abs against IL-6R α are already in clinical usage in patients with rheumatic diseases, there is a strong rationale for better understanding this novel role for IL-6R α in regulating ERK activation.

Acknowledgments

We thank the University of Cincinnati Gene-Targeted Mouse Service for expert assistance with generating the *Il6ra*-targeted mice, Dr. Mark Magnusen for the EIIa-Cre mice, Dr. Jay L. Degen for the rabbit anti-mouse fibrinogen Ab, and Drs. Simon A. Jones and Patrick B. Dennis for advice. Expert graphical and editorial assistance was provided by Glenn Doerman and Maryellen Daston, respectively.

Disclosures

The authors have no financial conflicts of interest.

References

- Schuster, B., M. Kovaleva, Y. Sun, P. Regenhard, V. Matthews, J. Grötzinger, S. Rose-John, and K. J. Kallen. 2003. Signaling of human ciliary neurotrophic factor (CNTF) revisited: the interleukin-6 receptor can serve as an α -receptor for CNTF. *J. Biol. Chem.* 278: 9528–9535.
- Crabé, S., A. Guay-Giroux, A. J. Tormo, D. Duluc, R. Lissilaa, F. Guilhot, U. Mavoungou-Bigouagou, F. Lefouilli, I. Cognet, W. Ferlin, et al. 2009. The IL-27 p28 subunit binds cytokine-like factor 1 to form a cytokine regulating NK and T cell activities requiring IL-6R for signaling. *J. Immunol.* 183: 7692–7702.
- Taga, T., M. Hibi, Y. Hirata, K. Yamasaki, K. Yasukawa, T. Matsuda, T. Hirano, and T. Kishimoto. 1989. Interleukin-6 triggers the association of its receptor with a possible signal transducer, gp130. *Cell* 58: 573–581.
- Bravo, J., and J. K. Heath. 2000. Receptor recognition by gp130 cytokines. *EMBO J.* 19: 2399–2411.
- Murakami, M., M. Hibi, N. Nakagawa, T. Nakagawa, K. Yasukawa, K. Yamanishi, T. Taga, and T. Kishimoto. 1993. IL-6-induced homodimerization of gp130 and associated activation of a tyrosine kinase. *Science* 260: 1808–1810.
- Lütticken, C., U. M. Wegenka, J. Yuan, J. Buschmann, C. Schindler, A. Ziemiecki, A. G. Harpur, A. F. Wilks, K. Yasukawa, T. Taga, et al. 1994. Association of transcription factor APRF and protein kinase Jak1 with the interleukin-6 signal transducer gp130. *Science* 263: 89–92.
- Stahl, N., T. G. Boulton, T. Farruggella, N. Y. Ip, S. Davis, B. A. Witthuhn, F. W. Quelle, O. Silvennoinen, G. Barbieri, S. Pellegrini, et al. 1994. Association and activation of Jak-Tyk kinases by CNTF-LIF-OSM-IL-6 β receptor components. *Science* 263: 92–95.
- Stahl, N., T. J. Farruggella, T. G. Boulton, Z. Zhong, J. E. Darnell, Jr., and G. D. Yancopoulos. 1995. Choice of STATs and other substrates specified by modular tyrosine-based motifs in cytokine receptors. *Science* 267: 1349–1353.
- Haan, S., J. F. Keller, I. Behrmann, P. C. Heinrich, and C. Haan. 2005. Multiple reasons for an inefficient STAT1 response upon IL-6-type cytokine stimulation. *Cell. Signal.* 17: 1542–1550.
- Wegenka, U. M., J. Buschmann, C. Lütticken, P. C. Heinrich, and F. Horn. 1993. Acute-phase response factor, a nuclear factor binding to acute-phase response elements, is rapidly activated by interleukin-6 at the posttranslational level. *Mol. Cell. Biol.* 13: 276–288.
- Fukada, T., M. Hibi, Y. Yamanaka, M. Takahashi-Tezuka, Y. Fujitani, T. Yamaguchi, K. Nakajima, and T. Hirano. 1996. Two signals are necessary for cell proliferation induced by a cytokine receptor gp130: involvement of STAT3 in anti-apoptosis. *Immunity* 5: 449–460.
- Ohtani, T., K. Ishihara, T. Atsumi, K. Nishida, Y. Kaneko, T. Miyata, S. Itoh, M. Narimatsu, H. Maeda, T. Fukada, et al. 2000. Dissection of signaling cascades through gp130 in vivo: reciprocal roles for STAT3- and SHP2-mediated signals in immune responses. *Immunity* 12: 95–105.
- Ernst, M., and B. J. Jenkins. 2004. Acquiring signalling specificity from the cytokine receptor gp130. *Trends Genet.* 20: 23–32.

14. Rose-John, S., J. Scheller, G. Elson, and S. A. Jones. 2006. Interleukin-6 biology is coordinated by membrane-bound and soluble receptors: role in inflammation and cancer. *J. Leukoc. Biol.* 80: 227–236.
15. Müllberg, J., H. Schooltink, T. Stoyan, P. C. Heinrich, and S. Rose-John. 1992. Protein kinase C activity is rate limiting for shedding of the interleukin-6 receptor. *Biochem. Biophys. Res. Commun.* 189: 794–800.
16. Horiuchi, S., Y. Koyanagi, Y. Zhou, H. Miyamoto, Y. Tanaka, M. Waki, A. Matsumoto, M. Yamamoto, and N. Yamamoto. 1994. Soluble interleukin-6 receptors released from T cell or granulocyte/macrophage cell lines and human peripheral blood mononuclear cells are generated through an alternative splicing mechanism. *Eur. J. Immunol.* 24: 1945–1948.
17. Jones, S. A., S. Horiuchi, D. Novick, N. Yamamoto, and G. M. Fuller. 1998. Shedding of the soluble IL-6 receptor is triggered by Ca^{2+} mobilization, while basal release is predominantly the product of differential mRNA splicing in THP-1 cells. *Eur. J. Immunol.* 28: 3514–3522.
18. Peters, M., S. Jacobs, M. Ehlers, P. Vollmer, J. Müllberg, E. Wolf, G. Brem, K. H. Meyer zum Büschenfelde, and S. Rose-John. 1996. The function of the soluble interleukin 6 (IL-6) receptor in vivo: sensitization of human soluble IL-6 receptor transgenic mice towards IL-6 and prolongation of the plasma half-life of IL-6. *J. Exp. Med.* 183: 1399–1406.
19. Rabe, B., A. Chalaris, U. May, G. H. Waetzig, D. Seeger, A. S. Williams, S. A. Jones, S. Rose-John, and J. Scheller. 2008. Transgenic blockade of Interleukin-6-trans-signaling abrogates inflammation. *Blood* 111: 1021–1028.
20. Chalaris, A., B. Rabe, K. Paliga, H. Lange, T. Laskay, C. A. Fielding, S. A. Jones, S. Rose-John, and J. Scheller. 2007. Apoptosis is a natural stimulus of IL6R shedding and contributes to the proinflammatory trans-signaling function of neutrophils. *Blood* 110: 1748–1755.
21. Hurst, S. M., T. S. Wilkinson, R. M. McLoughlin, S. Jones, S. Horiuchi, N. Yamamoto, S. Rose-John, G. M. Fuller, N. Topley, and S. A. Jones. 2001. IL-6 and its soluble receptor orchestrate a temporal switch in the pattern of leukocyte recruitment seen during acute inflammation. *Immunity* 14: 705–714.
22. McLoughlin, R. M., J. Witowski, R. L. Robson, T. S. Wilkinson, S. M. Hurst, A. S. Williams, J. D. Williams, S. Rose-John, S. A. Jones, and N. Topley. 2003. Interplay between IFN- γ and IL-6 signaling governs neutrophil trafficking and apoptosis during acute inflammation. *J. Clin. Invest.* 112: 598–607.
23. Vermes, C., J. J. Jacobs, J. Zhang, G. Firsicz, K. A. Roebuck, and T. T. Glant. 2002. Shedding of the interleukin-6 (IL-6) receptor (gp80) determines the ability of IL-6 to induce gp130 phosphorylation in human osteoblasts. *J. Biol. Chem.* 277: 16879–16887.
24. Kopf, M., H. Baumann, G. Freer, M. Freudenberg, M. Lamers, T. Kishimoto, R. Zinkernagel, H. Bluethmann, and G. Köhler. 1994. Impaired immune and acute-phase responses in interleukin-6-deficient mice. *Nature* 368: 339–342.
25. Poli, V., R. Balena, E. Fattori, A. Markatos, M. Yamamoto, H. Tanaka, G. Ciliberto, G. A. Rodan, and F. Costantini. 1994. Interleukin-6 deficient mice are protected from bone loss caused by estrogen depletion. *EMBO J.* 13: 1189–1196.
26. Cressman, D. E., L. E. Greenbaum, R. A. DeAngelis, G. Ciliberto, E. E. Furth, V. Poli, and R. Taub. 1996. Liver failure and defective hepatocyte regeneration in interleukin-6-deficient mice. *Science* 274: 1379–1383.
27. Wallenius, V., K. Wallenius, B. Ahren, M. Rudling, H. Carlsten, S. L. Dickson, C. Ohlsson, and J. O. Jansson. 2002. Interleukin-6-deficient mice develop mature-onset obesity. *Nat. Med.* 8: 75–79.
28. Mendel, I., A. Katz, N. Kozak, A. Ben-Nun, and M. Revel. 1998. Interleukin-6 functions in autoimmune encephalomyelitis: a study in gene-targeted mice. *Eur. J. Immunol.* 28: 1727–1737.
29. Hatzi, E., C. Murphy, A. Zoepfel, H. Rasmussen, L. Morbidelli, H. Ahorn, K. Kunisada, U. Tontsch, M. Klenk, K. Yamauchi-Takahara, et al. 2002. N-myc oncogene overexpression down-regulates IL-6; evidence that IL-6 inhibits angiogenesis and suppresses neuroblastoma tumor growth. *Oncogene* 21: 3552–3561.
30. Mulé, J. J., J. K. McIntosh, D. M. Jablons, and S. A. Rosenberg. 1990. Antitumor activity of recombinant interleukin 6 in mice. *J. Exp. Med.* 171: 629–636.
31. Hong, D. S., L. S. Angelo, and R. Kurzrock. 2007. Interleukin-6 and its receptor in cancer: implications for translational therapeutics. *Cancer* 110: 1911–1928.
32. Martin, P., and S. J. Leibovich. 2005. Inflammatory cells during wound repair: the good, the bad and the ugly. *Trends Cell Biol.* 15: 599–607.
33. Simpson, D. M., and R. Ross. 1972. The neutrophilic leukocyte in wound repair: a study with antineutrophil serum. *J. Clin. Invest.* 51: 2009–2023.
34. Dovi, J. V., L. K. He, and L. A. DiPietro. 2003. Accelerated wound closure in neutrophil-depleted mice. *J. Leukoc. Biol.* 73: 448–455.
35. Leibovich, S. J., and R. Ross. 1975. The role of the macrophage in wound repair: a study with hydrocortisone and antimacrophage serum. *Am. J. Pathol.* 78: 71–100.
36. Gallucci, R. M., P. P. Simeonova, J. M. Matheson, C. Kommineni, J. L. Guriel, T. Sugawara, and M. I. Luster. 2000. Impaired cutaneous wound healing in interleukin-6-deficient and immunosuppressed mice. *FASEB J.* 14: 2525–2531.
37. Lin, Z. Q., T. Kondo, Y. Ishida, T. Takayasu, and N. Mukaida. 2003. Essential involvement of IL-6 in the skin wound-healing process as evidenced by delayed wound healing in IL-6-deficient mice. *J. Leukoc. Biol.* 73: 713–721.
38. Buchholz, F., P. O. Angrand, and A. F. Stewart. 1998. Improved properties of FLP recombinase evolved by cycling mutagenesis. *Nat. Biotechnol.* 16: 657–662.
39. Postic, C., M. Shiota, K. D. Niswender, T. L. Jetton, Y. Chen, J. M. Moates, K. D. Shelton, J. Lindner, A. D. Cherrington, and M. A. Magnuson. 1999. Dual roles for glucokinase in glucose homeostasis as determined by liver and pancreatic β cell-specific gene knock-outs using Cre recombinase. *J. Biol. Chem.* 274: 305–315.
40. Clausen, B. E., C. Burkhardt, W. Reith, R. Renkawitz, and I. Förster. 1999. Conditional gene targeting in macrophages and granulocytes using LysMcre mice. *Transgenic Res.* 8: 265–277.
41. Berry, M. N., H. J. Halls, and M. B. Grivell. 1992. Techniques for pharmacological and toxicological studies with isolated hepatocyte suspensions. *Life Sci.* 51: 1–16.
42. Drew, A. F., A. H. Kaufman, K. W. Kombrinck, M. J. Danton, C. C. Daugherty, J. L. Degen, and T. H. Bugge. 1998. Ligneous conjunctivitis in plasminogen-deficient mice. *Blood* 91: 1616–1624.
43. Fattori, E., M. Cappelletti, P. Costa, C. Sellitto, L. Cantoni, M. Carelli, R. Faggioni, G. Fantuzzi, P. Ghezzi, and V. Poli. 1994. Defective inflammatory response in interleukin 6-deficient mice. *J. Exp. Med.* 180: 1243–1250.
44. Kaibara, A., N. J. Espat, T. Aufferberg, A. S. Abouhamze, D. Martin, S. Kalra, and L. L. Moldawer. 1998. Interleukin 6, but not ciliary neurotrophic factor or leukemia-inhibitory factor, is responsible for the acute phase response to turpentine-induced myositis. *Cytokine* 10: 452–456.
45. Geisterfer, M., C. Richards, M. Baumann, G. Fey, D. Gywnne, and J. Gaudie. 1993. Regulation of IL-6 and the hepatic IL-6 receptor in acute inflammation in vivo. *Cytokine* 5: 1–7.
46. Mackiewicz, A., H. Schooltink, P. C. Heinrich, and S. Rose-John. 1992. Complex of soluble human IL-6-receptor/IL-6 up-regulates expression of acute-phase proteins. *J. Immunol.* 149: 2021–2027.
47. Butterweck, V., S. Prinz, and M. Schwaninger. 2003. The role of interleukin-6 in stress-induced hyperthermia and emotional behaviour in mice. *Behav. Brain Res.* 144: 49–56.
48. Luckett, L. R., and R. M. Gallucci. 2007. Interleukin-6 (IL-6) modulates migration and matrix metalloproteinase function in dermal fibroblasts from IL-6KO mice. *Br. J. Dermatol.* 156: 1163–1171.
49. Nesbitt, J. E., N. L. Fuentes, and G. M. Fuller. 1993. Ciliary neurotrophic factor regulates fibrinogen gene expression in hepatocytes by binding to the interleukin-6 receptor. *Biochem. Biophys. Res. Commun.* 190: 544–550.
50. Zhu, B. M., Y. Ishida, G. W. Robinson, M. Pacher-Zavisin, A. Yoshimura, P. M. Murphy, and L. Hennighausen. 2008. SOCS3 negatively regulates the gp130-STAT3 pathway in mouse skin wound healing. *J. Invest. Dermatol.* 128: 1821–1829.
51. Jones, S. A., P. J. Richards, J. Scheller, and S. Rose-John. 2005. IL-6 transsignaling: the in vivo consequences. *J. Interferon Cytokine Res.* 25: 241–253.
52. Polgár, A., M. Brózik, S. Tóth, M. Holub, K. Hegyi, A. Kádár, L. Hodinka, and A. Falus. 2000. Soluble interleukin-6 receptor in plasma and in lymphocyte culture supernatants of healthy individuals and patients with systemic lupus erythematosus and rheumatoid arthritis. *Med. Sci. Monit.* 6: 13–18.
53. Schiemann, W. P., J. L. Bartoe, and N. M. Nathanson. 1997. Box 3-independent signaling mechanisms are involved in leukemia-inhibitory factor receptor α - and gp130-mediated stimulation of mitogen-activated protein kinase: evidence for participation of multiple signaling pathways which converge at Ras. *J. Biol. Chem.* 272: 16631–16636.
54. Lai, C. F., J. Ripperger, Y. Wang, H. Kim, R. B. Hawley, and H. Baumann. 1999. The STAT3-independent signaling pathway by glycoprotein 130 in hepatic cells. *J. Biol. Chem.* 274: 7793–7802.
55. Hirano, S., R. S. Rees, and R. R. Gilmont. 2002. MAP kinase pathways involving hsp27 regulate fibroblast-mediated wound contraction. *J. Surg. Res.* 102: 77–84.
56. Müllberg, J., W. Oberthür, F. Lottspeich, E. Mehl, E. Dittlich, L. Graeve, P. C. Heinrich, and S. Rose-John. 1994. The soluble human IL-6 receptor: mutational characterization of the proteolytic cleavage site. *J. Immunol.* 152: 4958–4968.
57. Ernst, M., D. P. Gearing, and A. R. Dunn. 1994. Functional and biochemical association of Hck with the LIF/IL-6 receptor signal transducing subunit gp130 in embryonic stem cells. *EMBO J.* 13: 1574–1584.
58. Wang, X. Y., D. K. Fuhrer, M. S. Marshall, and Y. C. Yang. 1995. Interleukin-11 induces complex formation of Grb2, Fyn, and JAK2 in 3T3L1 cells. *J. Biol. Chem.* 270: 27999–28002.
59. Lee, I. S., Y. Liu, M. Narazaki, M. Hibi, T. Kishimoto, and T. Taga. 1997. Vav is associated with signal transducing molecules gp130, Grb2 and Erk2, and is tyrosine phosphorylated in response to interleukin-6. *FEBS Lett.* 401: 133–137.
60. Kim, H., and H. Baumann. 1999. Dual signaling role of the protein tyrosine phosphatase SHP-2 in regulating expression of acute-phase plasma proteins by interleukin-6 cytokine receptors in hepatic cells. *Mol. Cell Biol.* 19: 5326–5338.
61. Holub, M. C., H. Hegyesi, P. Igaz, A. Polgár, S. Toth, and A. Falus. 2002. Soluble interleukin-6 receptor enhanced by oncostatin M induces major changes in gene expression profile of human hepatoma cells. *Immunol. Lett.* 82: 79–84.
62. Qiu, Y., L. Ravi, and H. J. Kung. 1998. Requirement of ErbB2 for signalling by interleukin-6 in prostate carcinoma cells. *Nature* 393: 83–85.
63. Badache, A., and N. E. Hynes. 2001. Interleukin 6 inhibits proliferation and, in cooperation with an epidermal growth factor receptor autocrine loop, increases migration of T47D breast cancer cells. *Cancer Res.* 61: 383–391.
64. Grant, S. L., A. Hammacher, A. M. Douglas, G. A. Goss, R. K. Mansfield, J. K. Heath, and C. G. Begley. 2002. An unexpected biochemical and functional interaction between gp130 and the EGF receptor family in breast cancer cells. *Oncogene* 21: 460–474.
65. Wang, Y. D., J. De Vos, M. Jourdan, G. Couderc, Z. Y. Lu, J. F. Rossi, and B. Klein. 2002. Cooperation between heparin-binding EGF-like growth factor and interleukin-6 in promoting the growth of human myeloma cells. *Oncogene* 21: 2584–2592.
66. Colomiere, M., A. C. Ward, C. Riley, M. K. Trenerry, D. Cameron-Smith, J. Findlay, L. Ackland, and N. Ahmed. 2009. Cross talk of signals between EGF and IL-6R through JAK2/STAT3 mediate epithelial-mesenchymal transition in ovarian carcinomas. *Br. J. Cancer* 100: 134–144.
67. Zhao, L., S. Hart, J. Cheng, J. J. Melenhorst, B. Bieri, M. Ernst, C. Stewart, F. Schaper, P. C. Heinrich, A. Ullrich, et al. 2004. Mammary gland remodeling depends on gp130 signaling through Stat3 and MAPK. *J. Biol. Chem.* 279: 44093–44100.

Interleukin-6 receptor enhances early colonization of the murine omentum by upregulation of a mannose family receptor, LY75, in ovarian tumor cells

Premkumar Vummidi Giridhar · Holly M. Funk · Catherine A. Gallo · Aleksey Porollo · Carol A. Mercer · David R. Plas · Angela F. Drew

Received: 5 March 2011 / Accepted: 20 August 2011 / Published online: 2 September 2011
© Springer Science+Business Media B.V. 2011

Abstract One of the earliest metastatic events in human ovarian cancer, tumor spread to the omentum, may be influenced by expression of interleukin 6 (IL6) and its cognate receptor (IL6R α). Previous reports have shown that IL6 and IL6R α expression is elevated in the serum and ascites of patients with ovarian cancer and that this can influence in vitro processes such as cell survival, proliferation and migration. In this study, overexpression of IL6R α , and to a lesser extent IL6, enhanced tumor growth on the omentum. Moreover, adherence to plastic and to peritoneal extracellular matrix components was enhanced in tumor cells overexpressing IL6 or IL6R α . Host production of IL6 and IL6R α was also sufficient to influence tumor adherence to the omentum. Expression of LY75/CD205/DEC205, a collagen-binding mannose family receptor, was directly influenced by IL6R α expression. Blocking LY75 with antibody reduced the adherence of tumor cells overexpressing IL6R α to matrices in vitro and to the omentum. The association between IL6R α

expression and LY75 expression has not been previously reported, and the promotion of cellular adherence is a novel role for LY75. These studies indicate that overexpression of LY75 may be an additional mechanism by which IL6 signaling influences the progression of ovarian cancer, and suggests that blocking LY75 could be a valuable clinical strategy for reducing the early metastasis of ovarian cancer.

Keywords LY75 · CD205 · Interleukin-6 · Ovarian cancer · Omentum · Metastasis

Abbreviations

IL6	Interleukin-6
IL6R α	IL6 receptor alpha
JAK	Janus-associated kinase
Stat	Signal transducer and activator of transcription
ERK	Extracellular signal-regulated kinase
DMEM	Dulbecco's modified Eagles medium
RFP	Red fluorescent protein

Electronic supplementary material The online version of this article (doi:10.1007/s10585-011-9420-x) contains supplementary material, which is available to authorized users.

P. V. Giridhar · H. M. Funk · C. A. Gallo · D. R. Plas · A. F. Drew (✉)
Department of Cancer and Cell Biology, Vontz Center for Molecular Studies, University of Cincinnati, 3125 Eden Avenue, Cincinnati, OH 45267-0521, USA
e-mail: adrew41@gmail.com

A. Porollo
Department of Environmental Health, University of Cincinnati, 3223 Eden Avenue, Cincinnati, OH 45267-0056, USA

C. A. Mercer
PDS Biotechnology, 500 Industrial Drive, Suite A, Lawrenceburg, IN 47025, USA

Introduction

Although metastasis accounts for the majority of deaths associated with ovarian cancer, little is known of the processes involved. Difficulties in detecting and studying early disease have confounded the problem. While it is known that localized peritoneal tumor dissemination predominates over hematogenous and lymphatic routes of spread, especially in the early stages of disease, the exact mechanisms have remained obscure. Ovarian serosal involvement is known to be associated with tumor cell exfoliation and the development of malignant ascitic aggregates, but the

cellular interactions involved in ovarian tumor metastasis are not well defined.

The omentum, a peritoneal organ rich in adipose tissue and immune cells, has been shown to be a preferred site of metastatic dissemination in ovarian cancer patients. Immune cells such as macrophages and lymphocytes are localized to specialized structures in the omentum known as milky spots. Tumor cells colonize the omentum via initial contact with milky spots. The mesothelial layer overlying much of the omentum is fenestrated over the milky spots, exposing immune cells and extracellular matrices rich in fibronectin, vitronectin, and collagen. Ovarian tumor cells express integrin ligands for matrix molecules that may influence tumor cell adhesion. The role of immune cells in facilitating tumor cell colonization of the omentum is not well studied.

Interleukin-6 (IL6) has been associated with the progression of multiple cancer types, including ovarian cancer. Increased expression of IL6 in ascites fluid and serum of patients is associated with disease stage. Recently, we showed that the specific alpha receptor for IL6, IL6 receptor alpha (IL6R α), is also upregulated in ovarian cancer patients [1]. Both the membrane-bound and soluble isoforms of IL6R α function as agonists for IL6 signaling. IL6 binds IL6R α and a common family signaling receptor, gp130, as a hexameric complex resulting in the dimerization of gp130 and subsequent activation of the janus-associated kinase (JAK)-signal transducer and activator of transcription (STAT), Extracellular signal-regulated kinase (ERK), and PI3K pathways. The downstream effects of such diverse pathways can result in cell survival, proliferation, migration, and anchorage-independent growth, and affects processes such as wound healing, inflammation, and tumorigenesis.

Many of the effects of IL6 signaling can be attributed to activation of the Stat3 signaling pathway and the subsequent increases in genes involved in cell survival and inflammation. However, many other genes are also upregulated by IL6 signaling. LY75 has not previously been associated with IL6 signaling. LY75 is a mannose family receptor expressed on thymic cortical epithelium, myeloid dendritic cell subsets, and on other leukocytes to a lesser extent [2–4]. LY75 has been reported to play a role in endocytic uptake of antigen and presentation to lymphocytes via MHC class II molecules [2, 5]. An endogenous ligand for LY75 has not yet been defined, but targeting antigens such as HIV gag protein, *Yersinia pestis* PLA protein, and the EBNA1 nuclear antigen of Epstein Barr Virus to LY75-specific antibodies has resulted in lymphocyte expansion [6, 7]. Undefined ligands for LY75 have been reported in apoptotic cells and in a subset of dendritic cells, indicating possible roles in the recognition of dying cells and in self-tolerance, respectively [8].

Downregulation of LY75 has been reported in colorectal carcinoma cell lines and has been correlated with tumor differentiation [9, 10], indicating possible roles for LY75 in tumor suppression. In contrast to these findings, here we report that in ovarian cancer cells LY75 expression is upregulated in association with IL6R α overexpression, and results in enhanced adherence of ovarian tumor cells to the omentum, a process that can be blocked with antibodies specific to LY75.

Methods

Cell culture, transfection and transductions

ES2 and SKOV3 human clear cell and serous papillary ovarian carcinomas were obtained from ATCC. ID8, a spontaneously transformed murine ovarian epithelial cell line, was obtained from Dr. K. Roby (University of Kansas). All cells were maintained in Dulbecco's modified Eagles medium (DMEM) (Cellgro) with 10% serum (HyClone) and without antibiotics, and tested regularly for mycoplasma. Cells were initially transfected with red fluorescent protein (RFP; DsRed, Clontech) as previously described [11]. The transfection of human IL6 and IL6R α sequences (ATCC) cloned into pcDNA plasmid (Invitrogen) or empty vector (pcDNA) was carried out by using JetPEI (PolyPlus Transfection). Selection was performed with hygromycin (Invitrogen). For transductions, we used prevalidated shRNA specific for human IL6, IL6R α (Sigma), or a scramble sequence known to show no cross-reactivity to human or murine RNA (Sigma). RNA was cloned in the pLKO.1 vector and packaged in lentivirus. Selection was performed with puromycin (InvivoGen).

Cell proliferation and survival assays

The thiozoly blue tetrazolium bromide (MTT) assay was performed as described [12] with the following modifications. ES-2 (500 cells/well) and SKOV3 (1,000 cells/well) were plated in 96-well plates in quadruplicate for 5 and 7 days, respectively. Monoclonal antibodies specific for CD205 (10 μ g/ml; AbD Serotec) and keyhole limpet hemocyanin (mouse IgG_{2B} isotype control antibody; 10 μ g/ml; R&D Systems) and recombinant human IL6 and IL6R α (10 and 100 ng/ml, respectively; PeproTech) were added as indicated. Each assay was performed a minimum of three times.

Growth in soft agar was assessed by plating 2,500 cells suspended in 0.4% soft agar in complete DMEM in triplicate in 6-well plates precoated with 0.6% agar in complete growth medium, followed by incubation at 37°C, 5%

CO₂. After 12 to 14 days, colonies were stained with 0.1% crystal violet, photographed, and counted.

Anoikis was assessed on 6-well plates precoated with poly-HEMA (Sigma) as previously described [13]. 1×10^6 cells per well were plated and incubated on a shaking platform at 37°C, 5% CO₂ for 24 h. Viable cells were counted with a hemocytometer after trypan blue staining.

Adhesion and migration assays

Migration was assessed by plating 50,000 cells in the top chamber of cell-culture inserts (8 μm pore size, Thincert, Geiner Bio-One) in serum-free media. Medium containing 10% serum was placed in the lower chamber. After 24 h, media was removed and the top of the filter was wiped with a Q-tip to remove non-migrated cells. Migrated cells on the lower side of the filter were stained with Kwik-Diff (Thermo Shandon), photographed, and counted in three fields at 100× magnification. Assays were performed in triplicate.

Cell adhesion was assessed by plating 20,000 cells on uncoated 96-well polystyrene plates (Costar 3596) or on plates precoated with human collagen I (5 μg/well; BD Biosciences, 354243), collagen II (2 μg/well; EMD, 234184), or laminin (2 μg/well; BD Biosciences, 354232). After 30 min, non-adherent cells were gently removed by washing with PBS. Remaining adherent cells were quantified by adding 0.1% crystal violet and then measuring absorbance at 570 nm (Molecular Devices Thermomax Microplate Reader). Adherence to other matrix proteins was assessed with ECM Fluorometric Cell Adhesion Array Kit (Millipore) as per the manufacturer's instructions. Antibody blocking experiments were performed with antibodies specific for human integrin αL (eBioscience), LY75 (AbD Serotec), LYVE-1 (R&D Systems), integrin α2 (R&D Systems) and MMP-2 (Oncogene) and IgG (control antibody) at a concentration of 10 μg/ml.

In vivo and ex vivo tumor models

We used mice of the following genotypes: SCID, IL6^{-/-}, IL6Rα^{fl/fl} (Jackson Laboratories), IL6Rα^{-/-}, IL6Rα^{fl/fl}/LysMCre⁺, IL6Rα^{fl/fl}/AlbCre⁺ [14]. All mice were maintained on a C57Bl6 background and housed in PIV cages. Tumor implant formation in mice was assessed in vivo after injection of 5×10^5 cells into the peritoneum. RFP-expressing tumor cells were imaged with a panoramic macrofluorescence imaging system (Lighttools Research, Encinitas, CA). Images were analyzed with ImagePro Express software (Image Processing Solutions, North Reading, MA) to assess fluorescent tumor coverage of the diaphragm as a percentage of total diaphragm area.

For ex vivo experiments, omental tissue was identified and isolated as previously described [15]. Briefly, the omentum, pancreas, and spleen were removed en bloc, placed in ice cold PBS, and the floating omentum was excised. Omenta were harvested either from mice in which tumor cells were administered in vivo 6 h prior to harvest or from naïve mice for ex vivo exposure to tumor cells. Ex vivo exposure was achieved by placing omenta in separate wells of a 24-well plate and adding 2×10^5 tumor cells and incubating for 6 h with gentle shaking in a CO₂ incubator at 37°C. After this time, the media was replaced, and omenta were maintained in ex vivo culture as previously described [15]. Conditioned media and fluorescent imaging (Xenogen IVIS) data were collected at various intervals for further analysis.

Detection of IL6 and IL6Rα mRNA and protein

Species-specific ELISAs for human and mouse IL6 (eBioscience) and IL6Rα (R&D Systems) were performed according to the manufacturers' recommendations. RNA was isolated from cultured cells or murine omenta with a Nucleospin II kit (Clontech). RNA was prepared from patients samples with RNeasy Lipid Tissue kit (Qiagen). cDNA was generated by gene-specific priming with the ThermoScript II reverse transcription kit (Invitrogen). Quantitative real-time PCR (Q-PCR) was performed with HotStar Taq DNA polymerase (Qiagen), using the primers listed in Supplementary Table I, and detected with the Realplex Mastercycler (Eppendorf). Primer specificity was confirmed by checking product sizes on an agarose gel and by performing a melt-curve analysis on each run. Gene expression was normalized against the human and mouse ribosomal L32 genes.

Gene expression analysis

Publicly available datasets on ovarian cancer were taken from the NCBI GEO database. For this study, the following ovarian carcinoma datasets were analyzed: GSE2109 (241 samples, IntGen, 2005, <https://expo.intgen.org/geo/>), GSE3149 (153 samples) [16], and GSE6008 (103 samples) [17]. These datasets were subsequently reduced to retrieve relevant and well represented cancer subtypes. The following subsets were used for analysis in this study: GSE2109—normal ovarian tissue (4 samples) and serous adenocarcinoma (41 samples); GSE3149—ovarian cancer stages III (111 samples) and IV (21 samples); GSE6008—serous surface papillary carcinoma (106 samples) and serous adenocarcinoma (24 samples). Statistical analysis of gene expression was conducted using the R package. Significance of differential expression and coexpression was set to *P*-value <0.0001.

Results

Tumor Expression of IL6 and IL6R α increase metastasis to the omentum

We and others have previously shown that the greater omentum is an early and preferred site of metastasis for ovarian cancer cells [15, 18, 19]. Moreover, expression of IL6 and IL6R α has been associated with the progression of ovarian cancer in patients [1, 20, 21], though no causative relationship or mechanism have been demonstrated. To investigate whether overexpression of IL6 and its receptor in ovarian tumor cells can influence early tumor metastasis, we generated expression variant cell lines using overexpression vectors and shRNA knockdown constructs of IL6, IL6R α , and control sequences. We used two human ovarian carcinoma cell lines (ES-2, clear cell carcinoma; and Skov-3, serous papillary carcinoma) each with low endogenous expression of IL6 and IL6R α , in which we had previously established stable expression of RFP. The level of expression of RFP was not different in the IL6 and IL6R α expression variants, as assessed by fluorometric readings of precounted cells (data not shown). Successful overexpression and knockdown of IL6 and IL6R α in stable cell lines was confirmed for ES-2 by Q-PCR (Fig. 1a, b). Protein overexpression was determined by ELISA (Fig. 1c) but levels were below the limit of detection for knockdown cell lines. Expression levels in Skov-3 cell lines was also assessed (Supplementary Fig. 1A–C). Interestingly, a modest increase in IL6R α levels occurred in IL6 overexpressing cells but these levels were much lower than that achieved by IL6R α overexpression. No increase in IL6 was seen in IL6R α overexpressing cells.

To determine an appropriate means of assessing early tumor colonization, we next injected the tumor cells into the peritoneum of mice and confirmed that (i) the earliest tumor colonization occurred on the omentum, as previously shown by Khan et al. [15]; and that (ii) similar proportional results were obtained by quantifying fluorescent tumor cells in omental homogenate preparations or by imaging the surface fluorescence of intact omenta (Supplementary Fig. 1D). Thus, analyses were performed on intact omenta to allow assessment at multiple time points. At 6 and 48 h after intraperitoneal injection, tumor cells overexpressing IL6 or IL6R α accumulated on the omentum at a greater rate than control vector-expressing cells (Fig. 1d, e). Although the duration of in vivo tumor cell exposure was insufficient for the development of adaptive immune responses, the experiments were repeated in immunocompromised SCID mice to ensure that results were not influenced by specific lymphocyte responses. Consistent with the results in immune-competent mice, IL6R α overexpression enhanced

the early accumulation of tumor cells to the omentum in SCID mice (Fig. 1f).

Effect of IL6 and IL6R α on proliferation, survival, and migration in ovarian cancer cell lines

As IL6R α expression, and to a lesser extent IL6, increased early metastasis to the omentum, we used a series of in vitro assays to determine whether the effects were mediated by increased proliferation and/or survival, enhanced migration, or increased adherence of tumor cells in vitro. We found minor increases in metabolic activity by MTT assay (Supplementary Fig. 2a), and increased anchorage-independent growth in both IL6 and IL6R α overexpressing cells (Supplementary Fig. 2B). This finding is consistent with the proliferative effects previously attributed to IL6 signaling in some cell lines [22, 23]. Reduced anoikis rates have been reported in ovarian cancer cell lines in response to stress, a process that also induces IL6 production [13]. To determine if decreased anoikis accounted for enhanced survival rates in cells overexpressing IL6 and IL6R α , we assessed anoikis in the IL6 expression variants and did not observe differences between the cell lines (Supplementary Fig. 2C). Cell migration and invasion have also been shown to be influenced by IL6 signaling and may contribute to enhanced colonization of the omentum by tumor cells. To determine if this was occurring in ovarian cell lines, we examined the effect of IL6 and IL6R α expression on cell migration in vitro. Migration through uncoated cell culture inserts was not significantly different in cells overexpressing IL6 or IL6R α (Supplementary Fig. 2D).

IL6 and IL6R α expression influence tumor cell adhesion

We next examined the effect of altered IL6 and IL6R α expression on tumor cell adherence. Initial experiments indicated that overexpression of IL6, and to a greater extent IL6R α , increased adhesion of ES2 and SKOV3 cells to plastic (Fig. 2a). To determine the effect of IL6 and IL6R α expression on adherence to individual matrix proteins relevant to the peritoneal environment, cells were assayed on culture plates precoated with extracellular matrices. Overexpression of IL6 and IL6R α enhanced adherence to laminin and collagen I and II, compared with empty vector-expressing cells (Fig. 2b), but not to fibronectin, vitronectin, tenascin, or collagen IV (data not shown). Similar to the results with the plastic substratum, the enhancement of attachment was more pronounced in cells overexpressing IL6R α as opposed to IL6. Interestingly, knockdown of IL6 and IL6R α did not significantly reduce adherence in ES2 or Skov3 cell lines (Fig. 2b). This result may reflect the low

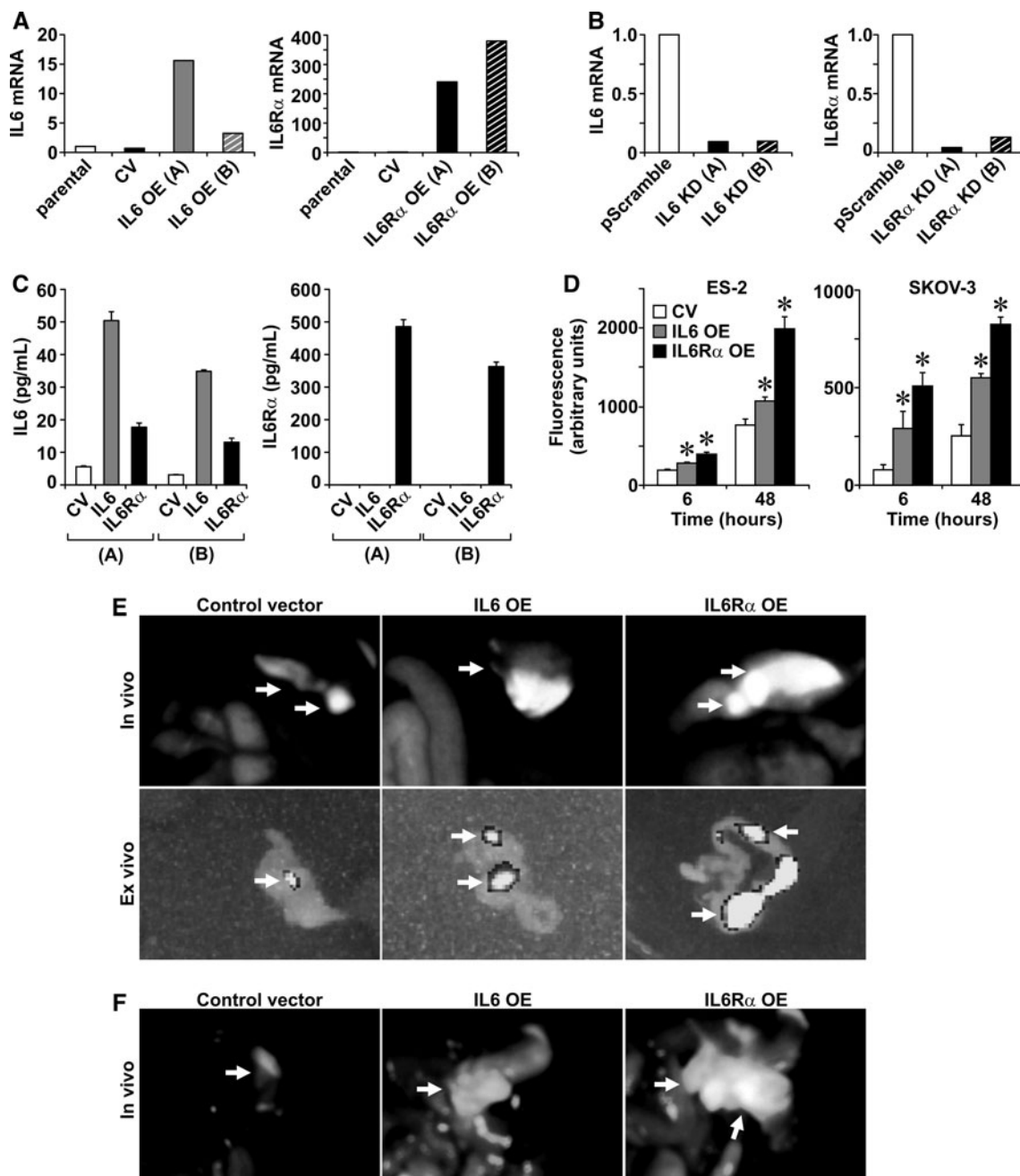


Fig. 1 IL6 and IL6R α expression increases early metastasis to the omentum. **a** ES-2 cell line overexpressing human IL6 (left panel) or IL6R α (right panel) and control vector (CV) were generated, and mRNA expression was analyzed by Q-PCR. Two lines (A and B) were tested for each construct. Data are expressed as fold change compared with cells expressing empty (control) vector (CV; overexpression experiments) or a scrambled sequence (pScramble; knockdown experiments). **b** ES-2 cell lines with knockdown constructs for IL6 (left panels) or IL6R α (right panel) were generated and analyzed for IL6 and IL6R α mRNA expression by Q-PCR. **c** Increased IL6 or IL6R α protein expression was detected by ELISA of conditioned media collected from

ES-2 cells (500 cells/well; 5 days). **d, e** Increased accumulation of RFP-positive tumor cells overexpressing IL6 or IL6R α was observed by fluorescent imaging of omenta exposed to ES-2 or Skov-3 tumor cells for 6 and 48 h (* $P < 0.05$). **e** Representative fluorescence images of omenta 6 h after intraperitoneal injection of ES-2 cells (top panels; in vivo imaging). Omenta were then excised and placed in ex vivo culture (lower panels, organ-specific imaging in culture plate). Areas of the omentum with fluorescent tumor implants are indicated with arrows. **f** Representative images of omenta 48 h after intraperitoneal injection of ES-2 cells (in vivo imaging)

levels of endogenous IL6 and IL6R α expression in the parental cell lines. In a scenario wherein IL6 signaling in tumor cells is minimal or low, adherence would be

determined by other adhesion molecules known to be expressed in ovarian cancer cells such as integrins, ICAM-1, and VCAM-1, and by proteolytic cleavage of matrix

proteins [24–26]. However, given that IL6 and IL6R α are frequently overexpressed in ovarian cancer, IL6 signaling may represent an additional important mechanism.

As IL6R α levels were more dramatically upregulated than IL6 by transfection with overexpression constructs, we incubated cell lines with exogenous IL6 and IL6R α to determine whether adhesion could be further enhanced in

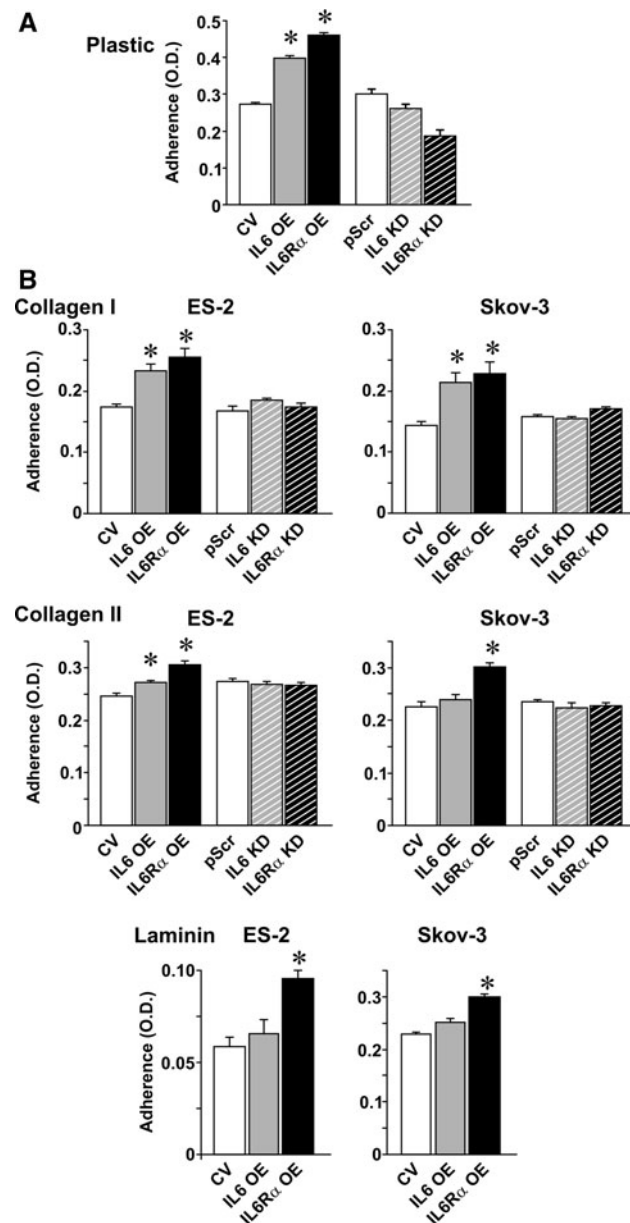


Fig. 2 IL6 and IL6R α overexpression enhances adhesion of ovarian tumor cell lines. **a** Adherence to plastic was increased in ES-2 cells overexpressing IL6 or IL6R α compared with empty vector (CV). Adherence was assessed by increased optical density (570 nm) after crystal violet staining. **b** Adherence to collagen I and II and to laminin was increased in ES-2 and Skov-3 cells, as assessed in (a). Results are expressed as percent inhibition relative to the same cell line exposed to vehicle alone \pm S.E.M. * P < 0.05

IL6 overexpressing cells to reach the level of adherence observed in IL6R α overexpressing cells. While soluble IL6 had only a minor effect on the adherence of cells overexpressing IL6R α , exogenous administration of soluble IL6R α enhanced the adherence of IL6-overexpressing cells to plastic almost to the levels of IL6R α -overexpressing cells (Supplementary Fig. 3). Control vector-expressing cells showed augmented adherence after exogenous administration of both IL6 and soluble IL6R α , but the levels did not reach those of IL6- or IL6R α -overexpressing cells. Doses of IL6 and IL6R α higher than those shown did not further enhance adherence. This may suggest limitations in the administration or availability of exogenous IL6/IL6R α or an adherence advantage in cells that express autocrine IL6 or IL6R α . These experiments indicate that the exaggerated adherence phenotype of cells overexpressing IL6R α compared with IL6 was at least partly accounted for by the greater expression of IL6R α , and perhaps that IL6R α rather than IL6 is the limiting factor in the cellular environment. The absence of IL6 in the culture media or FCS indicates that endogenous production of IL6 by tumor cells is the predominant source.

Host IL6R α expression contributes to tumor spread to the omentum

Although tumor cells are believed to be an important source of IL6 and IL6R α within the tumor microenvironment, both IL6 and IL6R α are secreted in soluble forms that contribute to IL6 signaling. Therefore, host expression of IL6 and IL6R α may be important in any phenotype conferred upon tumor cells. To determine whether host IL6 or IL6R α could influence tumor cell adherence to the omentum, we injected tumor cells expressing only the empty vector into mice with a complete genetic deficiency of IL6 or IL6R α . The absence of host-derived IL6 or IL6R α significantly reduced the adherence of tumor cells to the omentum, with the greatest effect on IL6R α ^{-/-} mice (Fig. 3a). This suggests that host IL6/IL6R α expression may also influence tumor adherence to the omentum. No additive effect was seen in mice with a double deficiency of IL6 and IL6R α (Fig. 3a) indicating that the tumor-promoting effects of IL6 and IL6R α utilize the same mechanism, most likely the IL6 signaling pathway.

Through our previous experiments involving mice with conditional IL6R α deficiency, we identified myeloid lineage cells as the primary source of circulating IL6R α , in both basal and inflammatory states, and hepatocytes as the secondary source [14]. To determine which source of IL6R α was important for tumor adherence to the omentum, tumor cells were administered to mice with IL6R α deficiencies in either hepatocytes (IL6R α ^{fl/fl}/AlbCre⁺) or myeloid lineage cells (IL6R α ^{fl/fl}/LysMCre⁺). The perturbation of tumor adherence

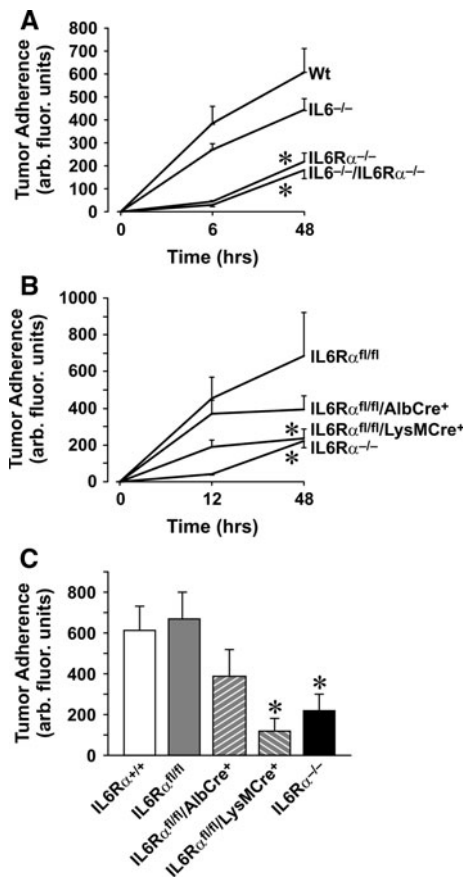


Fig. 3 Host IL6Rα expression contributes to tumor cell adherence to the omentum. **a** Mice with deficiencies in IL6 and/or IL6Rα were injected i.p. with 5×10^5 ES-2 cells expressing control vector. After 6 h, omenta were harvested, imaged to detect fluorescence, and cultured ex vivo for 48 h and then imaged again. Results represent the surface area of the omentum to which fluorescent tumor cells had adhered, expressed as arbitrary fluorescence units \pm S.E.M. **b** Mice with conditional deficits of IL6Rα were treated the same as in **(a)** and imaged after 12 and 48 h. **c** Naïve omenta were harvested from mice with conditional and complete IL6Rα deficits and ES-2 tumor cells (2×10^5) were added ex vivo. The graph shows tumor adherence after 6 h in ex vivo culture, expressed as arbitrary fluorescence units \pm S.E.M. * $P < 0.05$

was greater in IL6Rα^{fl/fl}/LysMCre⁺ mice (Fig. 3b). In fact, the level of adherence mirrored the contribution of each cell type to circulating levels of IL6Rα in that IL6Rα^{fl/fl} mice had the greatest tumor adherence, followed by IL6Rα^{fl/fl}/AlbCre⁺ mice, IL6Rα^{fl/fl}/LysMCre⁺, and IL6Rα^{-/-} mice. In order to determine if macrophages of the omentum could directly contribute to tumor cell adherence by production of IL6Rα, we administered tumor cells to omenta ex vivo. Without the contribution of extra-omental sources of IL6Rα, a greater reduction in tumor adherence was observed in omenta from IL6Rα^{fl/fl}/LysMCre⁺ mice than IL6Rα^{fl/fl}/AlbCre⁺ mice or IL6Rα^{fl/fl} mice (Fig. 3c). This finding may indicate an important and potentially targetable role for

milky spot macrophages of the omentum in facilitating ovarian tumor metastasis via IL6Rα production.

IL6Rα expression enhances LY75 production

To address the mechanism by which IL6 signaling may influence cellular attachment to the omentum, we investigated molecules known to be relevant to the omental environment. We asked whether IL6Rα overexpression in cell lines affected the expression of fibrillar collagen-binding receptors [integrin β1 (ITGB1), discoidin domain receptor 2 (DDR2), glycoprotein VI (GP6), leukocyte-associated IG-like receptor-1 (LAIR-1)] and the mannose receptor family members (MRC1, MRC2, LY75, PLA2R), and of several other adhesion molecules that are present in the ovarian tumor/omental microenvironment, including integrins β3, α2, α4, α5, α11, αL, αM, αV; ICAM1; and VCAM1. While IL6 and IL6Rα overexpression showed some correlation with the expression of MMP2, CLDN4, ITGA2, ITGAL, LYVE1, MUC16, and LY75, the most consistent effect involved LY75 mRNA. LY75 mRNA expression was upregulated in both ES-2 and Skov-3 cells overexpressing IL6 and IL6Rα and was decreased in cells in which endogenous IL6 and IL6Rα expression had been knocked down (Fig. 4a). Previously reported fusion proteins consisting of regions of LY75 and DCL-1 in human samples [27] were not detected by Q-PCR (data not shown). Addition of exogenous IL6 and IL6Rα to parental cells enhanced the expression of LY75 mRNA (Fig. 4a). Flow cytometry indicated that increased expression of LY75 protein was also observed on the surface of cells overexpressing IL6Rα (Fig. 4b).

Antibody blocking experiments were performed to determine whether the enhanced adherence exhibited by IL6Rα-overexpressing cells could be attributed to MMP2, CLDN4, ITGA2, ITGAL, LYVE1, MUC16, or LY75 expression. Only the antibody specific for LY75 resulted in decreased in vitro adherence of IL6Rα overexpressing cells (Fig. 4c). This antibody had little or no effect on control vector-expressing cells (Fig. 4c). Blocking LY75 did not affect cell proliferation in cells overexpressing IL6Rα or control vector (data not shown). Adherence to murine omentum was next tested in ex vivo cultures. Again, the blocking antibody to LY75 significantly reduced the attachment of tumor cells overexpressing IL6Rα (Fig. 4d). Perhaps not surprisingly, the antibody also had a significant effect on the empty-vector-expressing cells. The presence of host IL6Rα in the omenta may have contributed to this inhibitory effect. To determine the effect of the anti-LY75 antibody in mice lacking IL6Rα expression, the experiment was repeated on omenta from IL6Rα^{-/-} mice. Compared with the IgG2B-specific control antibody, the antibody against LY75 had a greater inhibitory effect on tumor

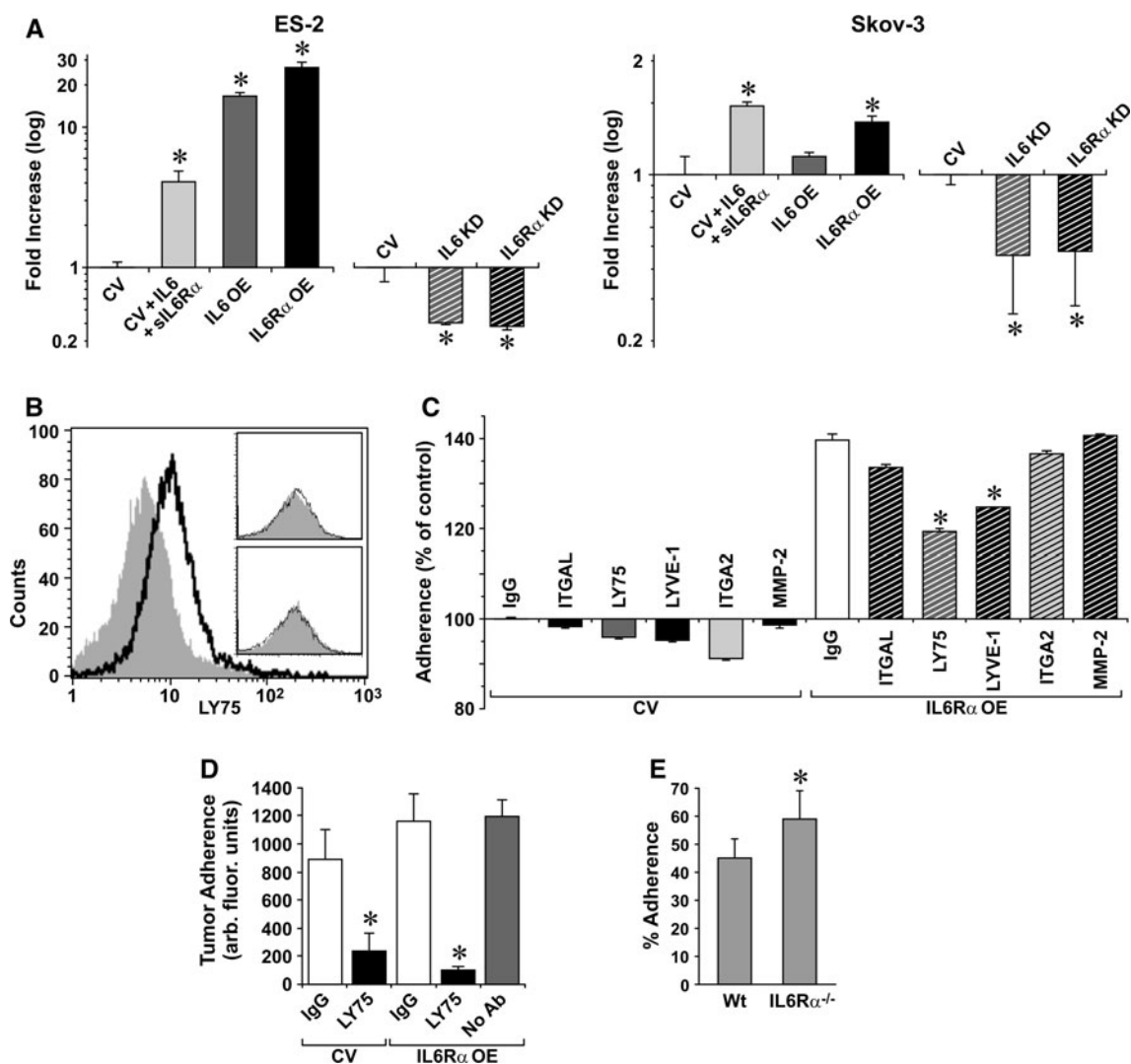


Fig. 4 IL6 and IL6R α expression correlates with LY75 expression and tumor adherence. **a** Q-PCR indicating that the manipulation of IL6 or IL6R α expression results in concomitant increases in LY75 mRNA expression in both ES-2 (*left panel*) and SKOV-3 (*right panel*) cell lines. Exogenous IL6 and IL6R α concentrations were 10 and 100 ng/ml, respectively. **b** Flow cytometric analysis of LY75 expression on ES-2 cells expressing control vector (*shaded histogram*) and IL6R α (*open histogram*). The *inset* shows the IgG control and LY75 antibody for the control vector-expressing cells. **c** Preincubation of tumor cells with anti-LY75 and anti-LYVE-1 antibodies (10 μ g/ml) significantly inhibited adherence of IL6R α -overexpressing

cells to plastic. Data are represented as percent adherence relative to control vector-expressing cells (CV) treated with IgG2B control antibody. Significance was assessed relative to IgG-treated cells expressing the same vector as the treatment group. **d** Ex vivo blocking studies performed with naïve omenta harvested from wild-type mice and exposed to tumor cells and antibodies, as indicated. **e** Tumor adherence to omenta from wild type and IL6R α ^{-/-} mice treated ex vivo with LY75 and control antibodies. Data are expressed as percent of surface area colonized by tumor compared with control antibody treatment

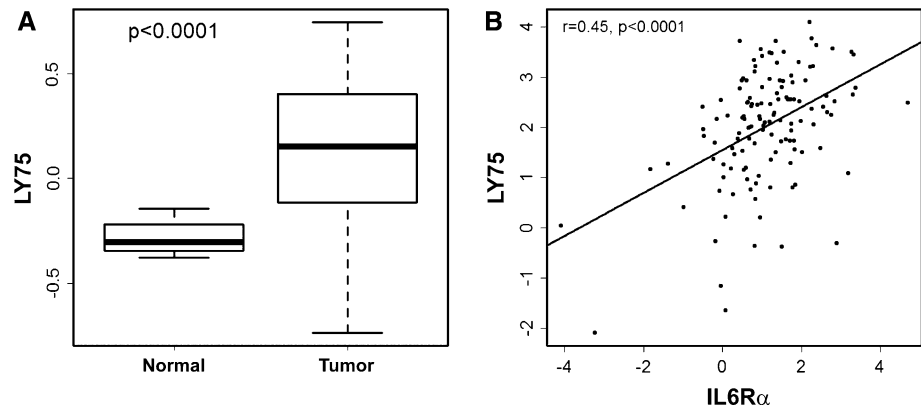
adherence in wild-type mice than in IL6R α ^{-/-} mice (Fig. 4e). These data indicate that both host- and tumor-derived IL6R α can influence LY75 expression and subsequent tumor adherence to the omentum.

LY75/CD205/DEC205 in ovarian cancer

As there was little available in the published data to explore a relationship between IL6R α and LY75 expression, we performed an analysis of studies deposited in the

NCBI GEO database. We found that LY75 is significantly overexpressed in serous adenocarcinoma compared with normal ovary (Fig. 5a), and consistent with our data, we found positive correlations between LY75 and IL6R α expression in two independent datasets on ovarian cancer [GSE2109, $n = 130$ (Fig. 5b) and GSE3149, $n = 132$ (data not shown)]. Insufficient information was provided to identify a potential correlation between tumor stage and LY75 expression. A significant correlation between LY75 and IL6 was not found. This may reflect the multiple

Fig. 5 IL6R α and LY75 expression in public databases. **a** Significant overexpression of LY75 in serous adenocarcinoma (grade I-III; $n = 41$) as compared with normal ovary ($n = 4$; dataset: GEO GSE6008). **b** Co-expression of LY75 and IL6R α in ovarian cancer: combined samples from ovarian serous surface papillary carcinoma and ovarian serous adenocarcinoma ($n = 130$; GSE2109). Intensity is log₂ scaled



pathways affecting IL6 production and/or that IL6R α rather than IL6 expression may be rate-limiting in IL6 signaling.

Discussion

IL6 expression, which has been linked to the progression of several cancer types, is upregulated in ovarian cancer. However, IL6 signaling influences tumor progression in both positive and negative ways and via multiple pathways. A clearer understanding of how IL6 influences particular cell types in the appropriate tumor microenvironment will be required to specifically target the metastatic pathways that influence tumor-induced mortality. Here we have shown that LY75 is upregulated as a result of IL6R α expression and that it contributes to ovarian tumor cell adherence to the omentum. This finding suggests that LY75 is a potential target for reducing the early metastasis of ovarian cancer within the peritoneum.

In the current study, we have shown that altering the expression of IL6 and IL6R α in tumor cells can affect the adherence of tumor cells to several substrates including plastic, collagen types I and II, laminin, and the surface of the omentum, and that this effect can be blocked by antibodies to LY75. Minor changes in cell proliferation were also seen with increased IL6 and IL6R α expression, but these changes were not blocked by antibodies to LY75. Given the increased expression of IL6 and IL6R α expression in ovarian cancer, we therefore propose that LY75 expression is increased in tumor cells as a result of increased IL6 signaling. Although murine IL6 exhibits species specificity for murine IL6R α , human IL6 does not. Therefore, the availability of tumor-derived human IL-6 in our model facilitates IL6 signaling and the subsequent induction of LY75 in tumor cells. However, according to our *in vitro* and *in vivo* data in knockout mice, both tumor- and host-derived IL6R α can influence tumor LY75 production and subsequent adherence. This is perhaps not surprising as it is known that IL6R α is secreted as a soluble

agonist in IL6 signaling. In fact, our data in conditional IL6R α -deficient mice suggest that myeloid cells within the omentum, most likely milky spot macrophages, may provide sufficient IL6R α to enhance tumor adherence. Given that the presence of a tumor, or the inflammation associated with the tumor, can induce increased expression of host IL6 and IL6R α [1, 11], it is likely that host proteins may be advantageous targets for reducing early metastasis of ovarian cancer.

Neither IL6 nor IL6R α expression have previously been linked to increased LY75 expression. However, both IL6 and LY75 are associated with dendritic cell maturation and lymphocyte expansion, and both are upregulated in human B cells treated with IL4 [28]. This suggests not only that their induction may occur as a result of a shared pathway, but that their function may be related. Our data showing that IL6R α expression leads to increased LY75 expression in tumor cells is supported by correlations revealed through the examination of large public databases that contain information on many patients with ovarian cancer.

The LY75 gene is located in a cluster of transmembrane C-type lectin receptors on chromosome band 2q24 [3]. The LY75 receptor is a single polypeptide chain receptor with a short cytoplasmic domain containing functional endocytosis motifs that direct its internalization through clathrin-coated pits to endosomes for MHC loading and subsequent immune responses [29]. The cytoplasmic domain is also believed to play a role in interleukin-4 receptor signal transduction. The extracellular domain consists of an N-terminal cysteine-rich domain, a fibronectin type II domain, and ten C-type lectin domains that lack carbohydrate-binding function [2, 5]. The undefined cellular ligand/s for LY75 are expressed by both live and necrotic cells, and bind within the C-type lectin domains [8]. The fibronectin domain is the most highly conserved of all the extracellular domains of the mannose receptor family and is predicted to bind collagen [30, 31]. Antigen presentation is the main function attributed to LY75. Targeting antigens to LY75 for uptake in the absence of dendritic cell

stimulatory factors leads to self-tolerance, while the addition of maturation stimuli such as toll-like receptor ligands or antibodies to CD40 induce specific immune responses [32–34]. Interestingly, unlike other mannose receptor family members, LY75 is upregulated in mature dendritic cells as a result of both increased transcription and increased shuttling to the cell surface, and this increase coincides with decreased endocytic activity [27]. These findings may indicate a role for LY75 that is independent of endocytosis and antigen presentation. As mature dendritic cells typically home to secondary lymphoid organs, LY75 may play a role in cell–cell or cell–matrix interactions. Likewise, tumor cells overexpressing LY75 may also home to secondary lymphoid organs such as the omentum, as suggested by our data.

The gene for DCL-1/CD302 is immediately adjacent to LY75 and forms an intergenic splice variant with LY75 consisting of the intracellular and transmembrane domains of DCL-1 and the extracellular domain of LY75 with an additional C-type lectin domain [27]. This fusion protein has been detected in Hodgkin's Lymphoma cell lines [35] and in small amounts in some myeloid dendritic cells [27]. We were unable to detect LY75/DCL-1 fusion protein in human ovarian tumor cell lines in our mouse model. However, similar to LY75, DCL-1 is predicted to have endocytic and cell-adhesion functions with little or no lectin-binding capacity [36]. The predicted collagen-binding properties of LY75 may enhance cell adhesion in the peritoneal environment.

Tumor expression of LY75 has been reported to be diminished in some malignancies such as breast and rectal carcinoma and unchanged in urothelial carcinoma, relative to non-tumorigenic tissue [9, 10, 37]. Interestingly, TERT immortalization of urothelial cells is associated with downregulation of LY75 [38]. The association of LY75 with higher differentiation and decreased proliferative potential in colorectal carcinomas suggests that LY75 may suppress tumor growth, a role similar to, and perhaps involving, interleukin-4 receptor [37]. No associations between LY75 expression and ovarian cancer have previously been reported, but depletion of LY75-positive dendritic cells delays ovarian tumor progression in a mouse model [39]. This antitumor effect also occurred when CD11c-positive dendritic cells were depleted, and the mechanism involved enhanced antitumor immunity and reduced tumor vascularization [39]. As we did not manipulate the number of LY75-expressing dendritic cells in vivo, and as our adherence phenotype occurred in vitro in the absence of immune cells, our IL6R α -induced LY75 adherence phenotype likely represents a novel function for LY75.

The combination of the specific tumor microenvironment, ascitic dissemination pathways, and early omental

colonization may create a situation in which LY75 expression favors the colonization of ovarian tumors. Increased expression of IL6 and IL6R α in patients with ovarian cancer may enhance LY75 expression in tumor cells and facilitate tumor adherence and colonization of the omentum. Indeed, we found a previously unreported correlation between IL6R α and LY75 expression in patients with ovarian cancer in large public databases, providing some clinical significance for our findings. Our study therefore demonstrates a novel mechanism by which IL6 signaling may contribute to tumor progression and suggests an opportunity for reducing the mortality associated with ovarian cancer.

Acknowledgments Funding was provided by a grant from the American Cancer Society (RSG-06-141-01; AFD) and the Department of the Army, DOD Ovarian Cancer Research Program (OC080273; AFD). We wish to thank Glenn Doermann for preparing the illustrations and Dr. Maryellen Daston for editing the manuscript.

References

- Rath KS et al (2010) Expression of soluble interleukin-6 receptor in malignant ovarian tissue. *Am J Obstet Gynecol* 203(3): 230.e1–230.e8
- Jiang W et al (1995) The receptor DEC-205 expressed by dendritic cells and thymic epithelial cells is involved in antigen processing. *Nature* 375(6527):151–155
- Kato M et al (1998) cDNA cloning of human DEC-205, a putative antigen-uptake receptor on dendritic cells. *Immunogenetics* 47(6):442–450
- Kato M et al (2006) Expression of human DEC-205 (CD205) multilectin receptor on leukocytes. *Int Immunol* 18(6):857–869
- McKay PF et al (1998) The gp200-MR6 molecule which is functionally associated with the IL-4 receptor modulates B cell phenotype and is a novel member of the human macrophage mannose receptor family. *Eur J Immunol* 28(12):4071–4083
- Cheong C et al (2010) Improved cellular and humoral immune responses in vivo following targeting of HIV Gag to dendritic cells within human anti-human DEC205 monoclonal antibody. *Blood* 116(19):3828–3838
- Gurer C et al (2008) Targeting the nuclear antigen 1 of Epstein-Barr virus to the human endocytic receptor DEC-205 stimulates protective T-cell responses. *Blood* 112(4):1231–1239
- Shrimpton RE et al (2009) CD205 (DEC-205): a recognition receptor for apoptotic and necrotic self. *Mol Immunol* 46(6): 1229–1239
- al-Tubuly AA et al (1996) Differential expression of gp200-MR6 molecule in benign hyperplasia and down-regulation in invasive carcinoma of the breast. *Br J Cancer* 74(7):1005–1011
- Tungekar MF, Gatter KC, Ritter MA (1996) Bladder carcinomas and normal urothelium universally express gp200-MR6, a molecule functionally associated with the interleukin 4 receptor (CD 124). *Br J Cancer* 73(4):429–432
- Robinson-Smith TM et al (2007) Macrophages mediate inflammation-enhanced metastasis of ovarian tumors in mice. *Cancer Res* 67(12):5708–5716
- Mosmann T (1983) Rapid colorimetric assay for cellular growth and survival: application to proliferation and cytotoxicity assays. *J Immunol Methods* 65(1–2):55–63

13. Sood AK et al (2010) Adrenergic modulation of focal adhesion kinase protects human ovarian cancer cells from anoikis. *J Clin Invest* 120(5):1515–1523
14. McFarland-Mancini MM et al (2010) Differences in wound healing in mice with deficiency of IL-6 versus IL-6 receptor. *J Immunol* 184(12):7219–7228
15. Khan SM et al (2010) In vitro metastatic colonization of human ovarian cancer cells to the omentum. *Clin Exp Metastasis* 27(3):185–196
16. Bild AH et al (2006) Oncogenic pathway signatures in human cancers as a guide to targeted therapies. *Nature* 439(7074):353–357
17. Hendrix ND et al (2006) Fibroblast growth factor 9 has oncogenic activity and is a downstream target of Wnt signaling in ovarian endometrioid adenocarcinomas. *Cancer Res* 66(3):1354–1362
18. Hagiwara A et al (1993) Milky spots as the implantation site for malignant cells in peritoneal dissemination in mice. *Cancer Res* 53(3):687–692
19. Krist LF et al (1998) Milky spots in the greater omentum are predominant sites of local tumour cell proliferation and accumulation in the peritoneal cavity. *Cancer Immunol Immunother* 47(4):205–212
20. Plante M et al (1994) Interleukin-6 level in serum and ascites as a prognostic factor in patients with epithelial ovarian cancer. *Cancer* 73(7):1882–1888
21. Scambia G et al (1995) Prognostic significance of interleukin 6 serum levels in patients with ovarian cancer. *Br J Cancer* 71(2):354–356
22. Ishikawa H et al (2006) Mitogenic signals initiated via interleukin-6 receptor complexes in cooperation with other transmembrane molecules in myelomas. *J Clin Exp Hematol* 46(2):55–66
23. Kanazawa T et al (2007) Interleukin-6 directly influences proliferation and invasion potential of head and neck cancer cells. *Eur Arch Otorhinolaryngol* 264(7):815–821
24. Kenny HA et al (2008) The initial steps of ovarian cancer cell metastasis are mediated by MMP-2 cleavage of vitronectin and fibronectin. *J Clin Invest* 118(4):1367–1379
25. Sawada K et al (2008) Loss of E-cadherin promotes ovarian cancer metastasis via alpha 5-integrin, which is a therapeutic target. *Cancer Res* 68(7):2329–2339
26. Slack-Davis JK et al (2009) Vascular cell adhesion molecule-1 is a regulator of ovarian cancer peritoneal metastasis. *Cancer Res* 69(4):1469–1476
27. Butler M et al (2007) Altered expression and endocytic function of CD205 in human dendritic cells, and detection of a CD205-DCL-1 fusion protein upon dendritic cell maturation. *Immunology* 120(3):362–371
28. Zhu YX et al (2004) The SH3-SAM adaptor HACS1 is up-regulated in B cell activation signaling cascades. *J Exp Med* 200(6):737–747
29. Mahnke K et al (2000) The dendritic cell receptor for endocytosis, DEC-205, can recycle and enhance antigen presentation via major histocompatibility complex class II-positive lysosomal compartments. *J Cell Biol* 151(3):673–684
30. Wu K, Yuan J, Lasky LA (1996) Characterization of a novel member of the macrophage mannose receptor type C lectin family. *J Biol Chem* 271(35):21323–21330
31. East L, Isacke CM (2002) The mannose receptor family. *Biochim Biophys Acta* 1572(2–3):364–386
32. Hawiger D et al (2001) Dendritic cells induce peripheral T cell unresponsiveness under steady state conditions in vivo. *J Exp Med* 194(6):769–779
33. Bonifaz L et al (2002) Efficient targeting of protein antigen to the dendritic cell receptor DEC-205 in the steady state leads to antigen presentation on major histocompatibility complex class I products and peripheral CD8+ T cell tolerance. *J Exp Med* 196(12):1627–1638
34. Trumpheller C et al (2008) The microbial mimic poly IC induces durable and protective CD4+ T cell immunity together with a dendritic cell targeted vaccine. *Proc Natl Acad Sci USA* 105(7):2574–2579
35. Kato M et al (2003) Hodgkin's lymphoma cell lines express a fusion protein encoded by intergenically spliced mRNA for the multilectin receptor DEC-205 (CD205) and a novel C-type lectin receptor DCL-1. *J Biol Chem* 278(36):34035–34041
36. Kato M et al (2007) The novel endocytic and phagocytic C-Type lectin receptor DCL-1/CD302 on macrophages is colocalized with F-actin, suggesting a role in cell adhesion and migration. *J Immunol* 179(9):6052–6063
37. al-Tubuly AA et al (1997) Inhibition of growth and enhancement of differentiation of colorectal carcinoma cell lines by MAb MR6 and IL-4. *Int J Cancer* 71(4):605–611
38. Chapman EJ, Kelly G, Knowles MA (2008) Genes involved in differentiation, stem cell renewal, and tumorigenesis are modulated in telomerase-immortalized human urothelial cells. *Mol Cancer Res* 6(7):1154–1168
39. Huarte E et al (2008) Depletion of dendritic cells delays ovarian cancer progression by boosting antitumor immunity. *Cancer Res* 68(18):7684–7691